Title

Striatal Indirect Pathway Dysfunction in a CNS-Specific Zfp521-Deficient Mouse Model of Tourette Syndrome-Like Behaviors

Author

Park, Chang Sin

Publication Date

2013

Peer reviewed|Thesis/dissertation

UNIVERSITY OF CALIFORNIA

Los Angeles

Striatal Indirect Pathway Dysfunction in a CNS-Specific Zfp521-Deficient Mouse Model of Tourette Syndrome-Like Behaviors

A dissertation submitted in partial satisfaction of the requirements for the degree of Doctor of Philosophy in Neuroscience

By

Chang Sin Park

2013

ABSTRACT OF THE DISSERTATION

Striatal Indirect Pathway Dysfunction in a CNS-Specific Zfp521-Deficient Mouse Model of Tourette Syndrome-Like Behaviors

by

Chang Sin Park

Doctor of Philosophy in Neuroscience

University of California, Los Angeles, 2013

Professor X. William Yang, Chair

Tourette Syndrome (TS) is a genetic, neurodevelopmental disorder that is characterized by the juvenile-onset of chronic motor and vocal tics and is often associated with other overlapping neuropsychiatric comorbidities including OCD, ADHD, self-injurious behaviors (SIBs), and social impairments. In this dissertation, we report novel TS-like behaviors in a CNS-specific conditional knockout mouse model of Zfp521 (Zfp521-BrKO). Zfp521 is a zinc finger transcription factor first identified as enriched in striatonigral MSNs from our laboratory's FACS-array profiling of striatal MSN subtypes (and later verified by the BAC-TRAP methodology) and is known to be critical in the differentiation of ES cells into early neuronal precursors. Converging evidence from the striatal expression of Zfp521 and the neurodevelopmental roles of Zfp423 (paralog) and Ebf1 (a physically interacting transcriptional partner of Zfp521) suggests Zfp521 may be involved in striatal development. Extensive studies of the behavioral and neuropathological phenotypes show that Zfp521-BrKO mice demonstrate robust TS-like face validity, exhibiting juvenile-onset

of several simple and complex tic-like motor behaviors that are exacerbated by stress or suppressed by attention, multiple TS-associated comorbidities, and select neuropathologies reported in TS patients. Pharmacological suppression of tic-like behaviors by haloperidol, a neuroleptic that is among the first-line treatments for TS, but not by fluoxetine, a SSRI used to treat OCD, reveals Zfp521-BrKO mice demonstrate selective predictive validity for tics associated with TS rather than the compulsive behaviors of OCD. Interestingly, Zfp521-BrKO mice are highly resistant to haloperidol-induced catalepsy, implicating hypofunctional indirect pathway D2-MSNs in the pathophysiology of the tic-like behaviors in the mutant mice, which was confirmed through immunohistochemical, electrophysiological, and optogenetic interrogation of the striatopallidal MSNs. Furthermore, supported by electrophysiological evidence of D1-MSN activation by haloperidol in Zfp521-BrKO, presumably by presynaptic D2-autoreceptor-mediated increase in DA release, we show that Zfp521-BrKO mice demonstrate unique predictive validity for tic-suppression by DA-agonism with pergolide and selective D1-receptor agonism. Our studies not only establish Zfp521-BrKO mice as a comprehensive animal model of TS with a distinct underlying BG circuitry dysfunction, but also highlights the potential of these mice as a powerful tool for TS drug discovery. Elucidating the molecular mechanisms of Zfp521, in both the normal and TS brain, will provide critical insights into the fundamental processes of striatal development and have significant implications for human genetic studies of TS.

This dissertation of Chang Sin Park is approved.

Daniel H. Geschwind

Michael S. Levine

S. Lawrence Zipursky

X. William Yang, Committee Chair

University of California, Los Angeles

2013

DEDICATION

This dissertation is dedicated to my wife, Traci Toy,

to my parents, Young Chul and Yoon Ja Park,

and to my friends, who are not special enough to name individually.

TABLE OF CONTENTS

LIST OF FIGURES AND TABLES

ACKNOWLEDGEMENTS

I would like to thank my mentor, William Yang, for providing me the opportunity to work on this endlessly intriguing (and sometimes frustrating) project. While William isn't always the easiest person to work for, I've come to appreciate and respect his drive, enthusiasm, and the high standards he demands of his lab, as well as of himself. In the end, I've become a better scientist by his example and I'm confident my future successes will be rooted in my education and experience in his lab. I would also like to thank the members of my doctoral committee: Dan Geschwind, Larry Zipursky, and especially Mike Levine, who always looked out for my best interest when I lost sight of what I needed to prioritize as a graduate student, and not just a researcher. As ridiculously quickly as the past six years have gone by, if it wasn't for my committee's insistence that I defend, I'm sure I will still be at this for another 20 years. I would like to thank members of the Yang lab, past and present: Xiaohong Lu, Yijun Cui, Xiaofeng Gu, Jeff Cantle, Nan Wang, Anthony Daggett, Daniel Lee, Monica Lee, Mary Kay Lobo, Michelle Gray, Erin Greiner, Tara Murphy, Richard Zhang, Margaret Chu, and Helena Tran for understanding that I don't mean to be a sarcastic ass, it's just how I come off because you obviously don't know me well enough. Special thanks to the other members of the D1/D2 team, Yijun and Xiaohong, for all their help in everything basal ganglia related. Apologies to Jeff Cantle, who desperately wanted a friend in the lab but was stuck with me (better luck with Anthony). Although Richard Zhang gave up on the noble pursuit of scientific research and lowered himself to become a medical doctor, I need to thank him for all the hours he spent as an undergraduate helping me with the data analysis and my mouse colonies. Of course, if I thank Richard, I need to also thank his later replacement, Suzie Sandoval. She was the absolute worst technician I had to work with but I thank her because she made me realize how much I lost when Richard graduated and left the lab. I also need to thank Mary Kay Lobo for

passing on such a great project to me. But at the same time, she set a ridiculously high standard to which William compares all his graduate students to, so maybe I'm not that thankful. Finally, special thanks to Margaret and Helena for keeping our lab functioning.

A very special thanks goes to Soren Warming and Neal Copeland. Not only did they provide us with an unpublished mouse, but they were incredibly patient in giving us the time to work with these mice and develop our model without having to worry about others scooping us with the same mice. I would also like to thank Sandra Holley and Carlos Cepeda in Mike Levine's lab for all their work on the electrophysiology with these mice. It was a lot of mice and a lot of work but in the end, they helped get me some very important pieces of data. I also appreciate all the help from Brian Zingg from Hong-Wei Dong's lab. We spent a lot of working on the tracer injections of my mice and it's a shame it couldn't go into this story, but I'm confident we're not done with it yet. I also need to thank Hong-Wei for all his help with the brain anatomy and circuitry of my mice, as well as for letting me spend countless hours with his lab's slide scanner. I love that thing so much that it hurt my heart when Hong-Wei's lab left with it to go to USC. A lot of thanks goes to Alexandra Nelson and Lex Kravitz from Anatol Kreitzer's lab. Not only did they train me in the ways of optogenetics, but spent more time than necessary trying to record from my mice. I would like to thank Giovanni Coppola for all his help on the microarray and bioinformatics work for my mice. I know I'll be seeing him again soon once I start on the RNA-seq experiments. Other collaborators I would like to thank for providing me mice and reagents and for working with me to track down every dead-end and head-scratching piece of data for my mice: Niall Murphy in Nigel Maidment's lab, Scott Barton in George Rebec's lab, Yun-Ping Deng in Tony Reiner's lab, Roland Baron, Eric Nestler, Istvan Mody, and Stewart Anderson. I'm not done with my work on these mice so this list is bound get longer. I would thank the graduate program's Neuroscience IDP, especially Suzie Vader and Mike Levine. The work in this dissertation was supported by the CSORDA P50 Grant to UCLA (NIDA), McKnight

Neuroscience of Brain Disorders Award, NIH ARRA Autism Challenge Grant, and the Neurogenetics Training Grant.

I would to thank my parents, Young Chul and Yoon Ja Park, who may have no idea what I've been working on for the past 6 years but it never stopped them from asking when I'll be done. But they are proud so I guess that should count for something. I want to thank my friends, who also have no idea what I've been working on despite the countless number of times I drunkenly explained it to them. But being a poor graduate student, they paid for my meals and drinks for years now so I guess that should count for something. Finally, I would like to thank my wife, Traci Toy, who doesn't really care what I've been working on as long as I finish up, get a job, and not go back to school for another degree. But she started this journey with me, and for whatever reason, was with me to the end, so I guess that should count for something.

VITA

2001 B.A., Neuroscience
Pomona College
Claremont, California

2001 - 2002 Research Technician
California Institute of Technology
Pasadena, California

2002 - 2006 Staff Research Associate/Lab Manager
University of California, Irvine
Irvine, California

2009 - 2011 UCLA Neurobehavioral Genetics Training Program Fellowship

2006 – 2013 Graduate Student Researcher
Major: Neuroscience
University of California, Los Angeles
Los Angeles, California

PUBLICATIONS AND PRESENTATIONS

Wilburn, B., Rudnicki, D.D., Zhao, J., Weitz, T.M., Cheng, Y., Gu, X., Greiner, E., **Park, C.S.**, Wang, N., Sopher, B.L., La Spada, A.R., Osmand, A., Margolis, R.L., Sun, Y.E., and Yang, X.W. (2011). An antisense CAG repeat transcript at JPH3 locus mediates expanded polyglutamine protein toxicity in Huntington's disease-like 2 mice. Neuron. 70, 427-440.

Park, C.S., Zhong, L., & Tang, S.J. (2009). Aberrant expression of synaptic plasticity-related genes in the NF1+/− mouse hippocampus. J. Neurosci. Res. 87, 3107-3119.

Park, C.S. and Tang, S.J. (2009). Regulation of microRNA Expression by Induction of Bidirectional Synaptic Plasticity. J. Mol. Neurosci. 38, 50-56.

Park, C.S., Gong, R., Stuart, J., and Tang, S.J. (2006). Molecular network and chromosomal clustering of genes involved in synaptic plasticity in the hippocampus. J. Biol. Chem. 281, 30195-30211.

Gong, R., **Park, C.S.**, Abbassi, N.R., and Tang, S.J. (2006). Roles of glutamate receptors and the mammalian target of rapamycin (mTOR) signaling pathway in activity-dependent dendritic protein synthesis in hippocampal neurons. J. Biol. Chem. 281, 18802-18815.

Chen, J., **Park, C.S.**, and Tang, S.J. (2006). Activity-dependent synaptic Wnt release regulates hippocampal long term potentiation. J Biol. Chem. 281, 11910-11916.

Park, C.S., Raskin, J., Nachtwey, J., and Parfitt, K.D. (2001) Changes with aging in adenylate cyclase-mediated forms of long term potentiation in hippocampal area CA1. Gordon Research Conference on Synaptic Plasticity, Newport RI.

Chapter 1

Introduction

1.1 Tourette Syndrome: Background and Clinical Features

In 1825, physician Jean Itard published an article in the *Archives Générales de Médecine* describing the inexplicable behavior of Marquise de Dampierre, who had gained public notoriety among Parisians for her uncontrolled outbursts of inappropriate shouts and crude obscenities, often in the middle of conversations. Sixty years later, the case history of Marquise de Dampierre, clinical observations of eight French patients with various involuntary motor twitches, movements, and vocal outbursts, as well as three examples from the United States, Malaysia, and Siberia of people exhibiting repetitive jumping and the echoing of words, all formed the basis of neurologist Georges Gilles de la Tourette's clinical description of "*maladie de tics*," published in his two-part "Study of a Nervous Affliction Characterized by Motor Incoordination with Echolalia and Coprolalia: Jumping, Latah, Myriachit" in 1885 (Kushner, 2009; Lajonchere et al., 1996). Soon renamed "*maladie de tics de Gilles de la Tourette*" by Tourette's mentor and clinical chief, Jean-Martin Charcot, this disorder was characterized by several, but not necessarily all, of the following features: involuntary movements and sounds, repetition of heard vocalizations (echolalia) and observed movements (echopraxia), and uncontrollable verbal cursing and obscenities (corprolalia). It was believed to manifest in childhood as a progressive disorder persistent through life and ultimately, incurable (Kushner, 2009; Lajonchere et al., 1996).

While this disorder continues to bear his name, the clinical features of Tourette syndrome (TS) have long since been extensively reassessed and expanded to more accurately define it as a juvenile-onset, neuropsychiatric disorder characterized by multiple motor and vocal tics that is often associated with various comorbidities (Leckman, 2002; Robertson, 2000).

Coming under the broader category of neurodevelopmental tic disorders in the current Diagnostic and Statistical Manual of Mental Disorders, 5th edition (DSM-V, APA, 2013), the diagnostic criteria for TS is the presence of both multiple motor and vocal tics, though not necessarily concurrent. Tics may fluctuate (wax and wane) in frequency but must have persisted for more than one year since the first tic onset, which must be before the age of 18 and not attributable to the physiological effects of a substance or other medical conditions. With an average age of tic onset around 5-8 years and the onset of 90-95% of TS cases occurring between 2 to 21 years of age (Leckman et al., 1998; Robertson, 2008a), the prevalence of TS among school-age children can range from 0.1% to 4%, depending on the adherence to diagnostic criteria and assessment methods (CDC, 2009; Hornsey et al., 2001; Robertson, 2008b). Furthermore, epidemiological studies suggest that while the overall clinical features and prevalence of TS generally remains consistent across race, culture, and geography, TS is 4 times more common in males than females (Freeman et al., 2000; Robertson et al., 2009; Staley et al., 1997).

Tics are clinically defined as sudden, rapid, and intermittent motor movements (motor tics) or vocalizations (vocal tics) that involve discrete muscle groups. These purposeless motor movements and vocalizations are often stereotyped and patterned, with stable intra-tic intervals between successive tics. Although individuals may have various types and patterns of tics over time (but usually stable for years), their repertoire of tics occur in a characteristically similar manner each time (APA, 2013; Jankovic, 1997; Leckman, 2002). Both motor and vocal tics can be further classified as either simple or complex. Simple motor tics involve only single muscle groups, producing brief, jerking movements or twitches (e.g., eye blinking, facial grimacing, head jerking, and shoulder shrugging), while complex motor tics consist of coordinated and sequenced movements of longer duration that resemble normal motor behaviors but are non-purposeful (e.g., head shaking, bending of body, touching, kicking, hitting, jumping, and

throwing). Furthermore, more specific forms of complex motor tics include imitating the gestures of others (echopraxia), repeating one's own gestures (palipraxia), and making lewd or obscene gestures (copropraxia). Simple vocal tics are also brief occurrences, involving single muscle groups such as the contraction of the diaphragm or muscles of the oropharynx to produce meaningless sounds (e.g., sniffing, throat clearing, grunting, squeaking, coughing, screaming, and blowing or sucking noises). On the other hand, complex vocal tics include linguistically meaningful utterances and verbalizations (e.g., syllables, words, and phrases usually in unusual speech patterns) that are still non-purposeful. As with motor tics, there are more specific forms of complex vocal tics that include repeating words or phrases of others (echolalia), repeating one's own words (palilalia), and shouting obscenities, profanities, or socially inappropriate words or phrases (coprolalia; Jankovic, 1997). A large majority of TS patients also report premonitory sensations or urges preceding motor and vocal tics. Previously characterized as sensory or internal tics, the premonitory sensations are distinct from the actual motor or vocal tics and are often described as localized discomforts, urges, tensions, or more generalized feelings of anxiety or anger that may be relieved following tics associated with the premonitory sensation (Kwak et al., 2003; Leckman et al., 1993).

Although the diagnostic criteria for TS includes the persistence of tics for at least one year, this is not an indication that individual tics are static and unchanging. In fact, the types and patterns, frequency, and severity of tics are often fluctuating through a patient's lifetime. Typically, motor tics manifest first in early childhood with the onset of vocal tics following months or years later. Tics often progress from simple to complex with age, although patients do present both simple and complex tics as part of their tic repertoire (Jankovic, 1997; Leckman et al., 1998). The severity of tics usually peaks at around 10-12 years of age and most typical cases of TS (about 75%) report a drastic reduction of tics by 18-20 years of age (Bruun, 1984; Erenberg et al., 1987; Leckman et al., 1998). However, there is a small percentage of patients

(approximately 5%) with severe or malignant forms of TS that persist or worsen into adulthood (Bloch and Leckman, 2009; Bloch et al., 2005; Jankovic et al., 2010).

Throughout the course of a day, tics can fluctuate greatly, waxing and waning in frequency, intensity, and severity, with varying tic-free intervals or periods of intensified tics. Furthermore the frequency and severity of tics can be affected by environmental or contextual factors. Stress, anxiety, and fatigue can often exacerbate tics while distraction, attention, and concentration on mental or physical tasks can temporarily suppress tics. Furthermore, there are some reports that there is a rebounding (buildup) effect in which momentary increases in the severity of tics occur immediately following temporary tic suppression (Conelea and Woods, 2008; Jankovic, 1997).

Although motor and vocal tics are the hallmark diagnostic features of TS, there are also a spectrum of related comorbid conditions which accompany tics and can sometimes overshadow the clinical picture of TS. Many neuropsychiatric conditions and behaviors are categorized as TS-associated comorbidities and include attention-deficit hyperactivity disorder (ADHD), obsessive-compulsive spectrum disorder (OCSD), impulse control disorders, self-injurious behaviors (SIBs), anxiety, depression, personality disorders, learning and social impairments (Kadesjö and Gillberg, 2000; Robertson, 2000). Among the various comorbidities that can manifest along with TS, OCSD, ADHD, and anxiety are the most common, occurring in 30-50% of reported cases of TS (Kadesjö and Gillberg, 2000; Khalifa and von Knorring, 2005; Robertson, 2000).

1.2 Genetics of Tourette Syndrome

One of the more contentious assertions made by Tourette in his published description of "*maladie de tics*" was that it was a hereditary disorder, despite the lack of evidence supporting such a claim (Kushner, 2009; Lajonchere et al., 1996). Although the genetic basis of TS has long since been well-established, the specific genetic factors and etiology of this phenotypically

complex disorder remains elusive. Early familial studies of TS reveal strong patterns and aggregation in families and estimate the risk of TS among first-degree relatives to be 10-15%, which is a 10- to 100-fold greater risk among first-degree relatives of individuals with TS compared to the general population (Paschou, 2013; Pauls, 2003; State, 2010). Despite the small and limited number of subjects and studies, data from twins provide the earliest and strongest evidence for the genetic basis of TS, with monozygotic twins showing 50-77% concordance (56% for TS and 77% for chronic motor tics) compared to 10-23% concordance for dizygotic twins (8% for TS and 23% for chronic motor tics; Hyde et al., 1995; Price et al., 1985). Segregation analyses of multi-generational TS family pedigrees, while benefiting from significantly larger sample sizes and studies, present widely inconsistent findings, ultimately supporting the genetic basis of TS but varying on the modes of inheritance. Earlier segregation analyses supported a single gene autosomal-dominant inheritance with incomplete penetrance but was eventually abandoned for the current model which characterizes TS a complex, multi-factorial heterogeneous genetic disorder (Pauls, 2003; Pauls and Leckman, 1986; Seuchter et al., 2000; State, 2010; Walkup et al., 1996).

To overcome the difficulties in modeling a complex genetic disorder, linkage and association studies, both genome-wide and targeting candidate genes and regions of chromosomal rearrangements, have been conducted to identify etiologically important loci and alleles that may contribute to TS susceptibility or risk. Although association and linkage studies to identify common variants in candidate genes, particularly those in the dopaminergic and serotonergic pathways believed to contribute to the neuropathology of TS, and in chromosomal regions implicated in TS (chromosomes 2, 3, 6, 14, 20, and 21) have been widely pursued, results have been inconsistent and poorly reproduced (Bloch et al., 2011; Paschou, 2013; State, 2010). More recently, the first genome-wide association study of TS was conducted to identify single nucleotide polymorphisms (SNPs) in a large cohort of 1285 cases and 4964 matched

controls of European ancestry, including two European-derived population isolates, Ashkenazi Jews from North America and Israel and French Canadians from Quebec, Canada. Although no loci reached genome-wide significance in this study, this study contributes to the systematic framework to identify and verify common variants associated with increased TS susceptibility and demonstrates the potential of increased sample sizes to provide insights into common variants of lower-penetrance as well as rare variants of complex genetic disorders (Scharf et al., 2013).

As the efforts to identify CNVs (copy number variants) expands from common variants (under the predominant “common variant, common disease” paradigm) to CNVs from rare variants with large effect sizes, several potentially relevant targets have emerged, some with no prior association with TS and others that may be implicated in TS through association with TS-related comorbidities such as OCD and ADHD (Bloch et al., 2011; Fernandez et al., 2012; Paschou, 2013; Sundaram et al., 2010). Among these rare variants, some that have generated interest and motivated further investigation because of strong associations with TS include genes for Slit and Trk-like 1 (SLITRK1), Contactin-associated protein-like 2 (CNTNAP2), L-histidine decarboxylase (HDC), and Neuroligin 4 (NLGN4), (Abelson et al., 2005; Ercan-Sencicek et al., 2010; Lawson-Yuen et al., 2008; Verkerk et al., 2003).

1.3 Basal Ganglia Circuitry and Neuropathology Implicated in Tourette Syndrome

The cortical-striatal-thalamo-cortical (CSTC) circuit consists of multiple parallel and overlapping sensorimotor, associative, and limbic circuits. The CSTC circuit processes and integrates information as it is directed from various cortical regions to the basal ganglia (BG) and then looped back to frontal cortical regions and brainstem nuclei to control motor and cognitive behaviors. The BG is further organized into a circuit consisting of interconnected subcortical nuclei including the striatum (subdivided into the putamen and caudate nuclei), the globus pallidus internal (GPi) and external (GPe) segments, the subthalamic nucleus (STN), the

substantia nigra pars compacta (SNc) and pars reticulata (SNr, Figure 1.1). The large majority (~95%) of the striatal neurons that process the excitatory glutamatergic inputs from the cortex are the medium-sized spiny neurons (MSNs) which are subdivided into two morphologically similar, but mosaically distributed subtypes: 1) the striatonigral (direct pathway) MSNs that project directly to the GPi and SNr and 2) the striatopallidal (indirect pathway) MSNs that project to the GPe, which indirectly modulates GPi and SNr via the STN. The classic model of BG circuitry (Figure 1.1) suggests that the two MSN subtypes provide antagonistic influences on BG output: activation of the direct pathway disinhibits the thalamus and activates the cortex, thus promoting desirable motor or cognitive behaviors, while activation of the indirect pathway can suppress the cortex by inhibiting thalamic output, thus inhibiting undesirable motor and cognitive behaviors (Albin et al., 1995; Alexander and Crutcher, 1990; DeLong, 1990; Mink, 1996). Furthermore, dopaminergic (DA) neurons from the SN differentially modulate these two MSN subtypes via dopamine D1-receptors (Drd1, stimulatory $G_{\alpha s}$-coupled) which are highly enriched on the striatonigral MSNs, and D2-receptors (Drd2, inhibitory $G_{\alpha i/o}$-coupled) which are highly enriched on the striatopallidal MSNs. D1-receptor activation will stimulate striatonigral MSNs and activate the direct pathway while D2-receptor activation will inhibit striatopallidal MSNs and suppress the indirect pathway; both of which promotes movement through synergistic activation of the thalamus and cortex by the BG (Gerfen et al., 1990).

In the context of the classic model of basal ganglia circuitry, it has long been suspected that the tic behaviors associated with TS are the consequence of dysfunctional BG output from an imbalance between the striatonigral direct pathway which facilitates wanted movements and the striatopallidal indirect pathway which inhibits the interfering unwanted movements (Albin et al., 1995; DeLong, 1990; Mink, 1996). Such a model allows for the possibility that tic behaviors are a result of an impaired indirect pathway, a dysfunctional direct pathway, or both: a reduction in the indirect pathway-mediated tonic inhibitory output from the BG which normally acts as a

"brake" on unwanted movements and behaviors (i.e., tics), a dysfunctional indirect pathway failing to selectively inhibit the unwanted tic behaviors which directly compete with volitional behaviors, or aberrant focal activation of the striatonigral MSNs that regulate the direct pathway, resulting in abnormal cortical excitability manifesting as tics (Albin et al., 1995; DeLong, 1990; Mink, 1996).

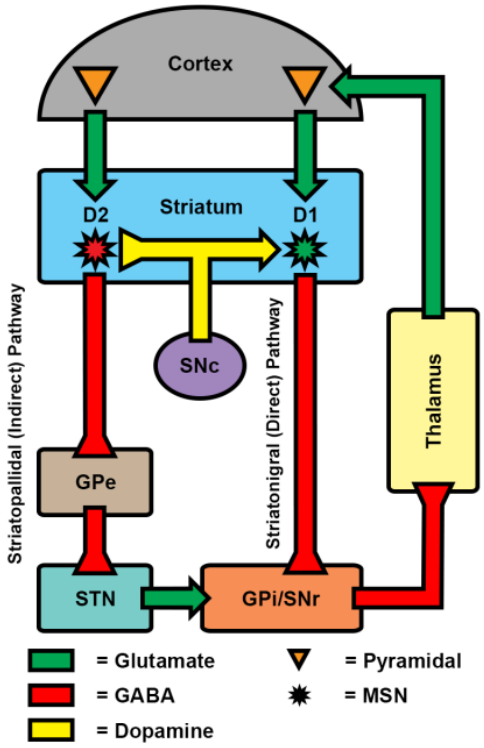

Figure 1.1 The classic basal ganglia circuitry. Glutamate from the cortex and dopamine from the substantia nigra pars compacta (SNc) modulate the activity of the medium spiny neurons (MSNs) in the striatum. MSNs are divided into two mosaically distributed subtypes: the D1-receptor enriched striatonigral and the D2-receptor enriched striatopallidal MSNs. The striatonigral D1-MSNs project to the globus pallidus interna (GPi) and the substantia nigra pars reticulata (SNr). The striatopallidal D2-MSNs project to the globus pallidus externa (GPe), which indirectly influence the SNr via the subthalamic nucleus (STN). The GPi and SNr are the output nuclei of the BG, sending inhibitory (GABA) outputs to the thalamus which in turn sends excitatory (glutamate) outputs to the cortex. Activation of the direct pathway disinhibits the thalamus, which activates the cortex, and promotes desirable motor or cognitive behaviors. Activation of the indirect pathway suppresses the cortex by inhibiting thalamic output, and inhibits unwanted motor and cognitive behaviors.

It isn't surprising that after 30 years of TS patient research, often guided under the conceptual framework of the classic basal ganglia circuitry model, converging evidence from pathological and imaging studies have reinforced the role of the BG as a critical component in the neurobiology of TS and tic disorders, in general (Felling and Singer, 2011; Ganos et al., 2013; Singer and Minzer, 2003). Volumetric MRI studies to image neuroanatomical changes in

TS patients report findings of reduced caudate or putamen (striatal) volumes in children and adult TS patients (Hyde et al., 1995; Peterson et al., 2003). Furthermore, longitudinal imaging studies suggest caudate volume in children with TS is inversely correlated to the severity of tics persisting into adulthood (Bloch et al., 2005). Stereological analysis of postmortem brains suggests a selective reduction of parvalbumin (PV) and cholinergic (ChAT) interneurons in the caudate and putamen which may also be indicative of a characteristic neuropathology in a subset of TS patients. PET and fMRI functional neuroimaging studies also correlate tic behaviors with BG activity and metabolism, often with decreased activity in the striatum and thalamus associated with tics and active tic suppression represented by increased BG activity (Braun et al., 1993; Eidelberg et al., 1997; Peterson et al., 1998; Pourfar et al., 2011; Stern et al., 2000).

Although numerous neurotransmitters, including dopamine, glutamate, GABA, serotonin, acetylcholine, and norepinephrine, are important to the proper function of the BG circuit, dopamine and its effect on striatal MSNs has long been the focus of the neurochemical component of TS pathophysiology. A small number of studies looking at dopamine receptor binding with functional imaging suggest increased dopaminergic input to the striatum along with increased, widespread dopamine release (Albin et al., 2003; Liu et al., 2010; Steeves et al., 2010; Wong et al., 2008). Additionally, the contribution of BG dopamine dysfunction in the pathophysiology of TS is supported by the efficacy of neuroleptics, primarily through suppression of D2-MSN activity in the striatum, in reducing tics (Robertson, 2000; Shapiro et al., 1989).

1.4 Animal Models of Tic-Like, Stereotypic, and OCD-Like Behaviors

Despite over 30 years of data from numerous TS patient studies, inconsistent and sometimes conflicting results have yielded ambiguous implications of BG involvement in TS. Instead, much of our more detailed understanding of the neurobiology of tics and stereotypy

(repetitive, rigidly patterned behaviors) common to TS, chronic tic disorders, OCD, and autism spectrum disorders (ASDs), have come from anatomical, physiological, pharmacological, and genetic studies of animal models (Felling and Singer, 2011; Macrì et al., 2013; Yang and Lu, 2011). Studies in non-human primates revealed that selective pharmacological disruption of GABA signaling to focally remove striatal inhibition induces stereotypy and tic behaviors (McCairn et al., 2009; Worbe et al., 2009). Similarly, a series of studies conducted in both primate (Saka et al., 2004) and rodent models (Berridge and Aldridge, 2000; Canales and Graybiel, 2000; Graybiel et al., 2000) also showed that pharmacologic activation of dopaminergic signaling in the striatum (amphetamines, cocaine, L-dopa, specific D1- and D2-receptor agonists) can lead to aberrant BG signaling and induce stereotypy and tic behaviors.

Allowing for more precise and sophisticated manipulation of dopaminergic signaling, genetic models not only complement the pharmacological models of tics and stereotypies, but also allow for detailed dissociation of D1- and D2-MSN activity (and their corresponding pathways) in BG-mediated normal and dysfunctional behaviors. Genetic knockdown of the dopamine transporter gene (DAT), a membrane transporter which clears DA out of the synapses and recycles it back into vesicles, results in a hyper-dopaminergic mutant mouse. The DAT-knockout mice are hyperactive and display increased behavioral stereotypy (excessive repetition of portions of the normal grooming pattern) consistent with OCD-like behaviors that are often comorbid with TS, though they lack the characteristic tic-like behaviors of TS (Berridge et al., 2005; Zhuang et al., 2001). In contrast, mutant mice that are selectively dopamine-deficient (genetic inactivation of tyrosine hydroxylase in only dopaminergic neurons) are hypoactive and show significant impairments in normal stereotyped activities, such as grooming (Zhou and Palmiter, 1995). However, selective activation of striatal D1-receptors restore stereotypy in these DA-deficient mice (Chartoff et al., 2001).

The apparent implication that striatal D1-receptors may be particularly important in the BG-mediated regulation of patterned behaviors (whether stereotypies or tics) was further demonstrated in behavioral studies of selective D1-receptor knockout mice, which display defective stereotypic grooming patterns (Cromwell et al., 1998). Additionally, in transgenic mice expressing a neuro-potentiating protein (the cholera toxin A1 subunit which activates $G_{\alpha s}$ and cAMP synthesis) in only D1-receptor expressing cortical pyramidal (but not striatal) neurons (D1CT-7 transgenic mice), increased cortical activity and glutamatergic excitation of cortically-driven striatal circuits results in hyperactivity and tic-like and OCD-like behaviors (Campbell et al., 1999; Nordstrom and Burton, 2002). Although most of these models emphasize the critical role of D1-receptors (and by extension, the D1-MSNs and striatonigral direct pathway) in modulating patterned behavior, studies of a D2-receptor knockout mouse show that while the D2-receptor signaling may not be necessary for expression of stereotyped behaviors, D2-receptor signaling can significantly attenuate D1-agonsim induced stereotypy, suggesting a synergistic role of both D1- and D2-receptor signaling in BG behavioral control (Glickstein and Schmauss, 2004).

The aforementioned pharmacological and genetic models all share the common connection of being firmly rooted in the classic model of BG circuitry and well-accepted interpretations from TS patient studies. However, there are other novel genetic models of aberrant stereotypic and OCD-like motor behaviors that have advanced our understanding of the neurobiology of tic disorders outside the simplified context of striatal dopaminergic signaling. Sapap3 (SAP90/PSD95-associated protein 3) a is highly striatal enriched postsynaptic density (PSD) protein that interacts with other postsynaptic scaffolding proteins such as PSD95 and is known to anchor or traffic NMDA and AMPA receptors at excitatory synapses. The knockout mouse model of Sapap3 exhibits increased anxiety and OCD-like excessive grooming behaviors which leads to the loss of facial hair and skin lesions; all of which have been shown to

be alleviated by chronic treatment with fluoxetine (an SSRI used to treat OCD) as well as lentiviral-mediated rescue of Sapap3 in the striatum. The deficits in excitatory cortical-striatal synapses reported in the Sapap3 knockout mice provide important insights into the role of abnormal cortical-striatal circuits in the control of patterned behaviors (Welch et al., 2007).

Slitrks are a family of transmembrane proteins similar to the axon guidance molecule, Slit and the neurotrophin factor, Trk. Although the function of Slitrk proteins (Slitrk1-Slitrk6) is not well understood (although it is thought they regulate neurite outgrowth during development), association of rare SLITRK1 sequence variants with TS (Abelson et al., 2005) have implicated Slitrk genes in TS as well as in associated disorders, such as OCD. A mouse model of Slitrk5 (SLIT and NTRK-like protein-5) deletion has been shown to exhibit excessive grooming associated with facial hair loss and skin lesions and increased anxiety-like behaviors. As with the Sapap3 knockout model, chronic fluoxetine treatment also alleviates the OCD-like excessive grooming in the Slitrk5 knockout mice. The Slitrk5 knockout model shares TS-like pathologies, including striatal volume loss, abnormal striatal MSN morphology, and diminished cortical-striatal excitatory neurotransmission. Although pathophysiological insights from Slitrk5 knockout mice are somewhat limited due to our inadequate understanding of the developmental and functional role of Slitrks, they may provide clues into the developmental course of TS and OCD neuropathology (Shmelkov et al., 2010).

Compared to the previously presented mouse models, the Hoxb8 knockout mouse presents a somewhat unusual model of abnormal grooming behavior that is derived from a hematopoietic lineage and associated with microglia. Hoxb8 knockout mice exhibit an excessive grooming phenotype (as well as excessive social grooming of cagemates), that leads to hair loss and self-inflicted lesions. Hoxb8 is a member of the Homeobox (Hox) family of transcription factors that is broadly expressed throughout both the body and CNS in early development (guidance of the anterior-posterior axis) and maintained through adulthood. To understand how

Hoxb8 regulates OCD-like grooming behavior, it was critical to elucidate its specific CNS cell-type expression and developmental function. Experiments to trace the Hoxb8 cell lineage revealed that the cells in the adult CNS that express Hoxb8 are microglia which originate from the yolk sac during early development and from hematopoietic cells in bone marrow postnatally. Surprisingly, bone marrow transplants from normal mice into Hoxb8 knockout mice rescues the excessive grooming, hair removal, and skin lesion deficits. Conversely, bone marrow transplants from the knockout mice into normal mice causes abnormal grooming in a subset of recipients. Additional genetic experiments to selectively delete Hoxb8 in the hematopoietic lineage also results in Hoxb8 conditional knockout mice with the excessive grooming phenotype. Taken together, these sets of studies revealed that Hoxb8 expression in bone marrow derived microglia may be causal to the pathological grooming phenotype in the knockout mice and may present important insights into the developmental pathophysiology of TS and OCD that may originate outside of our traditional views of the classic BG circuitry model (Chen et al., 2010; Greer and Capecchi, 2002). Many of the pharmacological and genetic models presented have shed significant insights into BG circuitry and provided an experimental context in which to study the neurobiology of TS and OCD-like behaviors. However, each model presents only a limited view of the pathology and developmental mechanisms of these disorders and brings to focus the need for a truly comprehensive model of TS and related tic disorders.

1.5 Zinc Finger Protein 521 (Zfp521) is a Striatonigral MSN-Enriched Gene Potentially Involved in Striatal Development

Thorough understanding of the BG circuitry in both normal and pathological behaviors requires elucidation of the molecular mechanisms which regulate the developmental and functional properties of the principal BG component cell-types; specifically, the striatal MSNs. Other than their projections though the direct or indirect pathways of the BG, the striatonigral (D1-) and striatopallidal (D2-) MSNs are morphologically identical and mosaically distributed

throughout the striatum, making it especially problematic to isolate these two cell-types in order to define their distinct developmental, functional, and molecular properties. To address this challenge, our laboratory developed the FACS-array methodology to perform gene expression profiling (microarray) of the striatonigral and striatopallidal MSN subtypes using fluorescent activated cell sorting (FACS) to isolate populations of genetically-labeled MSN-subtypes from bacterial artificial chromosome (BAC)-transgenic fluorescent reporter mouse brains (Lobo et al., 2006). The FACS-array method identified dozens of novel genes, and verified several previously known genes, that are differentially enriched in the two MSN subtypes. Subsequently, a critical subset of these striatonigral and striatopallidal differentially enriched genes was independently validated by a study which used BAC-transgenic mice expressing a fluorescence-tagged ribosomal protein in defined cell populations to purify and perform gene expression profiling of ribosome-associated transcripts (BAC-TRAP methodology; Doyle et al., 2008; Heiman et al., 2008). Among the group of striatonigral MSN-enriched genes that was validated by both FACS-array and BAC-TRAP, zinc finger protein 521 (Zfp521, also known as the ecotropic viral insertion site, or Evi3) is of particular interest because along with its interacting transcriptional partner (another striatonigral MSN-enriched gene), early B-cell factor 1 (Ebf1), Zfp521 may be involved in the transcriptional machinery regulating the differentiation of MSN subtypes, striatal development, and/or BG circuitry formation (Garel et al., 1999; Lobo et al., 2006, 2008).

Zfp521 is a zinc finger transcription factor and is one of only two mammalian proteins, the other being its paralog, Zfp423 or OAZ/EBFAZ, with 30 Kruppel-like zinc fingers (ZFs) that are highly conserved and mediate multiple protein-protein interactions (Bond et al., 2004; Warming et al., 2003). Zfp521 was initially identified as a common retroviral integration site in murine AKXD B-cell lymphomas and its functional mechanism was believed to involve its transcriptional repression of Ebf1 by physical interaction at the C-terminal ZFs, similar to the

transcriptional interaction between Zfp423 and Ebf1 (Bond et al., 2004; Hentges et al., 2005; Warming et al., 2003). However, the numerous studies which ensued revealed that Zfp521 regulates multiple developmental and cellular processes in a diverse range of cell-types and tissues, much of which is reflected in the multiple protein binding and transcriptional interaction domains of the zinc fingers that make up Zfp521 (Figure 1.2).

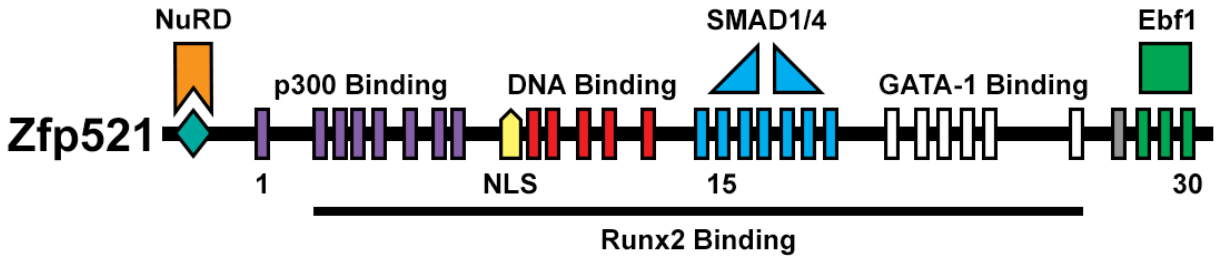

Figure 1.2 Structure and functional interaction domains of Zfp521. Thirty Kruppel-like zinc fingers (ZF) are distributed throughout Zfp521 in clusters (ZF1-30). A Nuclear Remodeling and Histone Deacetylation (NuRD) complex motif involved in transcriptional repression (via interaction with HDACs) is located at the N-terminus and a putative nuclear localization signal (NLS) lies between ZF8 and ZF9. ZF1-8 associate with p300 (a transcriptional co-activator), ZF14-20 are involved in TGFβ/BMP signaling through interaction with SMAD1 and 4 (transcriptional co-factors), ZF21-26 bind to GATA-1 (erythroid transcription factor) to regulate the differentiation of erythroid cells from hematopoietic progenitors, and ZF2-26 bind and attenuate the activity of Runx2 to promote cell differentiation. The C-terminal ZFs mediate the physical interaction of Zfp521 and its critical transcriptional partner, Ebf1.

In the N-terminus of Zfp521, upstream of the first ZF, is a 12 amino-acid motif called the nuclear remodeling and histone deacetylation (NuRD) complex which binds to histone deacetylases (HDACs) and functions in global transcriptional repression. Transcriptional repression through the NuRD motif of Zfp521 is critical in its function in regulating the differentiation of erythroid cells from hematopoietic progenitors. Zfp521 binds GATA-1 (erythroid transcription factor) via ZF21-26 and at the same time, recruits HDAC (and other members of the NuRD complex) at the NuRD domain which in turn inhibits GATA-1 and represses the differentiation of erythroid cells (Bond et al., 2008; Matsubara et al., 2009). As with its paralog, Zfp423, the transcriptional activity of Zfp521 in the hematopoietic system is also regulated by interactions with activated SMAD1 and SMAD4 (ZF14-20) to enhance the transcription activity of BMP2/4 responsive elements (BRE) to mediate TGFβ/BMP signaling and transcription (Bond et al., 2004; Hata et al., 2000).

Similar to the role of Zfp521 in regulating the differentiation of hematopoietic cells, several studies by Baron and colleagues also demonstrate the regulatory role of Zfp521 in various aspects of bone development. Zfp521 and HDACs forms a complex (though not necessarily at the NuRD motif) to bind and attenuate the activity of Runx2 (at ZF2-26), which promotes the differentiation of osteoblasts from mesenchymal precursors as well as regulate the proliferation and differentiation of growth plate chondroyctes in bone growth by parathyroid hormone-related peptide (PTHrP) signaling (Correa et al., 2010; Hesse et al., 2010; Wu et al., 2009). Furthermore, it was reported that both Zfp521 and Zfp423 promote the differentiation of preadipose fibroblasts to committed preadipoctyes through amplification of the TGFβ/BMP signaling pathway at the SMAD interaction domains (Gupta et al., 2010; Kang et al., 2012). In all the Zfp521-mediated transcriptional programs described above, Ebf1 remains a critical transcriptional co-regulator that functions independently, but in a coordinated manner with the other binding partners of Zfp521 to properly regulate proliferation and differentiation (Kang et al., 2012; Kiviranta et al., 2013; Nechanitzky et al., 2013).

Although the investigations of Zfp521 in regulating the determination of mesenchymal, hematopoietic, and preadipose cell fates provide important insights into the transcriptional function, partners, and signaling pathways of Zfp521, its *in vivo* role in the CNS remains obscure. The first indication about the neural function of Zfp521 comes from its expression pattern in the brain. While Zfp521 is expressed broadly throughout various cells and tissues in the body, its expression in the CNS is highly enriched the striatum and levels of expression varies with development. Combined with findings from cell-specific gene expression studies that show Zfp521 is highly enriched in striatonigral MSNs (Heiman et al., 2008; Lobo et al., 2006), it suggests Zfp521 may have a restricted, cell-type or region-specific function in neurodevelopment. As a caveat, it should also be noted that Zfp521 is also consistently expressed in the cerebellum and septum from early embryonic stages and persists through

adulthood. Zfp521 expression begins as early as E7 and shows strong, widespread striatal expression at later embryonic stages (E15.5) and up through the end of postnatal development (P14). However, after postnatal development, Zfp521 expression is significantly reduced and restricted to just the lateral striatum, lateral septum, and cerebellum in the adult mouse (Allen Institute for Brain Science, 2012; Kamiya et al., 2011).

Currently, much of our limited understanding of the role of Zfp521 in the brain is derived from studies of Zfp423 and Ebf1 in a neural context. Studies of mice with mutated or knocked out Zfp423 reveals its critical role in cerebellar development. Loss of Zfp423 reduces proliferation of granule cell precursors and creates deficits in Purkinje cell differentiation, resulting in severely ataxic mice with significantly reduced and underdeveloped cerebellums (Alcaraz et al., 2006; Cheng et al., 2007; Warming et al., 2006). Furthermore, a large-scale RNA interference-based screen of genes involved in retinoic-acid (RA) signaling identifies Zfp423 as a transcriptional regulator of RA-induced differentiation of several cell types, including neuroblastomas (Huang et al., 2009). This study adds another important signaling pathway through which Zfp423 (and by extension, Zfp521) may exert transcriptional regulation of cell differentiation in both the body and brain. Findings from Zfp423 studies are further added upon by investigation of its (and Zfp521's) closely co-regulated partner, Ebf1. Studies from our laboratory and others show that not only is Ebf1 important in down-regulating genes to drive postmitotic cells from the subventricular zone (SVZ) to differentiate into striatal neurons in the mantle (Garel et al., 1999), but deficits in Ebf1 it may specifically affect the postmitotic differentiation of striatonigral MSNs (Lobo et al., 2006, 2008).

In addition to regulating the proliferation and differentiation of neurons, both Zfp423 and Ebf1 have been shown to be involved in guiding the axonal projections of these neurons in various neural circuits. In early neural development, the loss of Zfp423 results in the mistargeting of axonal projections from dorsal telencephalic commissural neurons, which fail to

properly cross the midline to project to their intended targets (Cheng et al., 2007). Similarly, Zfp423 is also involved in olfactory neurogenesis in which Zfp423 deletion impairs the differentiation of olfactory-receptor neurons (ORN) and disrupts the pattern of ORN axonal projections to the olfactory bulb (Cheng and Reed, 2007). Studies show that while thalamocortical projections are present in a Ebf1 knockout mouse, the organization and topography of the connections between the thalamus and cortex is disrupted. Interestingly, the misrouting of the projections seems to first occur in the BG and suggests Ebf1 may mediate the function of the BG as regulatory point of axonal pathfinding for thalamocortical projections (Garel et al., 2002). Our own studies of an Ebf1 knockout also reveal that deletion of Ebf1 specifically disrupts the axonal projection pattern of striatonigral MSNs through the direct pathway of the BG, implicating the importance of Ebf1 and its partner zinc finger transcription factors, Zfp423 and Zfp521, in developmental axonal guidance within the BG circuitry (Lobo et al., 2006, 2008).

The first study to investigate the direct role of Zfp521 in neural development and function reveals that Zfp521 is required very early on in neural development and is both necessary and sufficient to induce neural differentiation of embryonic stem (ES) cells in culture (Kamiya et al., 2011). In addition to its critical role in the transition of epiblast to neuroectoderm, examination of the expression patterns of Zfp521 throughout early development of the mouse embryo (E3.5 to 9.5) also suggest it may contribute to the developmental regulation of the rostral neural tube following gastrulation. Zfp521 works downstream of BMP4 (a neural differentiation inhibitor) and once BMP inhibition is removed, Zfp521 directly activates early neural genes (Sox1, Sox3, Ncad, and Pax6) with a transcriptional co-activator, p300 (which associates with N-terminal ZF1-8), to drive the early neural differentiation of ES cells into a neuroectodermal lineage (Kamiya et al., 2011). More recently, in vitro studies of medullablastoma cells show that lentiviral

overexpression of Zfp521 induces the proliferation, growth, and migratory abilities of these cells, all of which require the NuRD domain of Zfp521 (Spina et al., 2013).

The findings from studies of Zfp521, Zfp423, and Ebf1 reveal characteristic transcriptional and regulatory functions that are common among these transcription factors, regardless of whether it is in development of the immune system, blood, bone, fat, or brain. Zfp521 has been shown, or indirectly implicated, to be involved in the developing brain, from early embryonic to late postnatal stages, specifically regulating proliferation, differentiation, and axonal guidance. Given the enrichment of Zfp521 specifically in striatonigral MSNs, what remains to be answered is whether Zfp521 is critical to BG circuitry development, BG function in behavioral control, and whether disruption of Zfp521-mediated cellular processes can result in neurodevelopmental disorders.

1.6 Summary

Tourette Syndrome is clinically defined as a juvenile-onset neuropsychiatric disorder characterized by multiple motor and vocal tics that is often associated with various comorbidities, including OCD, ADHD, self-injurious behaviors, anxiety, depression, and social impairments. What was once considered a rare condition is now understood to be a relatively common, but genetically complex disorder with a spectrum of behavioral and pathological manifestations that are at the intersection of various neurodevelopmental behavioral disorders. Extensive genetic, neuroimaging, and pharmacological studies have provided significant, but limited insights, implicating the BG as the pathological circuit that is the basis of the tic behaviors and interconnects the myriad of comorbidities associated with TS. To advance beyond our current understanding of the neurobiology of TS, genetic animal models provide a powerful tool to elucidate and manipulate the specific genetic factors, cellular processes, and signaling in the neural circuits of this phenotypically complex disorder.

Although several principles can be used to evaluate the validity of an animal model, a commonly accepted approach is based on three criteria: 1) face validity, which is the phenomenological similarity between the model and clinical features, 2) predictive validity, which is the determination of the response and efficacy of therapeutics used to treat the clinical conditions, and 3) construct validity, which is the consistency of the theoretical rationale or similarity of the underlying etiology between the model and the known pathophysiology of the disorder (Willner, 1984, 1986). While many of the previously discussed pharmacological and genetic models of stereotypic and tic-like behaviors present some TS-like clinical features and fulfill a few aspects of the validation criteria, each model fundamentally falls short of being considered a proper model of TS.

The studies presented in this dissertation will characterize a brain-specific conditional knockout mouse model of the striatonigral-enriched transcription factor, Zfp521, and present it as the first truly comprehensive mouse model of TS. Chapter 2 will address the face and predictive validity of this mouse model by examining the TS-like behavioral phenotypes, neuropathologies, and response to therapeutics commonly used to treat TS patients. The neural developmental studies of this mouse model will be described in Chapter 3. Construct validity will be discussed in Chapter 4, in the context of the pathogenic BG circuitry deficits in this mouse model of TS. In Chapter 5, we will examine the BG signaling involved in the suppression of the behavioral phenotype and discuss the significance of this mouse model in advancing TS research and its relevance to future TS-related therapeutics and drug discovery.

Chapter 2

Phenotypic Assessment of Tourette Syndrome-Like Behaviors and Neuropathologies in Zfp521-BrKO, a Brain-Specific Conditional Knockout Mouse Model of Zfp521

2.1 Introduction

Tourette Syndrome is a neurodevelopmental disorder characterized by the chronic presence of fluctuating motor and vocal tics that interferes with the daily lives of patients. With wide ranging severity, at best, TS can be a minor inconvenience and at worst, it can be completely debilitating. Both phenotypically diverse, with a spectrum of clinical comorbidities that overlap with other neuropsychiatric disorders (i.e., OCD and autism), and genetically complex, a critical challenge to advance TS research is to develop an animal model that accurately recapitulates the clinical phenomenology and offers insights into the underlying biology of TS. While many of the animal models described in the previous chapter added to our current understanding of the neurobiology of stereotyped and tic behaviors, none can be convincingly described as a model of TS.

The pharmacological models of dopaminergic-signaling may have strong construct validity based on functional imaging studies of BG dysfunction in TS patients, but the face validity of these models is very limited, often exhibiting only a single stereotyped behavior (pathological grooming) that only represents a small subset of the clinically defined tic behaviors and no developmental onset (Felling and Singer, 2011; Macrì et al., 2013). Similarly, genetic models such as Sapap3 and Slitrk5 knockout mice may also show construct validity (cortical-striatal signaling deficits from striatal MSN deficits), but are limited in their aspects of face validity (pathological grooming and TS-comorbid conditions such as facial hair loss and skin lesions similar to SIBs and anxiety). Furthermore, the pathological grooming for the Sapap3 and Slitrk5 knockout mice does not show juvenile-onset, and generally starts at 3 months and 4 to 6

months, respectively. The stereotypic, excessive grooming phenotypes of these models are more OCD-like rather than TS-like, as they show predictive validity only in response to pharmacological treatments for OCD, such as Fluoxetine (Shmelkov et al., 2010; Welch et al., 2007). The Hoxb8 knockout mouse model also exhibits hair loss and skin lesions due to pathological grooming, but the behavioral phenotype is not juvenile-onset and is confounded by the fact that this mouse model also engages in excessive social grooming of cage mates. Although the Hoxb8 knockout mouse model is limited as a model of TS, it is an interesting model of stereotypy with OCD-like features in that its excessive grooming phenotype is believed to originate from microglia derived from a hematopoietic origin and offers an alternate perspective of TS etiology outside the traditional BG-circuitry mechanisms (Chen et al., 2010; Greer and Capecchi, 2002).

Among the published animal models of pathological stereotyped and tic-like behaviors, the D1CT-7 transgenic mice have thus far presented the closest model of TS, with juvenile-onset of tic-like behaviors (rapid head and/or body shakes), excessive jumping, pathological grooming leading to hair loss and skin lesions, and response to TS-targeted pharmacological intervention (Clonidine, an α_2 adrenergic agonist). However, although a D1-receptor promoter is used to drive the expression of the neuropotentiating cholera toxin (CT) protein to create this "circuit-test" model of TS and OCD behaviors, CT expression (and excitatory activation) is limited to D1-expressing neurons in the piriform cortex, somatosensory cortex, and the intercalated nucleus of the amygdale (Nordstrom and Burton, 2002). With no expression in the striatum, no evidence of aberrant BG circuitry function, and no developmental pathophysiology, the D1CT-7 mouse model implicates a non- striatal effect on the pathological behaviors and is severely limited in its construct validity in the context of the BG deficits and dysfunctions reported in TS patients. Thus, despite various conceptual approaches and diverse animal

models, the need for a genetic tool to elucidate the complex etiology and genetics of TS still remains unfulfilled.

The brain-specific conditional knockout mouse model of the striatonigral MSN-enriched transcription factor, Zfp521 (Zfp521-BrKO mice), that was developed in our laboratory addresses this critical need for a comprehensive animal model of TS. The Zfp521-BrKO mouse model that is the central focus of this dissertation recapitulates multiple aspects of TS to a degree as yet unseen in previous mouse models of pathological stereotyped and tic-like behaviors, including: individually-distinct patterns of numerous diverse and robust juvenile-onset tic-like behaviors, several comorbid conditions, response to TS pharmacology, critical BG neuropathologies, and novel BG-circuit signaling deficits. In this chapter, we will briefly discuss the generation of Zfp521-BrKO mice and then report the detailed characterization of the TS-relevant behavioral phenotypes and neuropathologies of this mouse model.

2.2 Generation of a CNS-Specific Zfp521 Conditional Knockout Mouse

The transcription factor Zfp521 was first identified as among the top striatonigral MSN-enriched genes from our laboratory's FACS-array study to identify the novel genes that are differentially expressed in the morphologically identical striatonigral and striatopallidal MSNs that make up the striatum (Lobo et al., 2006). Furthermore, Zfp521 was later independently verified as a striatonigral MSN-enriched gene in a study using the BAC-TRAP methodology (Doyle et al., 2008; Heiman et al., 2008). In the FACS-array study, it was also demonstrated that Ebf1, a physically-interacting partner of Zfp521, regulates the postmitotic differentiation of striatonigral MSNs. In light of Ebf1's role in striatal development and its close transcriptional interaction with Zfp521, which had not been previously implicated in any striatal development or function, our laboratory obtained a previously unpublished Zfp521 conditional knockout mouse from our collaborators, Drs. Soren Warming and Neal Copeland (both at the National Cancer Institute at the time), to further examine the developmental or functional role Zfp521 in

striatonigral MSNs. In the time we have been conducting our *in vivo* studies of Zfp521, the bone-specific model of this conditional knockout mouse and the role of Zfp521 in the differentiation of precursors from a mesenchymal lineage has been extensively characterized and published (Correa et al., 2010; Hesse et al., 2010; Kiviranta et al., 2013; Wu et al., 2009). However, the CNS role of Zfp521 and its potential contribution to TS pathophysiology remains unexplored.

The mice we initially received had Zfp521 conditional alleles ($Zfp521^{2loxP}$) in which exon 4 (the largest exon) was flanked by two loxP sites (this mouse was termed, $Zfp521^{flox/flox}$). Homologous recombination at the two loxP sites mediated by Cre-recombinase excises exon 4 and results in the null or knockout allele, $Zfp521^{1loxP}$ (Figure 2.1A). In the early stages of this study, a full-body Zfp521-null mouse was generated after a series of crosses involving $Zfp521^{flox/flox}$ with a β-actin-Cre mouse line. However, these Zfp521-null mice required continuous supportive care (wet food and hydrogel on cage floor and saline injections, as needed, and weaning after 28 days instead of 21 days) to survive to 4 weeks, with very few surviving to 8 weeks (less than 5%).

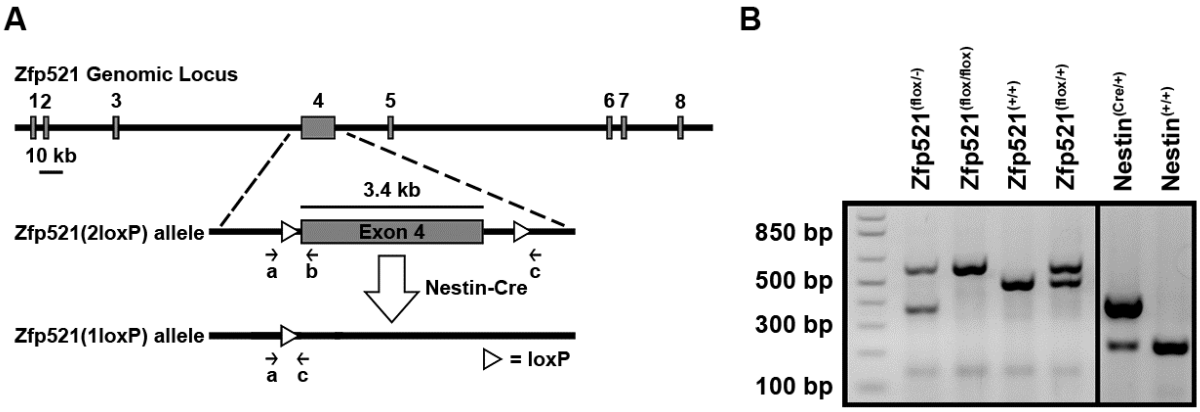

Figure 2.1 Generation and genotyping of Zfp521 conditional and knockout alleles. (A) Schematic representation of the Zfp521 genomic locus (not drawn to scale). The conditional allele, Zfp521(2loxP), has two loxP sites flanking exon 4, which is excised by Cre-mediated recombination at the loxP sites resulting the in the knockout allele, Zfp521(1loxP). To restrict Zfp521 deletion to a neuronal cell population (CNS-specific deletion), Cre-recombinase expression is driven by the Nestin promoter. Positions of the PCR genotyping primers are indicated by arrows (lowercase letters) . (B) Genotyping PCR of genomic DNA to determine Zfp521 alleles and Nestin-Cre. The genotypes are indicated above each lane and the basepairs are indicated to the left of the DNA ladder. The PCR amplicon of the conditional Zfp521 allele (>500 bp; "flox") includes a loxP site and is larger than the wild-type Zfp521 allele (~500 bp, no loxP site; "+"). Under the genotyping PCR conditions, the Zfp521 knockout amplicon (~350 bp; "-") can only be generated when exon 4 is excised. Nestin-Cre genotyping primers identify the Nestin-Cre (~350 bp) and wild-type Nestin (~200 bp) alleles.

To increase the long-term survival of these mice and to focus our study on a CNS-specific deletion of Zfp521, the genetic and breeding strategy was revised and Zfp521$^{flox/flox}$ mice were crossed with a Nestin-Cre line (Tronche et al., 1999) to eventually generate the brain-specific conditional knockout of Zfp521, termed Zfp521-BrKO (Figure 2.1A). Nestin is an intermediate filament (IF) protein expressed at early embryonic stages in proliferating and migrating neural stem cells, sometime before neural tube formation (Dahlstrand et al., 1995). Deleting the conditional Zfp521allele with the Nestin-driven Cre insured early, efficient, and specific CNS deletion of Zfp521. Mouse genotypes were determined by polymerase chain reaction (PCR) to identify the specific Zfp521 allele (wild-type allele, conditional allele, or knockout allele) and the presence of Nestin-Cre. The Zfp521 allele was identified with: 1) 5' primer in the intron upstream of the 5' loxP site, 2) 3' primer in the 5' region of exon 4, and 3) 3' primer in the intron downstream of the second 3' loxP site after exon 4. Nestin-Cre was genotyped with: 1) 5' Nestin primer, 2) 3' Nestin primer, and 3) 3' Cre primer to genotype both the wild-type Nestin allele and the transgenic Nestin-Cre allele (Figure 2.1A-B). To create Zfp521-BrKO mice, Zfp521$^{flox/flox}$ mice were first crossed with a Nestin-Cre line and the resulting Zfp521$^{flox/+}$; Nestin-Cre double transgenic mice were crossed with Zfp521$^{flox/flox}$ mice to generate Zfp521$^{flox/flox}$; Nestin-Cre (Zfp521-BrKO), Zfp521$^{flox/flox}$ and Zfp521$^{flox/+}$ (control), and Zfp521$^{flox/+}$; Nestin-Cre (Zfp521-Het) mice (Figure 2.2).

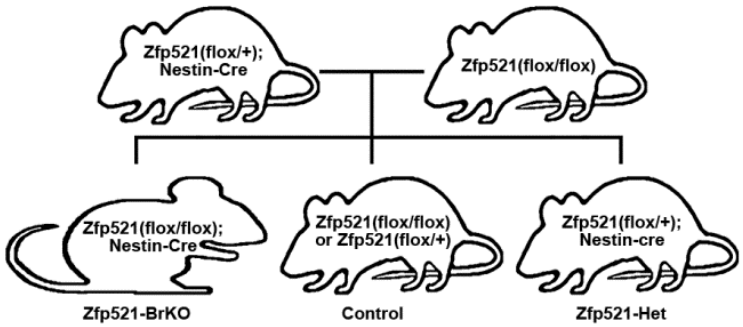

Figure 2.2 Breeding strategy to generate Zfp521-BrKO mice. The first generation of crosses were of Zfp521$^{flox/flox}$ mice with a Nestin-Cre line to generate Zfp521$^{flox/+}$; Nestin-Cre double transgenic mice. These Zfp521-Het mice were crossed with Zfp521$^{flox/flox}$ mice to generate Zfp521-BrKO and control (Zfp521$^{flox/flox}$ and Zfp521$^{flox/+}$) mice for behavioral, pharmacological, and pathological studies and Zfp521-Het mice for additional breeding.

As shown in the *in situ* hybridizations of Zfp521 expression at 2 months of age, the expected Zfp521 mRNA expression in the lateral striatum and septum in control brains was significantly reduced in Zfp521-BrKO brains (Figure 2.3A). Furthermore, relative quantification of Zfp521 genomic DNA (targeting the deleted exon 4) by quantitative PCR (qPCR) assays showed conditional deletion of Zfp521 in the brain (striatum, cortex, and cerebellum) but not the body in Zfp521-BrKO mice (Figure 2.3B)

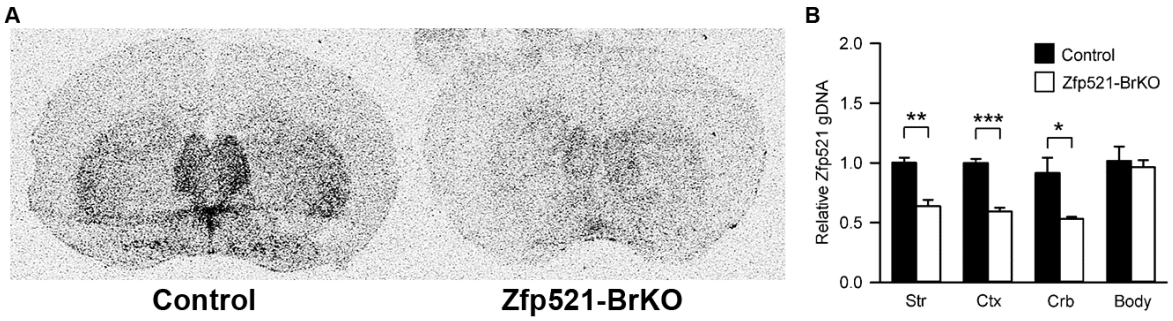

Figure 2.3 Brain-specific reduction of Zfp521 expression in Zfp521-BrKO mice. (A) *In situ* hybridization of Zfp521 (with a RNA probe against the floxed exon 4) revealed expression in the lateral striatum and septum in 2 month-old control mice which was significantly reduced in Zfp521-BrKO mice. (B) SYBR Green qPCR of Zfp521 genomic DNA (gDNA) with primers targeting the deleted exon 4 showed conditional deletion of Zfp521 in the striatum (str), cortex (ctx), and cerebellum (crb), but not in the body (Control, n = 3; Zfp521-BrKO, n = 3; Student's t-test; Str, $p = 0.00264$; Ctx, $p < 0.001$; Crb, $p = 0.0249$; Body, $p = 0.696$). Values are mean± SEM (* $p \leq 0.05$; ** $p \leq 0.01$; *** $p \leq 0.001$).

All genotypes were born at the expected Mendelian ratios and unlike Zfp521-null mice, Zfp521-BrKO could generally live up to at least 6 months without supportive care and under the same conditions as littermate control and Zfp521-Het mice (although we are often required by DLAM to euthanize Zfp521-BrKO at around 3-4 months due to complications from phenotype-related lesions). Although Zfp521-BrKO were comparable in size to control at birth, a marked reduction in growth and body weight became apparent by P20 and at 2 months, both male and female Zfp521-BrKO mice were significantly smaller compared to control (Student's t-test; $p < 0.001$ for both male and female; Figure 2.4A). Corresponding to the reduced body weight, both male and female Zfp521-BrKO mice also showed a significant reduction in both forebrain (Student's t-test; $p = 0.00458$ for male and $p = 0.00043$ for female) and cerebellum (Student's t-test; $p = 0.004$ for male and $p = 0.00938$ for female) weights compared to control mice at 2

months of age (Figure 2.4B-C). However, unlike the underdeveloped cerebellum reported in the knockout mouse model of the Zfp423 (the paralog of Zfp521; Cheng et al., 2007; Warming et al., 2006), a comparison of the relative weight between the cerebellum and forebrain did not show a significant difference between genotypes and suggested a global reduction of brain weight in Zfp521-BrKO that was not specific to either the forebrain or cerebellum (Figure 2.4D). Besides the overall smaller size of Zfp521-BrKO mice (Zfp521-Het were indistinguishable from control mice), no other prominent or apparent physical abnormalities were observed.

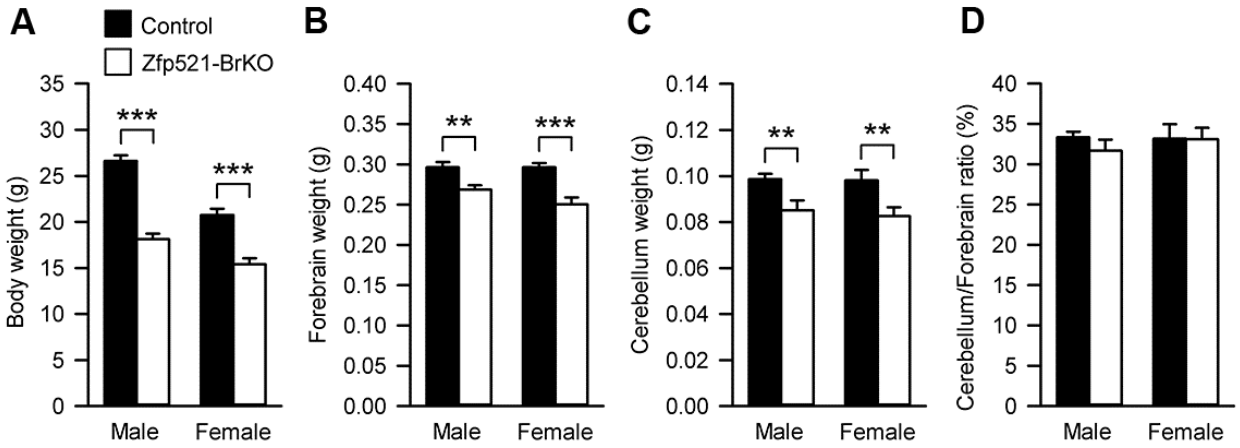

Figure 2.4 Body and brain weights are reduced in Zfp521-BrKO mice. (A) Although control and Zfp521-BrKO mice were comparable in size at birth, by 2 months, both male and female mutant mice weighed significantly less than control littermates (Male: Control, n = 20; Zfp521-BrKO, n = 18; Student's t-test; $p < 0.001$; Female: Control, n = 15; Zfp521-BrKO, n = 14; Student's t-test; $p < 0.001$). (B and C) The forebrain and cerebellum of perfused and fixed brains from 2 month-old control (Male: n = 11 and Female: n = 7) and Zfp521-BrKO (Male: n = 7 and Female: n = 9) mice were weighed. The forebrains of both male and female Zfp521-BrKO weighed significantly less than control mice (Student's t-test; $p = 0.00458$ for male; $p = 0.00043$ for female). Similarly, both male and female Zfp521-BrKO mice showed significant reductions in cerebellar weight compared to control mice (Student's t-test; $p = 0.004$ for male; $p = 0.00938$ for female). (D) The weight ratio between the cerebellum and forebrain did not show a significant difference in both male and females between control and Zfp521-BrKO mice (Male: Student's t-test; $p = 0.257$; Female: Student's t-test; $p = 0.964$), indicating a general reduction in brain size in mutant mice that was not specific to either the forebrain or cerebellum. Values are mean± SEM (* $p \leq 0.05$; ** $p \leq 0.01$; *** $p \leq 0.001$).

2.3 Characterization of the Tic-Like Behavioral Phenotype in Zfp521-BrKO Mice

Over the course of observing the development of Zfp521-BrKO mice from the time of birth to adulthood, it was apparent that the mutant mice spent a significant portion of their time engaged in a multitude of tic-like behaviors reminiscent of the motor tics that are the hallmark clinical features of TS (APA, 2013; Leckman, 2002). To better differentiate and quantify the various tic-like behaviors that were first observed in the home cage, behavioral analysis of Zfp521-BrKO and control littermates was conducted in a behavioral recording chamber with a

transparent floor through which an angled mirror allowed video-recording of mouse behaviors from below. This bottom-up view allowed for clear, unobstructed observation and analysis of even the most subtle or slightest of mouse behaviors. Mice were video-recorded for 15 minutes, with the first 12 minutes for mice to acclimate to the behavioral chamber and the last 3 minutes analyzed for behavior. Both tic-like and non-tic motor behaviors (horizontal movement and rearing) were quantified as "behavioral counts" by hand-scoring the prominent behaviors for each 1-second bin of the 180-second analysis period (Kelley, 2001).

Behavioral analysis of 2 month-old mice (control, n = 10; Zfp521-BrKO, n = 14) revealed that in contrast to control mice, Zfp521-BrKO mice usually spent approximately 70% of the 3 minute analysis period engaged in multiple tic-like motor behaviors, categorized as: 1) excessive head grooming, 2) excessive body grooming, 3) head twitch, 4) hind-limb flapping, and 5) repetitive jumping (Figure 2.5A). Unlike the normal, purposeful grooming observed in control mice, which usually proceed from head to body in a well-characterized chain of sequences (Aldridge et al., 2004), the grooming behavior of Zfp521-BrKO was fixed at a particular component (either grooming of just the head or the body) and continued in excessive, recurring bouts that was significantly greater than observed in control mice (Student's t-test; $p < 0.001$; Figure 2.5A). Similarly, while jumping is also a normally observed behavior in mice, the mutant mice engaged in prolonged bouts of repetitive jumping, clearly distinct from the jumping behavior of littermate controls (Mann-Whitney U-test; $p < 0.001$; Figure 2.5A). On the other hand, the head twitch and hind-limb flapping bouts, both of which are rapid and abrupt (less than 100 msec in duration), occurred in frequencies and durations that were unique to the behavioral phenotype of Zfp521-BrKO mice and rarely observed in control mice (Mann-Whitney U-test; $p < 0.001$ for both head twitch and hind-limb flapping; Figure 2.5A). Although it was reported that TS is 4 times more common in males than females (Freeman et al., 2000;

Robertson et al., 2009; Staley et al., 1997), we did not observe a sex difference in the likelihood of occurrence or severity in the behavioral phenotype of Zfp521-BrKO mice (data not shown).

Just as early childhood-onset is another defining clinical feature of TS-associated tics (APA, 2013; Leckman, 2002), the tic-like behaviors of Zfp521-BrKO mice were also characterized by juvenile-onset. Motor behaviors were indistinguishable between Zfp521-BrKO and control mice at P10 (control, n = 5; Zfp521-BrKO, n = 5) but the pathological behavioral phenotypes emerged at around the age of weaning (P20), with significantly more tic-like behaviors observed in mutant compared to control mice (control, n = 10; Zfp521-BrKO, n = 14; Student's t-test; p = 0.00304; Figure 2.5B). From P20, the severity of the tic-like behaviors increased until stabilizing and persisting in the adult mutant mice (2 months; control, n = 10; Zfp521-BrKO, n = 14; Student's t-test; p < 0.001; Figure 2.5B).

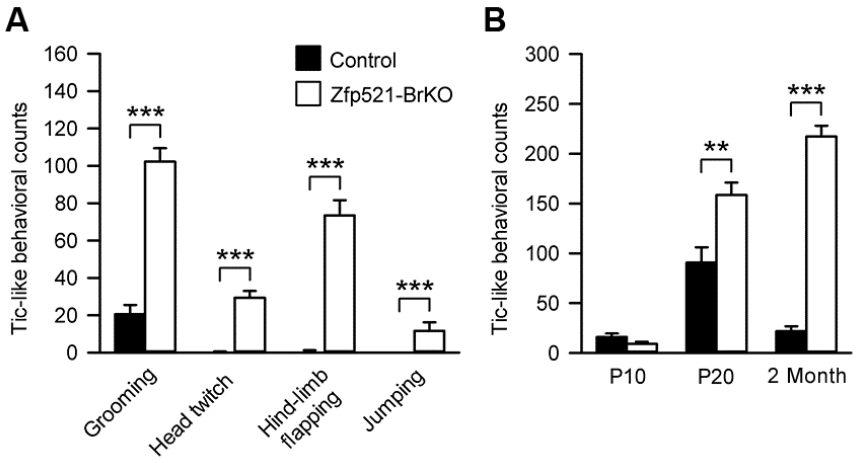

Figure 2.5 Zfp521-BrKO mice show juvenile-onset of multiple tic-like behaviors. (A) Extensive video-recorded behavioral analysis of 2 month-old Zfp21-BrKO mice revealed multiple pathological tic-like behaviors either rarely seen or observed in much lower frequencies in control mice. All behaviors were quantified as "behavioral counts" by hand-scoring the prominent behaviors for each 1-second bin of the 180-second analysis period (video-recorded and analyzed at half-speed playback). These tic-like behaviors included excessive grooming (head and/or body), quick head twitch, rapid hind-limb flapping, and repetitive jumping (Control, n = 10; Zfp521-BrkO, n = 14; Grooming: Student's t-test; p < 0.001; Head twitch: Mann-Whitney U-test; p < 0.001; Hind-limb flapping: Mann-Whitney U-test; p < 0.001; Jumping: Mann-Whitney U-test; p < 0.001). (B) Comparisons of the total tic-like behavioral counts (combined counts of all tic-like behaviors during the 3-minute analysis period) between control and Zfp521-BrKO mice at P10, P20, and 2 months revealed that at P10, tic-like behaviors were similarly low in both mutant and control mice (Control, n = 5; Zfp521-BrKO, n = 5; Student's t-test; p = 0.115). However, near the age of weaning at P20, Zfp521-BrKO mice showed juvenile-onset of the tic-like behaviors (Control, n = 10; Zfp521-BrKO, n = 14; Student's t-test; p = 0.00304) which increased in severity until stabilizing in young adult Zfp521-BrKO mice at 2 months (Control, n = 10; Zfp521-BrKO, n = 14; Student's t-test; p < 0.001). Values are mean± SEM (* p ≤ 0.05; ** p ≤ 0.01; *** p ≤ 0.001).

In addition to variety and complexity, the tic-like behaviors of Zfp521-BrKO mice also sharde some of the temporal features of the tics of TS, which are clinically described as

occurring in patterns of “burst-like” intermittent bouts of short duration with periodic intra-tic intervals between successive bouts (APA, 2013; Jankovic, 1997; Peterson and Leckman, 1998). As shown in the second-by-second timeline analysis of the behavioral phenotype of three individual Zfp521-BrKO mice, the predominant tic-like behaviors also occured in “burst-like” bouts of varying periodicity and duration. Furthermore, although all Zfp521-BrKO mice exhibited the tic-like phenotype, the types of predominant tic-like behaviors, the frequency, and the duration of bouts and intra-tic intervals all manifested in varying degrees in each individual mice (Figure 2.6).

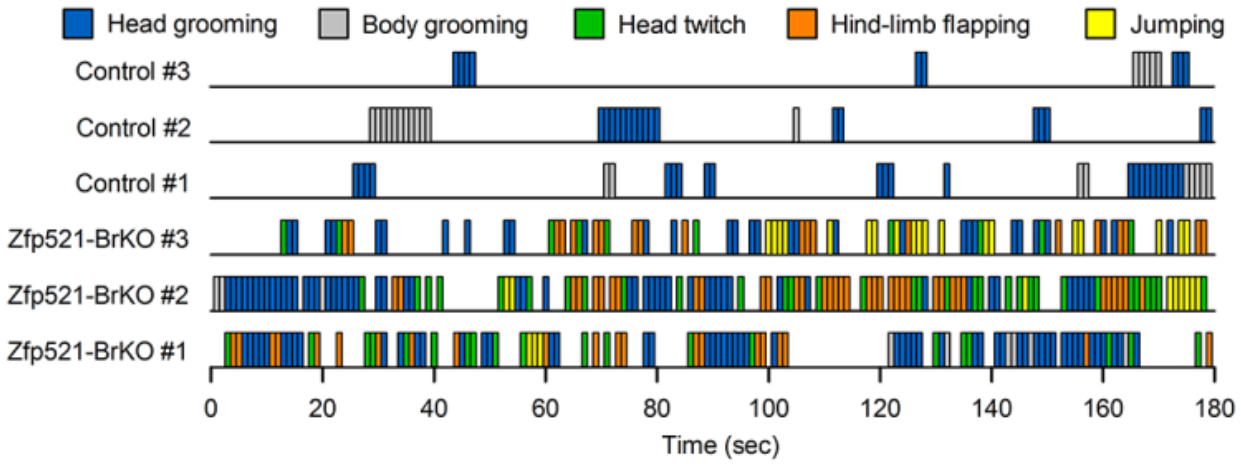

Figure 2.6 Zfp521-BrKO mice show individual variations in the presentation of tic-like behaviors. A second-by-second time line analysis of three representative control and three Zfp521-BrKO mice (2 months-old) showed that different aspects of the tic-like behaviors, including the types of predominant tics, the frequency, duration of bouts, and the length of intra-tic intervals are subject to individual variation. Furthermore, in Zfp521-BrKO mice, the tic-like behaviors occurred in “burst-like” patterns of short intermittent bouts with periodic intra-tic intervals between successive bouts .

An important clinical aspect of TS is that the incidence of tics can be directly influenced by environmental factors and internal processes, such as the exacerbation of tics by stress or anxiety and the temporary suppression of tics by focused attention or distraction (Conelea and Woods, 2008). To determine if such factors can also alter the severity of tic-like behaviors of Zfp521-BrKO mice, we compared the frequency of tic-like behaviors while mice were in a neutral environment (home cage), to when they were placed in a stressful environment (behavioral recording chamber under bright lights) or made to perform an attentionally-demanding task (balancing on a narrow, elevated beam, Figure 2.8A). When Zfp521-BrKO mice

were placed in a stressful environment, the total number of tic-like behavioral counts during a 3-minute analysis period was significantly increased when compared to the counts observed under home cage conditions (Student's t-test; $p < 0.001$; Figure 2.8B). In contrast, when Zfp521-BrKO were placed on a narrow (3cm, approximately body-wide), elevated beam, the attention required to remain on the beam and the distraction of a new, novel environment significantly suppressed the tic-like behaviors during a 3-minute period (Student's t-test; $p < 0.001$; Figure 2.8B). Two-way ANOVA revealed a significant effect of genotype ($F_{1,53} = 270.982$; $p < 0.001$) and condition ($F_{2,53} = 73.752$, $p < 0.001$) on total tic-like behavioral counts with a significant genotype x condition interaction ($F_{2,53} = 49.96$; $p < 0.001$). Post-hoc analysis revealed significantly greater tic-like behavioral counts for Zfp521-BrKO compared to control mice under each condition (Student's t-test; $p < 0.001$ for all three conditions). Similarly, when Zfp521-BrKO mice were placed in a novel, but less stimulating environment, such as a cage top or new home cage, there was a significant, but momentary, suppression of tic-like behaviors that waned along with interest or distraction (data not shown).

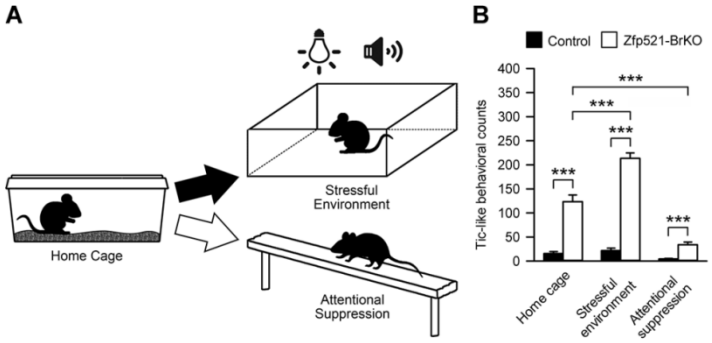

Figure 2.7 Tic-like behaviors in Zfp521-BrKO mice are exacerbated by stress and suppressed by attention. (A) Illustration of the behavioral testing paradigm in which the baseline tic-like behaviors were first quantified when mice were in their home cages (neutral environment) and then measured when mice were placed in the behavioral recording chamber under bright lights and noise from the laminar flow hood (stressful environment) or when mice were placed onto and attempted to stay on a 3 cm-wide (slightly larger than body-width), elevated beam (attentionally-demanding task). (B) Quantification of the total tic-like behavioral counts during a 3-minute analysis period comparing when mice were in the home cage, a stressful environment, or engaged in an attentionally-demanding task showed that environmental factors and internal processes significantly influenced the frequency of tic-like behaviors. Two-way ANOVA of 10 control and 10 Zfp521-BrKO mice (2 months-old) revealed a significant effect of genotype ($F_{1,53} = 270.982$; $p < 0.001$) and condition ($F_{2,53} = 73.752$; $p < 0.001$) on tic-like behavioral counts with a significant genotype x condition interaction ($F_{2,53} = 49.96$; $p < 0.001$). Post-hoc analysis revealed that compared to when in the home cage, the total tic-like behaviors were significantly increased in Zfp521-BrKO mice when in the stressful environment (Student's t-test; $p < 0.001$) but dramatically suppressed when engaged in an attentionally-demanding task (Mann-Whitney U-test; $p < 0.001$). Additionally, post-hoc analysis showed significantly greater tic-like behavioral counts for Zfp521-BrKO compared to control mice under each condition (Student's t-test; $p < 0.001$ for all three conditions). Values are mean± SEM (* $p \leq 0.05$; ** $p \leq 0.01$; *** $p \leq 0.001$).

2.4 Behavioral Phenotypes Relevant to TS Comorbidities

Adding to the etiological complexity of TS are a spectrum of related comorbidities that are often as persistent and prevalent as the tics that characterize this disorder. Many of these comorbid conditions share clinical and pathophysiological features that overlap with other developmental neuropsychiatric disorders and include attention-deficit hyperactivity disorder (ADHD), obsessive-compulsive spectrum disorder (OCSD), self-injurious behaviors (SIBs), anxiety, depression, learning and social impairments (Robertson, 2000). As with TS patients, many of these comorbidities are also present in Zfp521-BrKO mice.

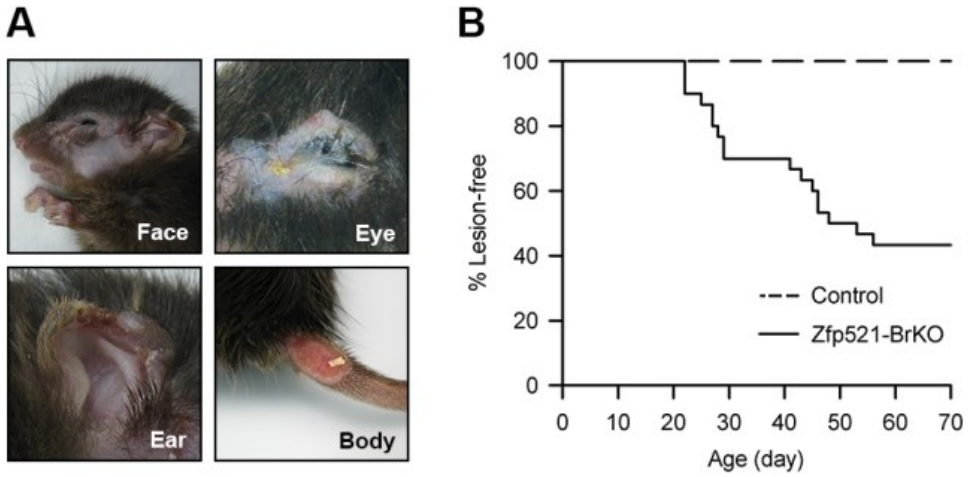

Figure 2.8 A large subset of Zfp521-BrKO exhibit self-injurious behaviors (SIBs) associated with excessive grooming and hind-limb flapping. (A) SIBs are among the TS-associated comorbidities and in Zfp521-BrKO mice, excessive head and body grooming, as well as hind-limb flapping (which scratches the face), first resulted in the loss of hair in the affected area and usually progressed to lesions (particularly evident on the face, eyes, ears, and around the base of the tail on the lower body). (B) The first appearance of SIB-related lesions were recorded in daily health checks of control (n = 30) and Zfp521-BrKO (n = 30) mice to generate a Kaplan-Meier curve tracking the percentage of lesion-free mice from P0 to 2.5 months. Among the mice observed, all control mice remained lesion-free while progressively more Zfp521-BrKO mice began to show lesions with age; by 2 months, at least 50% of Zfp521-BrKO mice exhibited SIB-related lesions.

Within a large subset of Zfp521-BrKO mice, the excessive head and body grooming and the hind-limb flapping behaviors escalated and could be categorized as SIBs as the tic-like behaviors caused bodily injuries. The repetitive grooming and scratching of particular areas of the head or body first resulted in a loss of hair and eventually progressed to lesions of the affected areas (usually the face, eyes, ears, and lower body, Figure 2.8A). As shown in the Kaplan-Meier curve (control, n = 30; Zfp521-BrKO, n = 30), while all control mice observed

remain lesion-free even after 2 months of age, some Zfp521-BrKO mice began to develop lesions from SIBs as early as P23 (a few days after the onset of tic-like behaviors at around P20) and by 2 months of age, at least 50% of mutant mice showed SIB-related lesions (Figure 2.8B).

To determine if there were also social impairments in Zfp521-BrKO mice, we examined nest building, a highly conserved and ethologically-relevant behavior, as a measure of social behavior in the home cage (Moretti et al., 2005). Zfp521-BrKO (n = 6) and control mice (n = 6) were temporarily single-housed in clean home cages, each with a new, intact nestlet (square of compressed cotton) for nest building. After 24 hours, nest building was assessed using an established 5-point rating scale: 1) Nestlet untouched, 2) Nestlet partially torn, 3) Nestlet mostly torn but no clear nest, 4) Well defined, but flat, nest, 5) Well defined nest with high walls (Figure 2.9A; Deacon, 2006). Control mice quickly built proper, high-walled nests (nest score = 5), often within a few hours. However, Zfp521-BrKO mice scored significantly lower in their nest building, often only able to partially shred their nestlets (nest score < 3) and failing to build normal nests even after 24 hours. This statically significant deficit in nest building (Mann-Whitney U-test; p = 0.002; Figure 2.9B) may reflect a form of behavioral dysfunction similar to the social impairment comorbidity associated with TS.

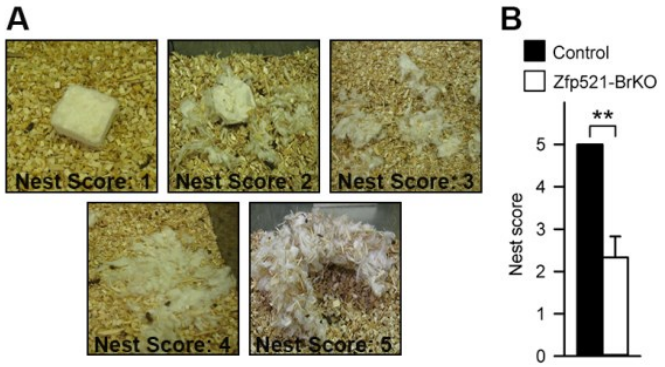

Figure 2.9 Social impairment in Zfp521-BrKO mice demonstrated by deficient nest building. (A) Nest building is an ethologically-relevant behavior that is used as a measure of normal social behavior in mice. Single-housed mice were given a compressed cotton nestlet for nesting material and after 24 hours, nest building is assessed using a 5-point scale: 1) Nestlet untouched, 2) Nestlet partially torn, 3) Nestlet mostly torn but no clear nest, 4) Well defined, but flat, nest, 5) Well defined nest with high walls. (B) After 24 hours control mice (n = 6) built proper, high-walled nests (nest score = 5) but the nests built by Zfp521-BrKO mice (n = 6) were scored significantly lower (nest score < 3; Mann-Whitney U-test; p = 0.002). Values are mean± SEM (* $p \leq 0.05$; ** $p \leq 0.01$; *** $p \leq 0.001$).

General locomotor activity, exploratory behavior, hyperactivity, and anxiety was assessed by automated open field test in which Zfp521-BrKO and control mice were observed in the open field chamber for 15 minutes. Although anxiety is a common comorbidity reported in TS patients and observed in select animal models of OCD-like behaviors (Sapap3, Slitrk5, and DAT knockout mouse models), open field analysis did not confirm an anxiety phenotype in Zfp521-BrKO mice. Reduced time or distance in the center of the open field chamber is indicative of a anxiety phenotype (Carola et al., 2002; Prut and Belzung, 2003). However, quantification of time spent in the perimeter and center of the open field chamber, as well as the number of center entries, did not indicate an anxiety phenotype in Zfp521-BrKO mice compared to controls (data not shown). In a follow-up, we also tested Zfp521-BrKO for an anxiety phenotype using the light-dark box paradigm, which relates anxiety to the time a mouse spends in the light compartment (less anxiety) as opposed the dark compartment (more anxiety; Bourin and Hascoët, 2003). As with the open field test, the light-dark box assessment did not indicate altered anxiety in Zfp521-BrKO as compared to control mice (data not shown).

However, as shown in the examples of the movement traces of Zfp521-BrKO and control mice during a 15-minute session in the open field box (Figure 2.10A), Zfp521-BrKO seemed to exhibit hyperactive movement in between bouts of tic-like behaviors (represented by small, concentrated clusters of movements in the same location). Quantification of the total distance traveled during the 15-minute period in the open field box showed significantly greater distances traveled by Zfp521-BrKO compared to control mice (control, $n = 14$; Zfp521-BrKO, $n = 14$; Student's t-test; $p < 0.001$; Figure 2.10B), reminiscent of the ADHD comorbidity of TS.

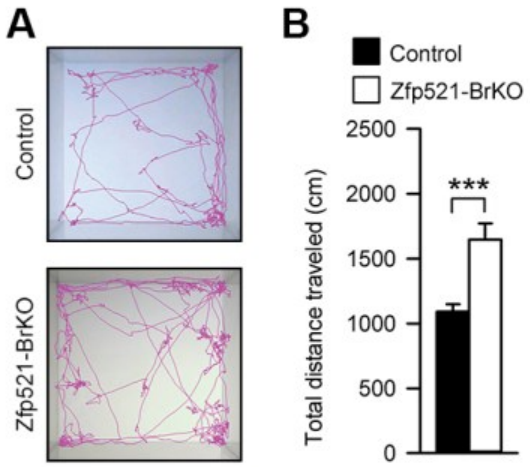

Figure 2.10 Hyperactivity in Zfp521-BrKO mice is analogous to the ADHD comorbidity associated with TS. (A) Representative movement traces of control and Zfp521-BrKO mice during a 15-minute open field analysis session. (B) 2 month-old Zfp521-BrKO mice (n = 14) traveled greater distances (in the intra-tic intervals) compared to control mice (n = 14) during the 15-minute sessions, indicating an ADHD-like hyperactivity in mutant mice (Student's t-test; $p < 0.001$). Values are mean± SEM (* $p \leq 0.05$; ** $p \leq 0.01$; *** $p \leq 0.001$).

2.5 Pharmacological Response to Common TS and OCD Treatments

As previously discussed, one of the important validation criteria for animal models of human disorders is to demonstrate a therapeutic response to pharmacotherapies comparable to that observed in patients. Haloperidol (mixed D2-antagonist) is among the class of neuroleptics often prescribed to TS patients to as a first-line treatment to effectively control motor tics (Robertson, 2000; Shapiro et al., 1989). To determine if haloperidol is similarly effective in reducing the tic-like behaviors in this mouse model of TS, Zfp521-BrKO and control mice were treated with 1.0 mg/kg haloperidol and tic-like behaviors were assessed 1 hour post-injection in the behavioral recording chamber. Two-way repeated measures ANOVA revealed a significant genotype effect ($F_{1,12} = 11.628$; $p = 0.005$), haloperidol treatment effect ($F_{1,12} = 19.028$, $p < 0.001$) on total tic-like behaviors, and a significant genotype x treatment interaction ($F_{1,12} = 12.327$; $p = 0.004$). As shown in Figure 2.11A, acute 1.0 mg/kg haloperidol treatment significantly reduced the total tic-like behavioral counts in Zfp521-BrKO mice compared to the pre-treatment counts (Student's t-test; $p < 0.001$). Furthermore, post-hoc analysis showed that

this alleviation of the tic-like behaviors in Zfp521-BrKO mice by haloperidol reduced the total tic-like behavioral counts to almost that of control levels (Student's t-test; p = 0.115; Figure 2.11A).

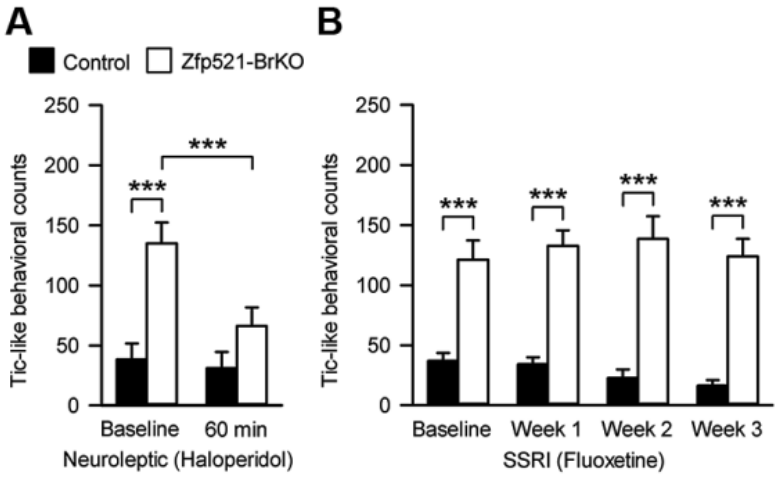

Figure 2.11 Suppression of tic-like behaviors in Zfp521-BrKO mice by pharmacological treatment for TS (haloperidol) but not by treatment for OCD (fluoxetine). (A) Haloperidol (mixed D2-antagonist) is among the classic neuroleptics used as a first-line treatment for tics in TS. Acute treatment with 1.0 mg/kg haloperidol (i.p. injected) significantly suppressed tic-like behaviors in Zfp521-BrKO mice one hour post injection (3-minute behavioral analysis). Two-way repeated measures ANOVA (Control, n = 7; Zfp521-BrKO, n = 7) showed a significant genotype effect ($F_{1,12}$ = 11.628; p = 0.005) and haloperidol treatment effect ($F_{1,12}$ = 19.028, p < 0.001) on tic-like behaviors, and a significant genotype x treatment interaction ($F_{1,12}$ = 12.327; p = 0.004). Post-hoc comparison of Zfp521-BrKO mice at untreated baseline and at 1 hour post-injection with haloperidol showed significant reduction of tic-like behaviors (Student's t-test; p < 0.001) to levels that are no longer significantly different from that of control mice (Student's t-test; p = 0.115). (B) In contrast, after 3 weeks of daily fluoxetine injections (20.0 mg/kg) there was no significant effect of fluoxetine treatment on tic-like behaviors (Control, n = 7; Zfp521-BrKO, n = 7; Two-way repeated measures ANOVA; Genotype: $F_{1,22}$ = 75.505; p < 0.001; Fluoxetine treatment: $F_{3,22}$ = 0.846; p = 0.484; Genotype x treatment interaction: $F_{3,22}$ = 0.613; p = 0.614). Values are mean± SEM (* p ≤ 0.05; ** p ≤ 0.01; *** p ≤ 0.001).

In order to differentiate Zfp521-BrKO mice as a mouse model that uniquely recapitulates TS-like motor behaviors, tic-like behaviors were also evaluated against chronic fluoxetine (SSRI) treatment. Although fluoxetine has been shown to be effective in suppressing compulsive behaviors in OCD patients and OCD-like stereotypic behaviors in genetic mouse models such as the Sapap3 and Slitrk3 knockout mice, it has also been shown to be ineffective in the suppression of TS-associated motor tics (Robertson, 2000; Scahill et al., 1997). Zfp521-BrKO and control mice were treated with daily injections of 20.0 mg/kg fluoxetine for 3 weeks. As shown in Figure 2.11B, even though was a clear genotype effect (two-way repeated measures ANOVA; $F_{1,22}$ = 75.505; p < 0.001), even after 3 weeks of chronic fluoxetine treatment, there was no significant fluoxetine treatment effect ($F_{3,22}$ = 0.846; p = 0.484) or

genotype x treatment interaction ($F_{3,22}$ = 0.613; p = 0.614) on the total tic-like behavioral counts in Zfp521-BrKO and control mice.

2.6 Characterization of TS-Associated Neuropathologies in Zfp521-BrKO Mice

While evidence from several lines of studies generally implicate the BG, and the striatum in particular, as the pathological center of TS, there is far less consensus on the specific anatomical changes and dysfunctions that may define the neuropathology of TS. However, among numerous volumetric and functional neuroimaging investigations of TS patients, a common theme has emerged; multiple studies report findings of reduced caudate volumes in children and adults TS patients (Felling and Singer, 2011; Hyde et al., 1995; Peterson et al., 2003). Furthermore, longitudinal imaging studies suggest caudate volume in children with TS is inversely correlated to with the severity of tics persisting into adulthood (Bloch et al., 2005).

Using DARPP-32 (dopamine- and cAMP-regulated neuronal phosphoprotein of 32 kDa) as a histological marker of striatal MSNs to immunohistochemically stain and anatomically define the striatum, we also observed a consistent decrease through all levels of the dorsal striatum in Zfp521-BrKO mice compared to controls (Figure 2.12A). To more accurately quantify the total dorsal striatal volume reduction in Zfp521-BrKO compared to control mice, we performed unbiased stereological volumetric analysis of 2 month-old mice (control, n= 5; Zfp521-BrKO, n = 5) using DARPP-32 immunohistochemical staining to define the striatum in coronal brain sections. Stereological volume measurements revealed both striatal and cortical volumes were significantly smaller in Zfp521-BrKO compared to control mice (Student's t-test; $p < 0.001$ for both striatal and cortical volumes; Figure 2.12B). To determine if there was a uniform decrease in both striatal and cortical volumes that is reflective of the global reduction in overall brain size (Figure 2.4B) or if there was a greater reduction specifically in striatal volume, we compared the striatal to cortical volume ratio in Zfp521-BrKO and control mice. As shown in Figure 2.12C, the striatal to cortical volume ratio was significantly smaller in Zfp521-BrKO mice

(Student's t-test; $p < 0.001$), indicating dorsal striatal atrophy in Zfp521-BrKO mice analogous to the caudate reduction reported in TS patients.

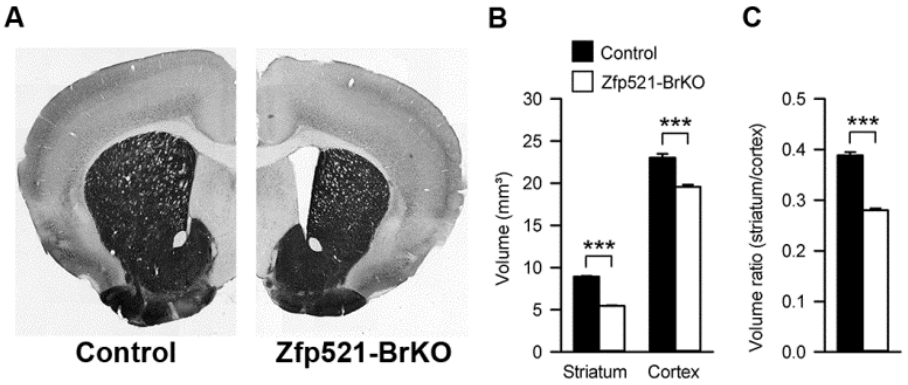

Figure 2.12 Zfp521-BrKO mice exhibit a significant reduction in dorsal striatal volume. (A) Immunohistochemical staining with DARPP-32 (striatal MSN marker) was used to define the striatum in matched coronal brain sections from 2-month old control and Zfp521-BrKO mice. Brain sections from Zfp521-BrKO mice showed a consistent reduction though all rostral-caudal levels of the dorsal striatum. (B) Unbiased stereological volumetric analysis of DARPP-32 immunohistochemically stained coronal sections revealed significant reductions in both striatal and cortical volumes in Zfp521-BrKO compared to control mice (Control, n = 5; Zfp521-BrKO, n = 5; Student's t-test; $p < 0.001$ for striatal and cortical volumes). (C) Comparison of the striatal-to-cortical volume ratios revealed a significantly greater reduction specifically in striatal volume in Zfp521-BrKO compared to control mice (Student's t-test; $p < 0.001$). Values are mean± SEM (* $p \leq 0.05$; ** $p \leq 0.01$; *** $p \leq 0.001$).

In addition to the MSNs which account for nearly 95% of striatal neurons, there are also four physiologically distinct classes of interneurons that that make up the remaining 5% of neurons in the striatum. These four immunohistochemically identified interneurons include parvalbumin (PV)-expressing GABAergic interneurons, somatostatin (SST)-expressing GABAergic interneurons, calretinin (CR)-expressing GABAergic interneurons, and choline acetyltransferase (ChAT)-expressing cholinergic interneurons (Gerfen and Surmeier, 2011; Tepper and Bolam, 2004). Although they only constitute a small percentage of the total neuronal population of the striatum, these interneurons regulate striatal signaling through localized inhibition (PV+ GABAergic interneurons) and DA modulation (cholinergic interneurons; Ding et al., 2010; Koós and Tepper, 1999). Interestingly, in a small neuropathological study, unbiased stereological analysis of postmortem brains from adult TS patients and matched controls found a selective reduction of PV+ interneurons in the caudate (Kalanithi et al., 2005). In a follow-up neuropathological study, the same laboratory also reported significant reductions in ChAT+ cholinergic interneurons in the striata of TS patients (Kataoka et al., 2010), suggesting striatal

reductions in these select interneuron subtypes may be indicative of a characteristic neuropathology in a subset of TS patients.

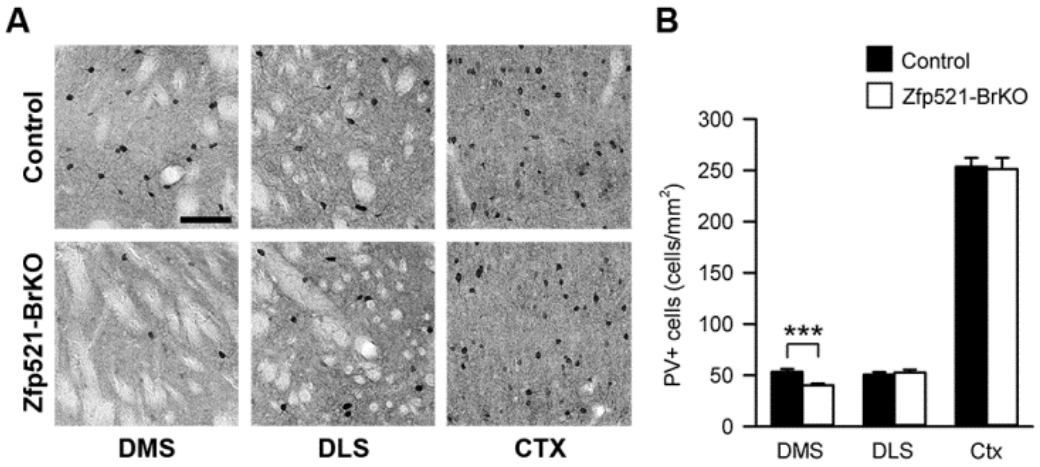

Figure 2.13 Selective reduction of parvalbumin (PV)-expressing interneurons in the DMS in Zfp521-BrKO mice. (A) Representative 20X images of immunohistochemically stained PV+ cells in the dorsomedial striatum (DMS), dorsolateral striata (DLS), and the cortices (CTX) of 2 month-old control and Zfp521-BrKO mice. Scale bar = 100μm. (B) Unbiased cell counting of PV+ cells in matched coronal sections revealed a significant reduction in the density of PV+ cells in the DMS, but not in the DLS or cortex in Zfp521-BrKO compared to control mice (Control, n = 5, Zfp521-BrKO, n = 5; Student's t-test; DMS: $p < 0.001$; DLS: $p = 0.600$; CTX: $p = 0.599$). Values are mean± SEM (* $p \leq 0.05$; ** $p \leq 0.01$; *** $p \leq 0.001$).

PV+ interneurons were identified by immunohistochemical staining in matched coronal brain sections from 2 month-old Zfp521-BrKO (n = 5) and control mice (n = 5; Figure 2.13A). Quantification of PV+ interneurons revealed Zfp521-BrKO mice also exhibited a PV+ interneuron neuropathology, with a selective reduction in the number of PV+ interneurons in the dorso-medial striatum (DMS; Student's t-test, $p < 0.001$) but no significant difference in the dorso-lateral striatum (DLS; Student's t-test; $p = 0.600$) or the cortex (Student's t-test; $p = 0.599$), compared to controls (Figure 2.13B). However, unlike the results of the second study by Kataoka and colleagues (2010), quantification of immunohistochemical labeled ChAT+ cholinergic interneurons in matched brain sections from Zfp521-BrKO and control mice did not indicate a ChAT+ interneuron neuropathology in mutant mice; there was no significant difference in the number of ChAT+ interneurons in the regions quantified (data not shown).

2.7 Discussion

From the time the transcription factor Zfp521 was first identified as a highly striatonigral-enriched gene from the our laboratory's FACS-array study (Lobo et al., 2006) and later verified by BAC-TRAP (Doyle et al., 2008; Heiman et al., 2008), we have attempted to elucidate developmental and functional role of Zfp521 in the CNS, specifically in the striatum. Through extensive behavioral, pharmacological, and pathological investigations presented in this chapter, we have demonstrated that a CNS-specific conditional knockout mouse of Zfp521 (Zfp521-BrKO) presents as a novel, phenotypically robust model of TS. In developing any animal model of human disorders, critical validation criteria must be met, including face validity (phenomenological similarity), predictive validity (comparable response to therapeutics), and construct validity (consistency of the theoretical etiology; Willner, 1984, 1986). As summarized in Table 2.1, the various tic-like behaviors, comorbid conditions, and key neuropathologies exhibited by Zfp521-BrKO mice overwhelmingly fulfilled the face validity criteria. Furthermore, pharmacological predictive validity was not only demonstrated, but differing responses to various drugs for TS and OCD suggested that Zfp521-BrKO was a distinct model of specifically TS-like, rather than OCD-like, pathological behaviors. Although construct validity will be discussed in more detail in later chapters, Zfp521-BrKO also demonstrated general construct validity in that Zfp521 is a highly striatonigral enriched gene and the striatum is focal to both the behavioral phenotype and primary neuropathologies of Zfp521-BrKO mice, similar to the well-accepted BG-centric pathophysiology of TS.

Table 2.1. Behavioral and pathological phenotypes of Zfp521-BrKO compared to the clinical and neuropathological features of Tourette Syndrome.

Clinical Features	Tourette's Syndrome	Zfp521-BrKO
Genetic Etiology	Complex	CNS-Specific Deletion of Zfp521
Onset	5 – 8 Years-old	P20
Sex Difference	4:1 (Male to Female)	No
Tics:		
Simple Tic	Yes	Yes (head twitch and hind-limb flap)
Complex Tic	Yes	Yes (excessive grooming and jumping)
Vocal Tic	Yes	Not Determined
Premonitory Urge	Yes	N/A
Tic modification:		
Exacerbation by Stress	Yes	Yes
Suppression by Attention	Yes	Yes
Comorbidity:		
Self-Injurious Behaviors (SIBs)	Yes	Yes
Attention Deficit Hyperactivity Behaviors	Yes	Yes (Hyperactivity)
Obsessive Compulsive Behaviors	Yes	Unlikely (see SSRI)
Social Impairment	Yes	Yes (Nest Building)
Pharmacological Suppression of Tics:		
Haloperidol	Yes	Yes
Fluoxetine	No	No
Neuropathology		
Striatal Atrophy	Yes	Yes
Striatal PV Interneuron Pathology	Yes	Yes

Zfp521-BrKO mice exhibited the human-equivalent of childhood-onset, with tic-like behaviors first fully emerging at around the age of weaning, P20. Although the tic-like behaviors were the most prominent phenotype of Zfp521-BrKO mice, much like the tics which are the clinical hallmarks of TS, the truly compelling features of the tic-like behaviors in the mutant mice were their robustness and variety. Unlike other previously discussed models of stereotyped and tic-like behaviors, which are usually limited to one or two primary behaviors (usually excessive grooming and head twitching), all Zfp521-BrKO mice exhibited multiple tic-like behaviors that can be further categorized as simple (head twitch and hind-limb flapping) and complex (excessive grooming and repetitive jumping) tics that constituted upwards of 70% of their active behaviors. Furthermore, although we labeled it as "grooming" behavior, this behavior was actually tic-like by definition, in that it was not purposeful and seemingly irrelevant to normal grooming behavior. Zfp521-BrKO mice were usually stuck in one component of the normal grooming syntactic chain (head or body grooming) and most mutant mice presented a poorly

groomed appearance. Detailed characterization of the pathological phenotype also revealed that while all Zfp521-BrKO mice exhibited most of the tic-like behaviors, there were clear individual variations in the types of predominant tic-like behaviors, the frequency, and the duration of intra-tic intervals, similar to the varying patterns of tics in TS patients. In contrast to aberrant, patterned motor outputs from brainstem nuclei that often proceed in an inflexible manner regardless of external input, the tic-like behaviors in Zfp521-BrKO were influenced by contextual factors, much like that of TS patients; tic-like behaviors were significant exacerbated by stress and attenuated by attention and distraction.

Although the presence of comorbidities is not a requisite criteria for the diagnosis of TS, conditions such as ADHD, OCD, SIBs , anxiety, and learning and social impairments which often accompany TS provide important insights into the neurobiological themes (i.e., BG circuitry) common to these broad, overlapping spectrum disorders. The comorbidities exhibited by Zfp521-BrKO mice, including hyperactivity, SIBs, and social impairment, may provide important clues into the shared pathophysiology among the different animal models of stereotyped and tic-like behaviors. Although Zfp521-BrKO mice also exhibited an excessive grooming phenotype which other studies of mouse models categorize as an OCD-like behavior, on the basis of the lack pharmacological response to fluoxetine, we categorized this behavior as a tic-like, rather than an OCD-like comorbidity.

Among the different hypotheses on the neurobiology of OCD, serotonin (5-HT) is generally regarded as playing an important role. Pharmacological manipulation of 5-HT receptors and genetic disruption of 5-HT signaling by knockout of the 5-HT_{2C} receptor induced OCD-like behaviors (excessive grooming, chewing, head-dipping, and disruptions in spontaneous alternation behaviors) in various animal models (Chou-Green et al., 2003; Yadin et al., 1991). In other models of OCD-behaviors, including the Sapap3 and Slitrk5 knockout mice, chronic fluoxetine (SSRI) treatment significantly reduced the OCD-like grooming behaviors.

However, none of the tic-like behaviors, including the excessive grooming, was significantly altered in Zfp521-BrKO mice by comparable fluoxetine treatments. On the other hand, acute treatment with haloperidol (neuroleptic), which is one of the first-line drugs often used to treat the motor symptoms of TS, significantly suppressed all of the individual tic-like behaviors in Zfp521-BrKO mice. These studies demonstrated that Zfp521-BrKO is a predictive model of pharmacological efficacy in suppressing the tic-like motor behaviors that are more representative of the motor tics associated with TS rather than the compulsive behaviors of OCD. Although this differentiation of the behavioral phenotypes as TS-like versus OCD-like may be regarded as nothing more than semantics, as there is clearly no drug or treatment that uniquely targets just TS or OCD, it is still important to acknowledge that there are likely physiological differences between the TS-like behavioral phenotype of Zfp521-BrKO mice and other animal models of OCD-like stereotypic behaviors.

While animal models often provide a powerful and experimentally tractable tool to study specific aspects of disorders, they are also narrowed representations of these conditions, with limitations and caveats. In the case of Zfp521-BrKO mice, one of the more apparent caveats is the significantly reduced body weight and size with corresponding reductions in overall brain weight. The CNS-specific conditional knockout mice were generated in place of the full Zfp521 knockout mice because Zfp521-null mice were severely smaller, with physical developmental issues, and less than 5% survived to 4 weeks of age. These early developmental and survival issues of Zfp521-null mice were likely due to the critical role of Zfp521 in the development of bone and adipose tissue (Correa et al., 2010; Kang et al., 2012; Wu et al., 2009). Although Zfp521-BrKO have no issues with survival into adulthood, the mice are all smaller compared to control and Zfp521-Het littermates (which are indistinguishable from controls). One possible reason may be that the larger energy expense of engaging in tic-like behaviors for significant periods of their active cycles starting from the age of weaning may adversely affect normal

growth and development of Zfp521-BrKO mice. However, this reduction in body size may be a minor issue in the overall context of Zfp521-BrKO mice as a model of TS as it does not interfere with the survival, overall development, and normal functioning of the mice, nor is it likely to be the source of the tic-like behaviors.

Although several epidemiological studies suggest TS is 4 times more common in males than females (Freeman et al., 2000; Robertson et al., 2009; Staley et al., 1997), we did not find evidence of a sex difference in any aspect the behavioral phenotype (age of onset, severity, or frequency of the different individual tic-like behaviors) of Zfp521-BrKO mice. In TS patients, this reported sex difference is likely due to the complex genetics of TS which cannot be replicated in our mouse model, which is concerned with the developmental consequences of a single gene. It has also been reported that in most typical cases of TS, there is often a drastic reduction of tics by late adolescence into young adulthood (Bruun, 1984; Erenberg et al., 1987; Leckman et al., 1998). However, the tic-like behaviors in Zfp521-BrKO mice persisted in adult mouse (2 months and older) with no indication of attenuation with age. Taken together with evidence that reduced caudate volumes can predict the severity of tics that persist into adulthood, the large striatal atrophy and stable tic-like behaviors that persist in the adult mice indicate that Zfp521-BrKO mice may be more accurately characterized as a model of a severe or malignant form of TS that persists into adulthood (Bloch et al., 2005; Cheung et al., 2007).

In this chapter, we extensively analyzed the characteristics of the TS-like pathological motor phenotypes of Zfp521-BrKO mice. However, vocal tics are another distinctive clinical feature of TS (APA, 2013) that are as equally disruptive to daily life as the motor tics. In mice, ultrasonic vocalizations are primarily emitted as distress calls by nursing pups when separated from their mothers and later in life, they are emitted during nonaggressive social interactions, particularly during mating behaviors (Portfors, 2007). In several mouse models of autism spectrum disorders (ASDs), alterations in ultrasonic vocalizations in pups have been reported,

though there is no clear consensuses as to whether disruptions in vocalization are really analogous to human vocal tics or language impairments (Peñagarikano et al., 2011; Schmeisser et al., 2012; Silverman et al., 2010; Tsai et al., 2012). Currently, alterations in ultrasonic vocalizations have not been determined in Zfp521-BrKO pups or adult mice. Although an investigation of altered ultrasonic vocalizations as a mouse-equivalent of a vocal tics in Zfp521-BrKO mice is of interest , we must consider the likelihood of detecting such a pathological phenotype in Zfp521-BrKO pups given our evidence indicating the tic-like phenotypes do not fully emerge until P20. Of course, this does not exclude the possibility of altered ultrasonic vocalizations in adult Zfp521-BrKO mice and may motivate future testing.

The two TS-like neuropathologies characterized in Zfp521-BrKO are important phenotypes which may provide direct insight into the construct validly of this mouse model of TS. Not only do the reductions in striatal volume and PV-expressing interneurons in Zfp521-BrKO mice match similar key neuropathologies reported from neuroimaging and postmortem studies (Hyde et al., 1995; Kalanithi et al., 2005; Kataoka et al., 2010; Peterson et al., 2003), it provides direct evidence of a possible striatal pathophysiology underlying the tic-like behaviors. This chapter detailed the extensive behavioral, pharmacological, and pathological studies performed to establish the face, predictive, and general construct validity of the Zfp521-BrKO mouse as a robust, novel, and comprehensive model of TS. In the following chapter, we will closely examine the molecular and cellular basis of the striatal volume and PV+ interneuron loss in the context of the known transcriptional functions of Zfp521 (as well as Zfp423 and Ebf1). Understanding the regulatory role of Zfp521 in early BG development and identifying striatal deficiencies resulting from the loss of Zfp521 will provide significant insights into BG circuitry dysfunctions which may underlie the pathological behaviors in Zfp521-BrKO mice and TS patients.

Chapter 3

Assessment of Zfp521's Role in the Striatal Neuropathologies of Zfp521-BrKO Mice

3.1 Introduction

In the previous chapter, we identified two prominent neurobiological deficits in Zfp521-BrKO mice that have also been reported in TS patients; dorsal striatal atrophy and selective reduction of PV-expressing interneurons in the dorsomedial striatum. Although the direct role of Zfp521 in striatal development remains largely unknown, our investigation of how the loss of Zfp521 can lead to the neuropathologies observed in Zfp521-BrKO mice is guided by the understanding of its function in the development of early neuronal precursors (Kamiya et al., 2011) as well as the role of Zfp423 (paralog) and Ebf1(transcriptional partner) in the differentiation of cerebellar, striatal, and olfactory neurons (Alcaraz et al., 2006; Cheng and Reed, 2007; Cheng et al., 2007; Lobo et al., 2008; Warming et al., 2006). Zfp521 is critical in the early neuroectodermal specification of undifferentiated embryonic stem cells. Fortunately, because Nestin is expressed after this critical transition, once these cells become proliferating neural progenitors, we are able to avoid embryonic lethality with Nestin-Cre mediated deletion of the conditional Zfp521 allele. Instead, Zfp521-BrKO mice provide the means to investigate the continued role of Zfp521 in various (though more restricted) aspects of neural development progressing from an extremely early embryonic stage (neural tube formation) to the first steps of striatal development at E12 (at the earliest indications of striatal-specific neurogenesis; Deacon et al., 1994; Olsson et al., 1998).

Although the striatum lacks the prominent cytoarchitecture to be arranged into morphologically different cellular groupings, it can be segregated into multiple functionally and histochemically distinct compartments beyond the basic organization of striatonigral and striatopallidal MSNs in the direct and indirect pathways. The striatum can be divided into dorsal,

ventral, lateral, and medial regions, each with topographically defined cortical afferent inputs and efferent projections (Berendse et al., 1992; Gerfen, 1985, 1992; Selemon and Goldman-Rakic, 1985). These regions have been shown to be associated with distinct forms of learning and behaviors, including goal-directed learning in the dorsomedial striatum, habit-formation in the dorsolateral striatum, and emotional and reward behaviors in the ventral striatum (Alexander et al., 1986; Cardinal et al., 2002; Graybiel, 2008). Furthermore, the striatal circuits can be further organized into striosomes (patch compartments) surrounded by the matrix compartment, which are histochemically defined by their characteristic signaling proteins and molecules (Graybiel, 1990). The striosomes are identified by high expression of mu-opiate receptors (MuOR), prodynorphin (Pdyn), and substance P (SP), receive inputs from the amygdala and limbic cortices, and project to the DA neurons of the substantia nigra pars compacta (SNc). The striatal matrix can be distinguished by enriched expression of acetylcholinesterase (AChE), calbindin (Calb1), and somatostatin (SST), receive inputs from association, oculomotor, and sensorimotor cortices and the thalamus, and project to GABAergic neurons of the pallidum and substantia nigra pars reticulata (SNr; Crittenden and Graybiel, 2011; Gerfen, 1984, 1985; Graybiel, 1990). Although there is no clear consensus on the exact functional roles of these compartments on BG-mediated learning and behavior, the expression of the specific signaling proteins, the characteristic inputs and outputs, are all likely to reflect specialized behavioral processing by these distinct striatal circuits and regions.

This compartmentalization is not only important from the perspective of functional circuitry, but also striatal development because the overall organization of the striatum occurs in stages (or waves) and the proper execution of an earlier developmental process sets up for the subsequent processes. During embryogenesis, the ventral telencephalic vesicles first form the medial ganglionic eminence (MGE) and then the lateral ganglionic eminence (LGE), which give rise to the pallidum and striatum, respectively (Deacon et al., 1994; Olsson et al., 1998). The

ventricular zone (VZ) and the subventricular zone (SVZ) are the two distinct proliferative zones of the MGE and LGE from which postmitotic neuronal precursors migrate out laterally into the mantle zone where they undergo terminal differentiation (Halliday and Cepko, 1992; Olsson et al., 1998). Pulse label experiments reveal two distinct waves of neurogenesis, beginning with striosome neurons migrating out of LGE between E11 and E15, followed by later-born matrix neurons emerging from the LGE between E17 and E20 in a caudal-to-rostral and lateral-to-medial gradient of migration (Fishell and van der Kooy, 1987; van der Kooy and Fishell, 1987; Krushel et al., 1995; Liu and Graybiel, 1992). The development of the striosomes correspond with the first innervation by dopaminergic nigrostriatal projections at E14 to form “dopamine islands” while the later development of the matrix occurs independent of dopaminergic input (Graybiel, 1984; Moon Edley and Herkenham, 1984).

While the striatal MSNs radially migrate out the from LGE to their final positions in the adjacent striatum, the vast majority of striatal interneurons (all cholinergic and a large subset of GABAergic interneurons) emerge from the MGE by tangential migration out from the VZ/SVZ proliferative zones and into the mantle zone of the developing striatum to undergo terminal differentiation (Marín and Rubenstein, 2001; Marin et al., 2000). Similar to the distinct developmental waves of striatal MSNs which organize the striosome/matrix compartmentalization of the striatum, various birth-dating, transplantation, and tracer experiments have revealed that the developmental regulation of striatal interneurons is also characterized by phases of early and late neurogenesis and migration from the proliferative zones of the MGE (Anderson et al., 1997; de Carlos et al., 1996; Marín and Rubenstein, 2001; Marin et al., 2000; Sussel et al., 1999; Xu et al., 2008). Though there is a considerable overlap of the windows of neurogenesis between the different interneuron subtypes, cholinergic interneurons are born earlier, between E12 and E15, followed by GABAergic interneurons generated between E14 and E17 (Phelps et al., 1989; Rymar et al., 2004; Sadikot and

Sasseville, 1997). Following migration and terminal differentiation in the later embryonic stages, these interneurons take on their distinct immunohistochemical and physiological identities in the critical first two to three weeks of postnatal development (Schlösser et al., 1999).

The selective reduction in both striatal volume (presumably due to some MSN deficits) and PV-expressing interneurons in Zfp521-BrKO mice suggests a possible regulatory role of Zfp521 in both the striatal MSN and interneuron developmental programs. Specifically, Zfp521 may be relevant to the differentiation of neurons from both the MGE and LGE through its association with Dlx1 and 2 (Distal-less) homeodomain transcriptions factors. Several extensive studies of a Dlx1/2 knockout mouse from the Rubenstein laboratory revealed that Dlx1 and 2 regulates the differentiation of both late-born striatal MSNs fated for the matrix and GABAergic interneurons (Anderson et al., 1997; Cobos et al., 2005; Marin et al., 2000). It has been shown that in Dlx1/2 knockout mice, there is an abnormal accumulation of partially differentiated neurons that failed to migrate out of SVZ, suggesting Dlx1 and 2 may promote the migration of neuronal precursors out of the proliferative zones through repression of axonal and dendritic development (Cobos et al., 2007). Furthermore, it was not only shown that Zfp521 is expressed in the MGE and LGE at E15.5, but its expression is significantly reduced in the Dlx1/2 knockout mice, indicating Zfp521 is likely one of the downstream targets of the Dlx1/2-mediated differentiation program (Long et al., 2009a, 2009b). This interaction may be mediated by some aspect of TGF-β signaling through binding of SMAD proteins, which physically interact with both Dlx and Zfp521 (Maira et al., 2010). In this chapter, through birth-dating and developmental examination of key striatal histological markers, we will attempt to examine whether the striatal neuropathologies of Zfp521-BrKO mice are a developmental consequence of disrupting a critical Zfp521-mediated transcriptional program common to both MSN and interneuron differentiation.

3.2 Assessment of Striatonigral and Striatopallidal MSNs and the Direct and Indirect Pathways in Zfp521-BrKO Mice

In the previous chapter, we performed unbiased stereological volumetric analysis of the striatum and cortex with DARPP-32 immunohistochemical staining to show that Zfp521-BrKO have a selective reduction in striatal volume compared control mice, similar to what has been reported in TS patients (Hyde et al., 1995; Peterson et al., 2003). The striatum is largely comprised of MSN cell bodies, neuropil (dendrites and axons), and synapses. The deficit of one, or a combination, of these elements may result in the observed striatal volume loss. Currently, there is no indication of the type of deficit that underlies the volume loss in TS patients, due to both the limitations of neuroimaging studies and the lack of detailed postmortem studies. However, immunohistological analysis of the striatal MSNs (and the specific striatonigral D1- and striatopallidal D2-MSN subtypes) in Zfp521-BrKO mice may provide clues as to the nature of the striatal volume loss in this model and in patients with TS.

To evaluate if there is a change in MSN composition (cell number or neuropil) in the striata of Zfp521-BrKO mice compared to controls, we assessed the density of MSNs in the dorsomedial (DMS) and dorsolateral striatum (DLS) by unbiased cell counting methods. As with the volumetric analysis, striatal MSNs were identified by DARPP-32 immunohistochemical staining (Figure 3.1A). Cells were counted under 100X magnification in multiple randomly selected regions-of-interest (ROIs) in the DMS and DLS of matched coronal brain sections from 2 month-old Zfp521-BrKO (n = 5) and control mice (n = 5). Quantification of DARPP-32 labeled cell densities did not show a significant difference in the DMS (Student's t-test; $p = 0.309$) or the DLS (Student's t-test; $p = 0.688$) between Zfp521-BrKO and control mice (Figure 3.1B).

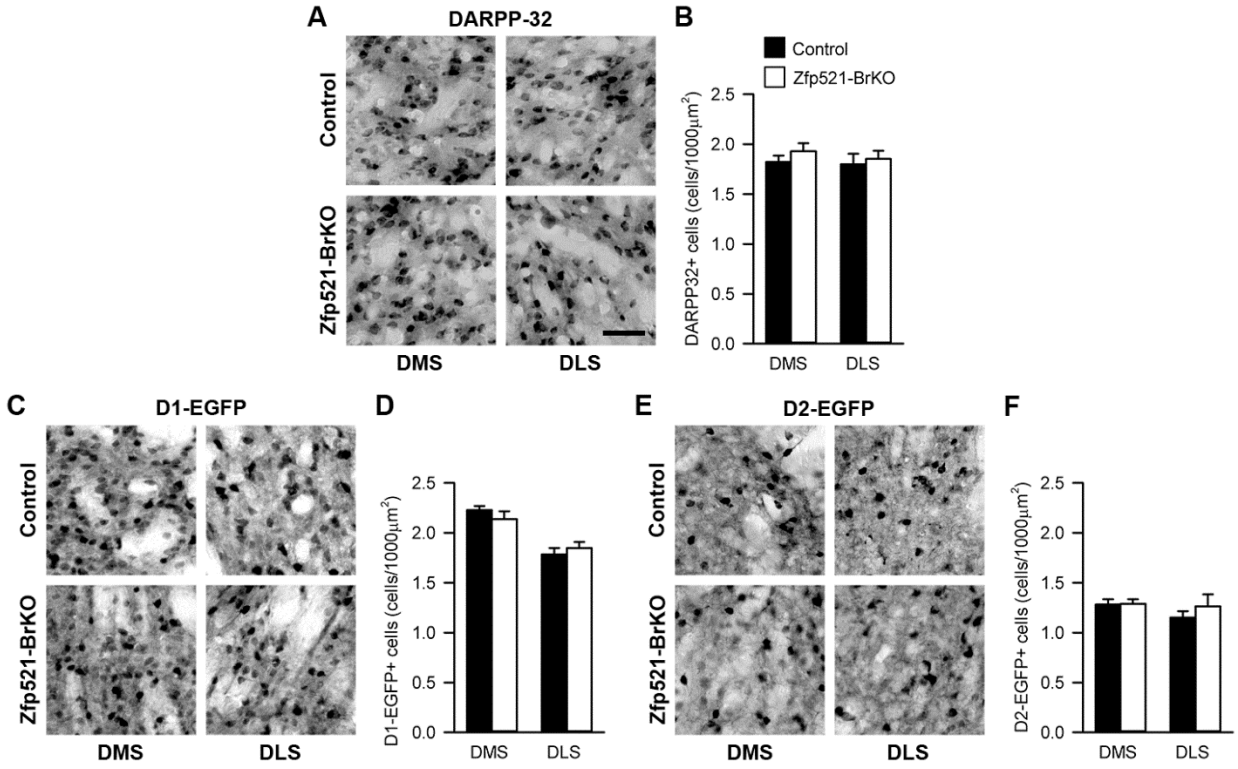

Figure 3.1 Striatal densities of D1- and D2-MSNs are preserved in Zfp521-BrKO mice. (A) Immunohistochemical stainings of DARPP-32 (MSN marker) in the DMS and DLS of control and Zfp521-BrKO mice and (C and E) EGFP (Enhanced Green Fluorescent Protein) in the DMS and DLS of control and Zfp521-BrKO mice expressing either D1-EGFP (to genetically label D1-MSNs) or D2-EGFP (to genetically label D2-MSNs), respectively. All images: 40X magnification, scale bar = 50μm. (B, D, F) Region-specific cell density was assessed under high magnification (100X for DARPP-32 and 40X for D1- and D2-EGFP) by unbiased cell counting in ROIs (regions of interest) that were randomly selected in the DMS and DLS of matched coronal sections from 2 month-old mice (DARPP-32: Control, n = 5; Zfp521-BrKO, n = 5; D1-EGFP: Control; D1-EGFP, n = 4; Zfp521-BrKO; D1-EGFP, n = 4; D2-EGFP: Control; D2-EGFP, n = 3; Zfp521-BrKO; D2-EGFP, n = 3). No significant difference was detected in the DMS or DLS density of DARPP-32+ MSNs (Student's t-test; p = 0.309 in DMS, p = 0.688 in DLS), D1-EGFP+ MSNs (Student's t-test; p = 0.3.11 in DMS, p = 0.494 in DLS), or D2-EGFP+ MSNs (Student's t-test; p = 0.466 in DMS, p = 0.402 in DLS) between control and Zfp521-BrKO mice. Values are mean± SEM (* $p \leq 0.05$; ** $p \leq 0.01$; *** $p \leq 0.001$).

Quantification of DARPP-32 labeled cells did not indicate a regional loss of MSNs or neuropil (which would have been likely indicated by a higher density of more closely associated MSNs in a given ROI) associated with the loss of striatal volume in Zfp521-BrKO. However, keeping in mind that Zfp521 is a striatonigral-enriched gene, it raises the possibility that Zfp521-BrKO may exhibit some subtle cell-autonomous striatonigral D1-MSN deficits or non-cell-autonomous striatopallidal D2-MSN deficits. Furthermore, if Zfp521 is involved in the determination of a D1- or D2-MSN subtype-specific fate, there may be a shift in the ratio of D1- versus D2-MSNs in Zfp521-BrKO mice that may not be reflected in total number of striatal

MSNs. To separately evaluate the D1- and D2-MSN subtypes, Zfp521-Hets were crossed with either BAC-Drd1a-EGFP or BAC-Drd2-EGFP reporter mouse lines from GENSAT (Gene Expression Nervous System Atlas project; www.gensat.org; Gong et al., 2003) to eventually generate Zfp521-BrKO and control mice with D1- (Zfp521-BrKO; D1-EGFP and control; D1-EGFP) or D2-MSNs (Zfp521-BrKO; D2-EFP and control; D2-EGFP) expressing EGFP.

As with the quantification of DARPP-32 labeled cells, we assessed the density of D1-EGFP and D2-EGFP labeled MSNs in the DMS and DLS by unbiased cell counting of cells immunohistochemically stained for EGFP (Figure 3.1C and E). For both D1- and D2-MSN quantification, cells were counted under 40X magnification in multiple randomly selected ROIs in the DMS and DLS of matched coronal brain sections from 2 month-old Zfp521-BrKO; D1-EGFP (n = 4), control; D1-EGFP mice (n = 4), Zfp521-BrKO; D2-EGFP (n = 3) and control; D2-EGFP (n = 3) mice. Quantification of D1-EGFP labeled cell densities did not show a significant difference in the DMS (Student's t-test; $p = 0.311$) or the DLS (Student's t-test; $p = 0.494$) between Zfp521-BrKO and control mice expressing D1-EGFP (Figure 3.1D). Similarly, we did not observe a significant difference in D2-EGFP labeled cell densities between Zfp521-BrKO and control mice expressing D2-EGFP in either the DMS (Student's t-test; $p = 0.466$) or the DLS (Student's t-test; $p = 0.402$; Figure 3.1F).

Previous studies have shown that the deletion of Zfp423 (paralog of Zfp521) disrupts the pattern of ORN axonal projections to the olfactory bulb (Cheng and Reed, 2007) and deletion of Ebf1 (transcriptional partner of Zfp521) disrupts both the thalamocortical projections (Garel et al., 2002) and the striatonigral MSN projections through the direct pathway (Lobo et al., 2006, 2008). Although we did not observe a clear D1- or D2-MSN neuronal deficit in the striatum, we used the same Zfp521-BrKO and control expressing D1-EGFP or D2-EGFP to get a sense of whether there is a visible disruption of the striatonigral direct or striatopallidal indirect pathways as a result of conditional deletion of Zfp521. We examined the regions of the direct (striatum,

GPi, and SNr) and indirect (striatum, GPe) pathways in 2 month-old Zfp521-BrKO and control mice expressing either D1- or D2-EGFP (immunohistochemically stained for EGFP) and found no observable disruptions or glaring deficits.

3.3 Examination of Neurogenesis and Developmental Organization of the Striatum in Zfp521-BrKO Mice

As previously discussed, several studies not only show that Dlx1 and 2 only is critical in the differentiation of neurons originating from the proliferative regions of the LGE (MSNs) and MGE (cholinergic and GABAergic interneurons), but Zfp521 is likely to be a direct downstream transcriptional target of Dlx1/2 in this developmental program (Anderson et al., 1997; Cobos et al., 2005; Long et al., 2009a, 2009b). Furthermore, in Dlx1/2 knockout mice, the loss of Dlx1/2-mediated repression of differentiation results in the accumulation of partially differentiated neurons (particularly those fated to be late-born matrix MSNs) in an aberrantly enlarged LGE (Anderson et al., 1997; Cobos et al., 2007). We therefore hypothesized Zfp521 is involved in the early differentiation program in the embryonic telencephalon and that the dorsal striatal atrophy (and potentially the loss of PV-expressing interneurons) in Zfp521-BrKO is a result of disrupted neuronal differentiation of cells originating and migrating out of the proliferative regions of the LGE (and MGE for interneurons).

BrdU (5-bromo-2-deoxyuridine, a synthetic nucleoside analogue of thymidine) birth-dating experiments were performed to label cells during critical time-points in striatal neurogenesis: E11.5 (early developmental wave of striosome MSNs), E15.5 and E17.5 (the later developmental waves of matrix MSNs). BrdU injected into pregnant dams is taken up by developing embryos. BrdU is permanently incorporated into dividing cells during DNA synthesis, passed down to daughter cells following division, and can be detected later through immunohistochemical staining with BrdU antibodies (Wojtowicz and Kee, 2006). We examined the migration of cells labeled at E11.5, E15.5, and E17.5 by BrdU immunohistochemical staining

of coronal brain sections from postnatal day 0 (P0) Zfp521-BrKO and control pups. At all three developmental time-points, we did not observe an aberrant accumulation of BrdU labeled cells in SVG nor an enlargement of the LGE in place of the striatum (Figure 3.2), which is what we would have expected if Zfp521 deletion resulted in premature differentiation of cells in the proliferative zones and failure to properly migrate out into the mantle zone. At P0, both Zfp521-BrKO and controls showed cells labeled at E11.5 were correctly organized into patch compartments, indicating normal neurogenesis and differentiation of striosome MSNs. Similarly, P0 examination of BrdU labeled cells at E15.5 and E17.5 showed matrix-like striatal distribution that was similar in Zfp521-BrKO and control pups (Figure 3.2).

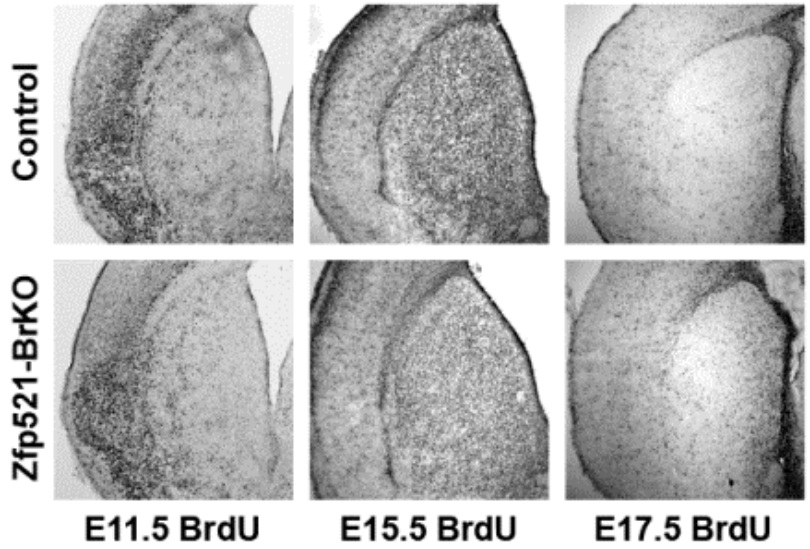

Figure 3.2 BrdU birth-dating shows intact neurogenesis and post-mitotic migration of developing striatal neurons in Zfp521-BrKO mice. Pregnant dams were injected with BrdU at critical time-points in striatal neurogenesis: E11.5 (early wave of striosome MSNs), E15.5 and E17.5 (the later waves of matrix MSNs). The BrdU taken up by developing embryos is permanently incorporated into dividing cells, passed down to daughter cells following division, and is detected at P0 through immunohistochemical staining with BrdU antibodies. At all three BrdU-injection time-points, the distribution and pattern of BrdU-labeled cells at P0 was indistinguishable between control and Zfp521-BrKO mice. In both control and mutant mice, cells labeled at E11.5 were organized into patch compartments and cells labeled at E15.5 an E17.5 showed matrix-like striatal distribution.

To further verify the results of the BrdU birth-dating and confirm that the overall striatal organization remained intact in Zfp521-BrKO mice, we examined select immunohistochemical markers for striosome/matrix MSNs and important striatal afferents in coronal sections from P0 Zfp521-BrKO and control mice. DARPP-32 staining showed that in both Zfp521-BrKO and

control mice, the MSNs were correctly organized into dense patches of striosome MSNs surrounded by uniformly distributed matrix MSNs (Figure 3.3). Furthermore, the mu-opioid receptor (MuOR) is a well-characterized marker of striosome MSNs (Graybiel, 1990) and immunohistochemical staining of MuOR verified that the dense patches of MSNs observed in P0 brain sections from both Zfp521-BrKO and control mice were striosome MSNs (Figure 3.3). Among the various striatal inputs, the two primary signaling afferents that are also the most implicated in TS are the dopaminergic nigrostriatal and glutamatergic corticostriatal projections, immunohistochemically identified by tyrosine hydroxylase (TH) and vesicular glutamate transporter 1 (VGluT1), respectively (Felling and Singer, 2011; Mink, 1996). As shown in Figure 3.3, these critical dopaminergic and glutamatergic signaling inputs to the striatum were intact in Zfp521-BrKO, comparable to control mice. Overall, the BrdU birth-dating and immunohistochemical studies suggest that in general, the embryonic neurogenesis, differentiation, and developmental organization of the striatum was largely maintained and comparable to controls, despite deletion of Zfp521 in the mutant mice.

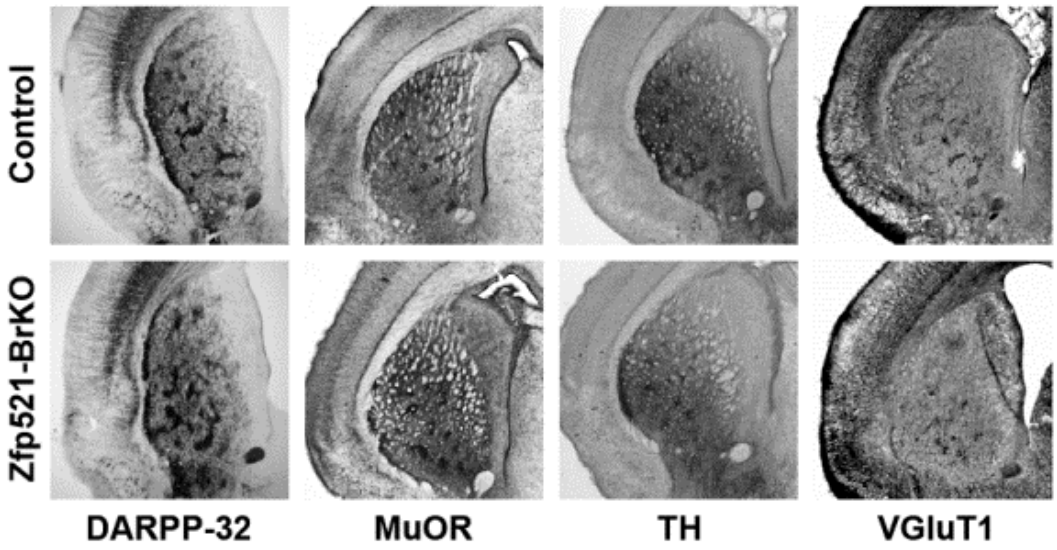

Figure 3.3 Organization of important striatal compartments and afferents implicated in TS are preserved in Zfp521-BrKO mice. Matched coronal sections from P0 control and Zfp521-BrKO mice were immunohistochemical stained for DARPP-32 (MSN marker),the mu-opioid receptor (marker for striosome MSNs), TH (marker for dopaminergic nigrostriatal afferents), and VgluT1 (marker for glutamatergic corticostriatal projections). Overall, the developmental organization of the MSNs and striatal afferents at P0 was intact in Zfp521-BrKO mice compared to controls; DARPP-32 and MuOR labeled cells were both organized into dense striosome compartments and both the TH and VGluT1 afferents were similarly distributed in control and Zfp521-BrKO striata.

3.4 Reduction of PV Expression in Select GABAergic Interneurons in Zfp521-BrKO Mice

As with the dorsal striatal volume loss examined in the previous sections, we wanted to assess the possible Zfp521-mediated developmental dysfunction underlying the selective loss of PV-expressing interneurons in the DMS of Zfp521-BrKO mice. Compelling evidence (Anderson et al., 1997; Cobos et al., 2005; Marin et al., 2000) suggests a significant overlap of the transcriptional mechanisms (mediated by Dlx genes) regulating the neurogenesis and differentiation of striatal MSN and interneurons originating from the LGE and MGE, respectively. We therefore initially hypothesized that the reduction of PV-expressing interneurons or the loss of PV gene expression in Zfp521-BrKO was also due to a similar disruption in the transcription program controlling the differentiation of interneuron precursors. However, in the absence of appreciable abnormalities in MSN differentiation in Zfp521-BrKO mice (as demonstrated in the previous section), we questioned whether the observed loss of PV interneurons was truly due to a developmental loss of the neurons themselves or a functional loss of PV expression in the intact GABAergic interneurons. Several studies of PV interneurons in the cortex (particularly the visual cortex) and striatum revealed that the postnatal expression of PV required for full maturation into the PV-expressing interneuron-subtype is strongly activity dependent (Cellerino et al., 1992; Patz, 2004; Rudkin and Sadikot, 1999; Schlösser et al., 1999; Vogt Weisenhorn et al., 1998) and increased in the presence of dopamine (Porter et al., 1999; Ross and Porter, 2002).

In order to assess actual striatal interneuron loss, independent of the postnatal activity-mediated expression of subtype-specific protein markers, we counted striatal cells expressing Nkx2.1 (NK2 homeobox 1), a transcription factor that is expressed in the VZ/SVZ of the MGE, upstream of Dlx1/2. Nkx2.1 regulates the neurogenesis of all interneuron subtypes originating from the MGE and remains expressed in fully differentiated, mature striatal cholinergic and GABAergic interneurons (Flandin et al., 2010; Marín and Rubenstein, 2001; Marin et al., 2000;

Sussel et al., 1999; Xu et al., 2008). We assessed the density of Nkx2.1-expressing cells in the DMS and DLS of matched coronal sections from 2 month-old Zfp521-BrKO (n = 5) and control (n = 5) mice (Figure 3.4A). Unbiased counting of cells immunohistochemically stained for Nkx2.1 did not reveal a significant difference in the density of Nkx2.1 expressing cells in the DMS (Student's t-test; p = 0.877) or the DLS (Student's t-test; p = 0.785) between Zfp521-BrKO and control mice (Figure 3.4B). Although far from conclusive, the finding that there was no significant interneuron loss in the dorsal striatum, specifically in the DMS where we observed the reduction of PV-expressing interneurons, suggested the regional deficit in PV interneurons was likely activity dependent rather than a developmental loss of neurons related to the loss of Zfp521.

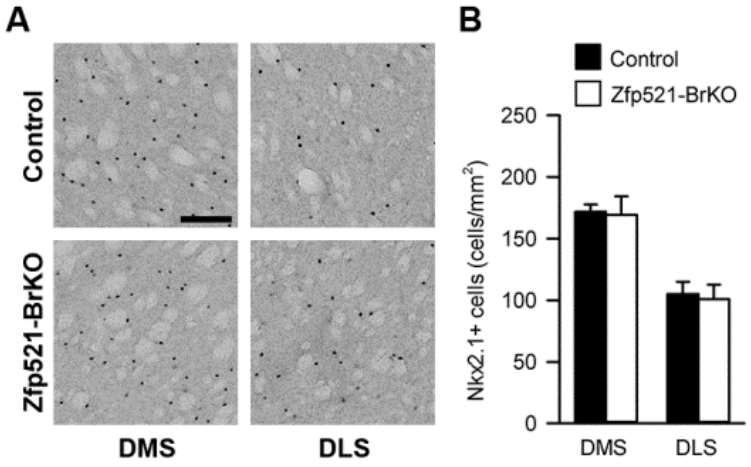

Figure 3.4 Region-specific striatal deficits in PV interneurons are more likely to be a reduction in activity-dependent PV expression rather than actual PV interneuron loss by cell death. (A) Nkx2.1 is a transcription factor expressed in all interneuron subtypes, including PV interneurons, that originate from the MGE. Nkx2.1 remains expressed in fully differentiated and mature cholinergic and GABAergic interneurons and can serve as a broad, non-subtype-specific interneuron marker. Representative Nkx2.1 immunohistochemical stainings in the DMS and DLS of matched coronal sections from 2 month-old control and Zfp521-BrKO mice. All images: 2.5X magnification, scale bar = 1mm. (B) Unbiased cell counting in the DMS and DLS did not reveal significant differences in the densities of Nkx2.1 labeled cells between control and Zfp521-BrKO mice (Control, n = 5; Zfp521-BrKO, n = 5; Student's t-test; p = 0.877 in DMS and p = 0.785in DLS). This suggested that overall, there was no significant interneuron loss (independent of subtype) in the striata of Zfp521-BrKO mice compared to controls and our earlier observation of PV interneuron loss in the DMS may actually reflect a reduction in activity-dependent PV-expression. Values are mean± SEM (* $p \leq 0.05$; ** $p \leq 0.01$; *** $p \leq 0.001$).

3.5 Discussion

The two prominent TS-like neuropathologies observed in Zfp521-BrKO mice were the reduction of dorsal striatal volume and the selective loss of PV-expressing GABAergic

interneurons specifically in the DMS. In this chapter, we attempted to elucidate the role of Zfp521 in developmental dysfunctions underlying these deficits through immunohistochemical staining of important striatal markers and BrdU birth-dating at critical embryonic time-points. Although Zfp521 is selectively enriched in striatonigral MSNs (Lobo et al., 2006) and has been shown to be critical in the early transition of embryonic stem cells into neural progenitors (Kamiya et al., 2011), very little is known about the transcriptional role of Zfp521 in later neural development, particularly in the differentiation of striatal MSNs and interneurons and the organization of the essential striatal compartments and circuits. It is through elucidating the developmental deficits of Zfp521-BrKO that we can provide insight into the normal transcriptional activity of Zfp521 in the context of BG development and function.

Overall, the developmental immunohistochemical and BrdU birth-dating studies detailed in this chapter were negative, indicating that striatal neurodevelopment up to P0 is largely intact in Zfp521-BrKO and comparable to control mice. In order to determine if the loss of striatal volume was due to a loss of MSN cell bodies or a reduction in MSN neuropil (dendrites and axons) we performed unbiased cell counting in the dorsomedial and dorsolateral striata of Zfp521-BrKO and control mice. An overall loss of MSNs cell bodies would have been reflected in lower MSN densities while increased cell densities may indicate a loss of neuropil or even cells being physically pressed closer together from increased pressure from aberrantly expanding ventricles. However, there was no discernible difference in the densities of MSNs between mutant and control mice in the ROIs selected.

Because Zfp521 is a striatonigral enriched gene, we next examined whether there would be a cell-autonomous difference in the number of striatonigral D1-MSNs or possibly a non-cell-autonomous difference in the number of striatopallidal D2-MSNs. A recent study using mice expressing both BAC-Drd1a-tdTomato and BAC-Drd2-EGFP (D1-MSNs labeled red and D2-MSNs labeled green) revealed that during early striatal development (E18), a significant

population of MSNs express both D1- and D2-reporter proteins. But by P0 and P14, there is extensive segregation of these D1- and D2-reporter proteins as the MSNs take on their mature, striatonigral or striatopallidal identities and express only D1-tdTomato or D2-EGFP, respectively (Thibault et al., 2013). A possible role of Zfp521 might be in the developmental segregation of D1- and D2-MSNs through a cell-autonomous transcriptional determination of a striatonigral fate or a non-cell-autonomous selection of a striatopallidal fate. We generated Zfp521-BrKO and control mice expressing BAC-Drd1a- or BAC-Drd2-EFGP to assess possible differences the D1- and D2-MSNs resulting from Zfp521 deletion. However, quantification of D1- and D2-EGFP labeled cells did not reveal a difference in densities or a shift in the relative numbers of D1- and D2-MSNs in the dorsal striata of Zfp521-BrKO compared to control mice. Furthermore, examination of the direct and indirect pathways in the D1- and D2-EGPF labeled mice did not reveal obvious disruptions or deficits in the MSN projections in Zfp521-BrKO mice.

Although the basic striatal composition of Zfp521-BrKO appeared comparable to control mice at the level of the striatonigral/striatopallidal (D1/D2) organization, it does not exclude the possibility of more subtle deficits at more complex levels of striatal organization, namely the striosome/matrix compartmentalization. While there is still much to be learned about the functional roles of the striosome and matrix, the general developmental pattern of these distinct striatal compartments is well-characterized. Neuronal precursors emerging from the proliferative zones (SV/SVZ) of the LGE migrate out to differentiate in the developing striatum of the mantle zone in two waves; an early wave consisting of striosome MSNs (starting around E11) and a later waves of matrix MSNs (E15 to E20). Currently, there is no direct evidence implicating Zfp521 in the differentiation of neurons originating from the ganglionic eminences of the embryonic telencephalon. However, several studies of a Dlx1/2 knockout and Ebf1 knockout suggest these transcription factors may all be intimately involved in the interconnected developmental programs of all striatal neurons (MSNs and interneurons). In our hypothesized

model, in the VZ/SVZ proliferative zones, downstream expression of Zfp521 by a Dlx1/2-medated transcriptional program (Long et al., 2009a, 2009b) leads to the down-regulation of Ebf1 by Zfp521 (Kiviranta et al., 2013). Inhibition of Ebf1's transcriptional activity, which normally down-regulates critical transcription factors that repress differentiation, keeps neuronal precursors in a non-differentiated, proliferative state in the VZ/SVZ (Garel et al., 1999). However, following migration out of the VZ/SVZ, neuronal precursors undergo differentiation in the mantle zone through down-regulation of Dlx1/2. Decreased Dlx1/2 activity eventually reduces the transcription of Zfp521 which in turn leads to an up-regulation of Ebf1 to block the transcription of genes that suppressed neuronal differentiation in the VZ/SVZ. Although speculative, our preliminary microarray analysis of Zfp521-BrKO mice (data not shown) showed an up-regulation of Dlx1 in the striatum in the absence of Zfp521, suggesting a possible feedback down-regulation of Dlx1 by Zfp521 once cells are out of the cell cycle in the VZ/SVZ. Instead of Zfp521, it is just as likely that part of Ebf1's role in promoting differentiation in the mantle zone is through feedback down-regulation of Dlx1/2.

In the context of this hypothesized neural developmental role of Zfp521, we used BrdU birth-dating label to neuronal precursors at time-points critical for striosome (E11.5) and matrix (E15.5 and E17.5) neurogenesis and examined the migration and differentiation of these cells at P0. These birth-dating experiments revealed that the neurogenesis and migration of striosome and matrix MSNs were largely intact in Zfp521-BrKO mice. Immunohistochemical staining of striatal markers for MSNs, striosome/matrix, and important afferents (both dopaminergic and glutamatergic) at P0 further verified the results of the birth-dating experiments by showing that the overall organization of the striatal compartments and circuits were comparable between Zfp521-BrKO and control mice.

Without strong evidence supporting the role of Zfp521 in neurogenesis and early neuronal differentiation, we attempted to confirm whether the apparent deficit of PV-expressing

neurons in Zfp521-BrKO was a result of PV-interneuron cell body loss through disrupted development, or a reduction of activity-dependent PV expression in mature, fully differentiated GABAergic interneurons. Quantification of cells immunohistochemically labeled for Nkx2.1, an early transcription factor that remains expressed in most mature striatal cholinergic and GABAergic interneurons, revealed that there was no significant interneuron loss in the dorsal striata of Zfp21-BrKO mice.

The implication that the reduction in PV-expressing interneurons in the DMS of Zfp521-BrKO mice may actually be due to a postnatal, activity-dependent reduction in PV-expression is an important insight to understanding the developmental deficits in the striata of the mutant mice. While we spent considerable effort trying to elucidate the role of Zfp521 in striatal MSN and interneuron neurogenesis and differentiation, the true Zfp521-related developmental dysfunction may be occurring in the final stages of neuronal maturation that occurs during the first few weeks of the critical postnatal period. Several axonal tracing studies have shown that while striosome MSNs establish their striatonigral projections by P0, the later-born matrix neurons are sending out and establishing their axonal projections during the first postnatal week (Fishell and van der Kooy, 1989). This first postnatal week also coincides with a critical period of pruning and cell death during which striatal neurons without established axonal projections (predominately late-born matrix MSNs) are considerably less likely to survive (Fentress et al., 1981; Fishell and van der Kooy, 1991; van der Kooy and Kooy, 1996). Furthermore, studies show that the differentiation and functional maturation of late-born matrix neurons (Butler et al., 1998; Liu and Graybiel, 1992; Partridge et al., 2000) and the activity-dependent expression of PV and maturation of PV-interneurons (Schlösser et al., 1999) in the dorsal striatum occurs in a lateral-to-medial gradient through the first two weeks of postnatal development.

In Zfp521-BrKO mice, both the reduced striatal volume and loss of PV-expression in interneurons was specifically localized to the dorsomedial striatum. Although we quantified the

volume of the dorsal striatum as a whole, in looking at the irregular shape of the dorsal striata of Zfp521-BrKO mice, it was apparent the most medial region of the dorsal striatum was missing (with an expanded lateral ventricle replacing it). Furthermore, the other remaining regions of the dorsal striatum appeared completely intact (both MSNs and interneurons) and properly organized. Taken all together, it suggested that the neuropathologies observed in Zfp521-BrKO mice were a result of a selective postnatal developmental dysfunction or deficits of late-born MSNs and interneurons specifically in the DMS. Currently, it is difficult to speculate whether Zfp521 is directly involved in the postnatal activities required for the maturation and survival of these region-specific neurons. We do not know if deletion of Zfp521 somehow selectively disrupts the embryonic differentiation of the late-born MSNs targeted to the DMS and initiates the pathological conditions for the later postnatal deficits. Although the studies discussed in chapter have been limited and are far from what we can consider a complete and thorough investigation, there is sufficient evidence to suggest that we need to expand our research focus and the examine the critical postnatal period of Zfp521-BrKO mice. Furthermore, although it is now outside the scope of this dissertation, continued studies to elucidate the transcriptional role of Zfp521, in both its normal and pathological function in this mouse model of TS, requires new genetic tools, such as Zfp521-EGFP reporter mice, to identify the lineage of cells developmentally regulated by Zfp521.

Chapter 4

Striatopallidal D2-MSN and Indirect Pathway Dysfunction in Zfp521-BrKO Mice

4.1 Introduction

Decades of anatomical, physiological, pharmacological, and lesion studies of the BG have established the generally well-accepted view that this circuit is critical in gating the multitude of competing excitatory motor (behavioral) inputs generated from throughout the cortex. During the default resting state, the tonically active indirect pathway maintains the inhibitory output of the basal ganglia that puts the “brake” on unwanted movements and behaviors. During the execution of desired, volitional movement, focal activation of specific striatonigral MSNs releases the inhibition of select circuits of the direct pathway which regulates the motor output of the BG. Concurrently, the inhibition of competing direct pathway outputs from the surrounding striatonigral MSNs is further strengthened, thus ensuring the regulated BG output of just the intended motor behavior (Albin et al., 1989; DeLong, 1990; Mink, 1996, 2001).

The various circuitry and signaling dysfunctions within this classic model (such as hyperinnervation by excitatory corticostriatal inputs) can account for the pathological motor behaviors in TS patients. More specifically, the dopamine-mediated imbalance between the striatonigral direct pathway and the striatopallidal indirect pathway in modulating BG output is considered to be the primary functional deficit in TS (Buse et al., 2013; Felling and Singer, 2011). It has been hypothesized that this DA imbalance could be due to hyperinnervation by nigrostriatal DA terminals, supersensitive postsynaptic striatal DA receptors, increased phasic (spike- or activity-dependent) DA release, reduced tonic (homeostatic) DA, or increased DAT activity which lowers extracellular DA levels and directly disrupts the regulation both the postsynaptic phasic and presynaptic tonic DA components (Buse et al., 2013; Singer and Minzer, 2003). However, there is currently no strong consensus on the nature of this

dopaminergic dysfunction and consequently, there is also a lack of comprehensive understanding of the molecular and signaling mechanisms of the common TS pharmacologies.

Interestingly, just as this DA hypothesis of TS originated from early clinical studies which reported the successful treatment of motor tics with low doses of the neuroleptic, haloperidol (Mink, 2001; Shapiro and Shapiro, 1968; Singer et al., 1982), our own insights into the circuitry dysfunction of our mouse model of TS also developed from the behavioral response of Zfp521-BrKO mice to haloperidol; specifically, from the differing adverse cataleptic responses to high doses of haloperidol between mutant and control mice. In TS patients, careful adjustment of low doses of haloperidol is important in effectively treating motor tics while minimizing the lesser side-effects such as sedation and avoiding the more serious adverse effects such as tardive dyskinesia and catalepsy (Sallee et al., 1997; Sandor, 2003; Shapiro and Shapiro, 1968; Shapiro et al., 1989). In rodents, haloperidol-induced catalepsy (postural rigidity and the lack of spontaneous motor activity) has been long studied to understand the adverse effects of classic neuroleptics and used to pharmacologically model aspects of movement disorders (such as Parkinson's Disease) to elucidate the role of striatal dopaminergic signaling in regulating motor behaviors (Degos et al., 2005; Hoffman and Donovan, 1995; Kapur and Mamo, 2003; De Ryck et al., 1980; Sanberg, 1980).

Ligand-binding and receptor occupancy experiments have shown that haloperidol is a mixed D2-antagonist and haloperidol-induced catalepsy is mediated by postsynaptic D2 receptors on striatopallidal MSNs (Creese et al., 1975; Natesan et al., 2006; Sanberg, 1980; Wadenberg et al., 2001). The role of D2 receptors in haloperidol-induced catalepsy was further demonstrated in studies which showed that D2 receptor knockout mice do not present spontaneous or haloperidol-induced catalepsy (Boulay et al., 2000; Kelly et al., 1998). Furthermore, high doses of haloperidol injected into mice expressing either BAC-Drd1a-EGFP or BAC-Drd2-EGFP to genetically label the D1- and D2-MSNS, respectively, revealed that

haloperidol selectively activates the phosphorylation of important signaling proteins in dorsal striatal D2-MSNs, including ERK (extracellular signal-regulated kinase), MSK1 (mitogen- and stress-activated kinase-1), and H3 (histone H3; Bertran-Gonzalez et al., 2008, 2009). By crossing an Cre-inducible diphtheria toxin receptor (DTR) mouse line with either D1- or D2-Cre mouse lines and then stereotaxically injecting diphtheria toxin into discrete regions of the striatum, Durieux and colleagues (2011) were able to selectively ablate D1- or D2-MSNs in functionally distinct dorsal striatal regions and revealed that the striatopallidal D2-MSNs in the DMS are required for the cataleptic effect of haloperidol.

In Chapter 2, we showed that low doses of haloperidol can suppress the tic-like behaviors in Zfp521-BrKO mice, similar to pharmacological treatment of motor tics in TS patients. In this chapter, we present evidence that Zfp521-BrKO mice are highly resistant to the cataleptic effect of haloperidol, suggesting that the striatopallidal D2-MSNs and the indirect pathway are dysfunctional in mutant mice. By examining the striatal D1- and D2-MSN activity of Zfp521-BrKO mice in response to haloperidol, we may gain circuitry insights into the suppression of tic-like behaviors and elucidate details on the regulation of unwanted behaviors by tonic indirect pathway activity, an often overlooked aspect of the DA signaling imbalance in TS.

4.2 Zfp521-BrKO Mice Are Highly Resistant to Haloperidol-Induced Catalepsy

An important concern in using haloperidol to treat the pathological behaviors of TS is the selection of the correct dose to treat the motor tics without overly sedating, or worse, inducing catalepsy in patients. Similarly, to determine the correct dose of haloperidol that would balance tic-suppression with minimal adverse side-effects in both Zfp521-BrKO and control mice, we performed dose-response experiments, with 0.1, 0.25, 0.5, 1.0, 2.0, and 5.0 mg/kg body weight doses of haloperidol and examined both tic-suppression and catalepsy. Two commonly used tests for catalepsy in rodents include the grid test and the bar test and both essentially involve

placing the animal into an unusual posture or position and recording the time taken to correct their posture or move from the awkward position (Hoffman and Donovan, 1995; Sanberg et al., 1988). In the grid test, rodents are placed on a wire grid that is inclined between 45 to 60 degrees and catalepsy is measured as the time taken to move down this inclined surface to level ground; normal animals will quickly move down the grid and away from this awkward position while cataleptic animals will generally stay immobile and not attempt to reposition themselves or move down this slanted surface (Figure 4.1A). In the bar test, the forepaws of the animals are placed on a bar several centimeters above the testing surface to position them into an unusual rearing-like posture (they are hanging upright by their forepaws on the bar) and again, catalepsy is measured as the time taken to correct their bodies into a normal posture; normal animals will quickly move themselves off the bar and onto the ground while cataleptic animals will stay immobile in that unusual posture (Figure 4.1B).

Using the grid test as our primary measure of catalepsy (and verified with the bar test; data not shown), we generated a haloperidol dose-response curve for catalepsy (2 month-old; control, n = 6; Zfp521-BrKO, n = 6). We found that control mice became significantly cataleptic at haloperidol doses greater than 1.0 mg/kg while Zfp521-BrKO are highly resistant to haloperidol-induced catalepsy, even at doses as high as 5.0 mg/kg (Figure 4.1C). Two-way repeated measures ANOVA revealed a significant effect of genotype ($F_{1,60} = 132.990$; $p < 0.001$) and haloperidol dose ($F_{6,60} = 209.891$, $p < 0.001$) on catalepsy times, with a significant genotype x dose interaction ($F_{6,60} = 74.445$; $p < 0.001$). Although Zfp521-BrKO mice began to show indications of catalepsy at the highest dose of haloperidol tested, post-hoc analysis revealed mutant are significantly less cataleptic compared to control mice at the following doses of haloperidol: 0.5 mg/kg (Student's t-test; $p = 0.004$), 1.0 mg/kg (Student's t-test; $p = 0.009$), 2.0 mg/kg (Student's t-test; $p < 0.001$), 5.0 mg/kg (Student's t-test; $p < 0.001$).

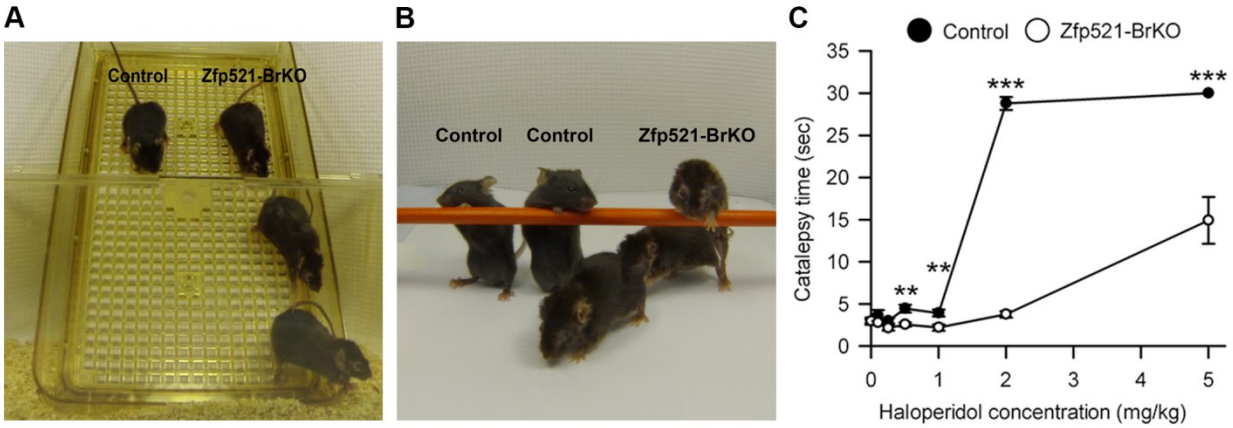

Figure 4.1 Zfp521-BrKO are highly resistant to haloperidol-induced catalepsy. (A) The grid test is one of the more commonly used methods to assess catalepsy (postural rigidity) in mice. Mice are place on a wire grid that is inclined between 45 to 60 degrees and catalepsy is measured as the time taken to move down this inclined surface. (B) The bar test is another commonly used assessment of catalepsy in which mice are positioned with their forepaws placed on a bar that is elevated several centimeters above the surface (hanging upright by their forepaws in an unusual rearing-like posture) and catalepsy is measured as the time taken to correct their bodies into a normal position on the ground. In both the grid test and bar test, haloperidol treated control mice were cataleptic and remained immobile while similarly treated Zfp521-BrKO mice were resistant to catalepsy and quickly moved or positioned themselves away from the awkward positions. (C) 2 month-old control (n = 6) and Zfp521-BrKO (n = 6) mice were injected with increasing doses of haloperidol (0.1, 0.25, 0.5, 1.0, 2.0, and 5.0 mg/kg) and catalepsy was assessed 1 hour post-injection using the grid test (and verified with the bar test; data not shown). While control mice become significantly cataleptic at haloperidol doses greater than 1.0 mg/kg, Zfp521-BrKO remained resistant to haloperidol-induced catalepsy even at 5.0 mg/kg. Two-way repeated measures ANOVA of the haloperidol dose-response curve revealed a significant effect of genotype ($F_{1,60}$ = 132.990; $p < 0.001$) and haloperidol dose ($F_{6,60}$ = 209.891, $p < 0.001$) on catalepsy times, with a significant genotype x dose interaction ($F_{6,60}$ = 74.445; $p < 0.001$). Post-hoc analysis further showed Zfp521-BrKO mice were significantly less cataleptic compared to control mice at 0.5 (Student's t-test; $p = 0.004$), 1.0 (Student's t-test; $p = 0.009$), 2.0 (Student's t-test; $p < 0.001$), 5.0 mg/kg haloperidol (Student's t-test; $p < 0.001$). Values are mean± SEM (* $p \leq 0.05$; ** $p \leq 0.01$; *** $p \leq 0.001$).

Studies have shown that haloperidol-induced catalepsy is mediated by striatopallidal D2-MSNs, specifically those in the dorsomedial region of the striatum (Boulay et al., 2000; Durieux et al., 2011; Kelly et al., 1998). In order to determine if the resistance to haloperidol-induced catalepsy in Zfp521-BrKO mice was due to a dysfunction or deficit of D2-MSNs in the DMS, we quantified cells immunohistochemically labeled for phosphorylated-histone H3 (p-H3), which is a D2-MSN signaling protein selectively activated by haloperidol (Bertran-Gonzalez et al., 2008, 2009). Matched coronal sections from brains taken from 2 month-old Zfp521-BrKO (n = 6) and control (n = 7) mice one hour post-injection of 1.0 mg/kg haloperidol were immunohistochemically stained for p-H3 (Figure 4.2A). We assessed the density of p-H3 labeled cells in the dorsal striatum by unbiased cell counting methods and found that the density of p-H3+ cells was significantly reduced in both the DMS and DLS (Student's t-test; $p = 0.005$ and $p = 0.01$, respectively) in Zfp521-BrKO compared to control mice. In the previous chapter,

we showed that the density of D2-MSNs in the dorsal striatum was comparable between mutant and control mice. This strongly suggested that this decrease in p-H3 labeled cells in Zfp521-BrKO was not a result of D2-MSN cell loss, but was likely due to reduced activation of p-H3 by haloperidol in hypofunctional D2-MSNs. Consequently, the resistance to haloperidol-induced catalepsy observed in Zfp521-BrKO mice could be specifically contributed to hypofunctional D2-MSNs in the DMS.

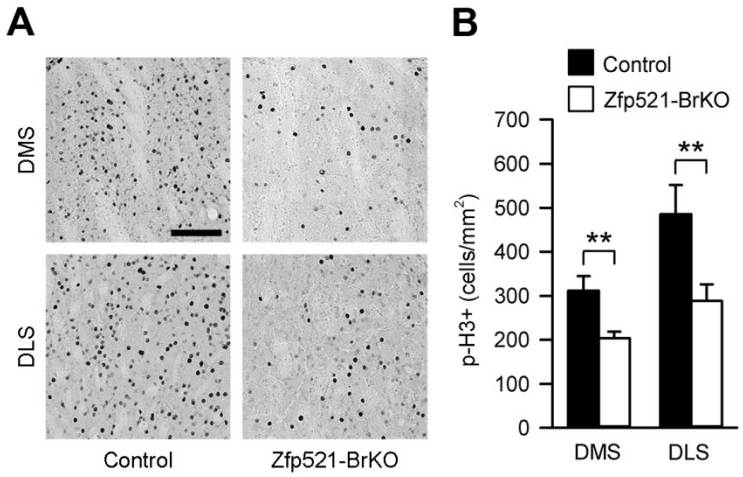

Figure 4.2 Haloperidol-induced activation of phosphorylated-H3 in D2-MSNs is reduced in the dorsal striata of Zfp521-BrKO mice. (A) Phosphorylated-histone H3 (p-H3) is a signaling protein selectively activated by haloperidol in striatopallidal D2-MSNs. 2 month-old control and Zfp521-BrKO mice were injected with 1.0 mg/kg haloperidol and brains were collected 1 hour post-injection. Immunohistochemically staining showed haloperidol-induced activation of p-H3 in the DMS and DLS of control and Zfp521-BrKO mice. All images: 2.5X magnification, scale bar = 1mm. (B) Density of p-H3 labeled cells in the DMS and DLS was assessed by unbiased counting methods. Compared to controls, Zfp521-BrKO mice showed a significant reduction in haloperidol-induced expression of p-H3 in both the DMS and DLS (Student's t-test; $p = 0.005$ in the DMS and $p = 0.01$ in the DLS). Values are mean± SEM (* $p \leq 0.05$; ** $p \leq 0.01$; *** $p \leq 0.001$).

4.3 Aberrant Electrophysiology of Haloperidol-Treated D1- and D2-MSNs in Zfp521-BrKO

Working with Sandra Holley and Carlos Cepeda in Michael Levine's laboratory (UCLA), we examined the electrophysiological properties of the D1- and D2-MSNs in Zfp521-BrKO and control mice to verify the apparent D2-MSN dysfunction inferred from the behavioral and immunohistochemical studies of haloperidol-treated mice. Zfp521-BrKO and control mice crossed with BAC-Drd1a- or BAC-Drd2-EGFP reporter lines (discussed in Chapter 3) were used to fluorescently label and visually distinguish the two MSN-subtypes for D1- and D2-MSN-specific patch-clamp electrophysiological recordings. Analysis of the basal membrane

properties, including capacitance, input resistance, and time constant, of the D1- and D2-EGFP labeled MSNs did not reveal significant differences in D2-MSNs between Zfp521-BrKO and control mice (Figure 4.3A). On the other hand, the time capacitance and time constant of D1-MSNs in Zfp521-BrKO (Figure 4.3B) was significantly reduced compared to controls, suggesting the size of D1-MSNs may be smaller in mutant mice (control, n = 28; Zfp521-BrKO, n = 20; Student's t-test; $p < 0.05$ for both).

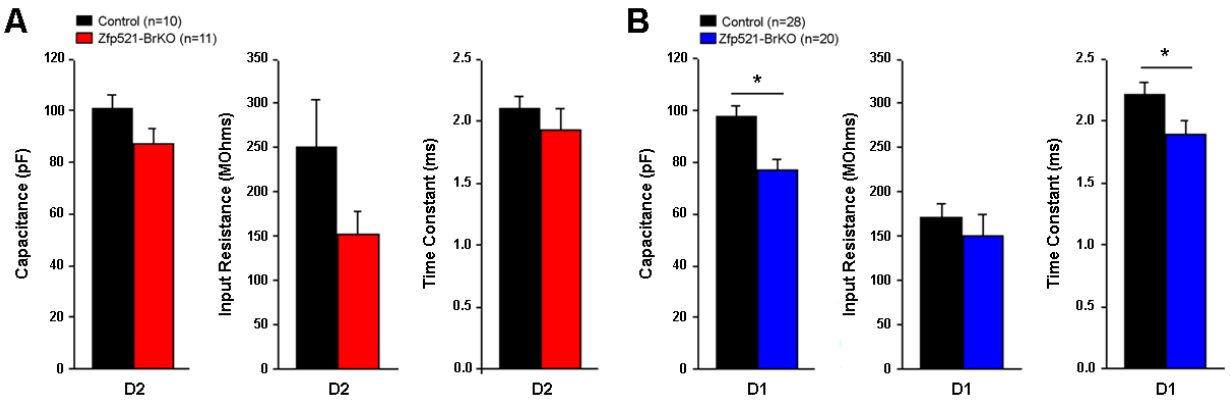

Figure 4.3 Compared to MSNs from control mice, striatal D1-MSNs from Zfp521-BrKO mice show significantly altered cell membrane properties while D2- MSNs do not differ. Measurements of cell membrane capacitance, input resistance and time constant in D2-MSNs (A) and D1-MSNs (B) compared to control cells (black). D1-MSNs from Zfp521-BrKO mice have reduced cell membrane capacitance and time constant values suggesting cell somas may be smaller in mutant animals compared to controls (Student's t-test; $p < 0.05$). Values are mean± SEM (* $p \leq 0.05$; ** $p \leq 0.01$; *** $p \leq 0.001$)

The spontaneous excitatory postsynaptic currents (sEPSCs) in D1- and D2-MSNs from the DMS were recorded before and after acute bath-application of 10 μM haloperidol in the presence of 10 μM bicuculline, a $GABA_A$ receptor antagonist used to block spontaneous inhibitory postsynaptic currents, or sIPSCs and measure only sEPSCs (Figure 4.4A). Because D2 receptors are inhibitory $G_{\alpha i/o}$-coupled, we expected an increase in sEPSC frequency in activated D2-MSNs in response to D2-receptor antagonism by haloperidol. In comparing the percent change in sEPSC activity in D1- and D2-MSNs after haloperidol treatment, we observed the expected increase in sEPSC frequencies in D2-MSNs from control but not Zfp521-BrKO mice (control, n = 10; Zfp521-BrKO, n = 11; Student's t-test; $p < 0.05$). Conversely, while D1-MSNs from control showed very little response to haloperidol, there was an unexpected

increase in sEPSC frequency in D1-MSNs from Zfp521-BrKO mice in response to haloperidol (control, n = 14; Zfp521-BrKO, n = 9; Student's t-test; $p < 0.05$). Although the mechanism by which haloperidol paradoxically activated D1-MSNs in Zfp521-BrKO mice is not entirely clear, it suggested the possibility that haloperidol suppression of tic-like behaviors in mutant mice may function through a D1-MSN-mediated mechanism; this will be further explored in Chapter 5.

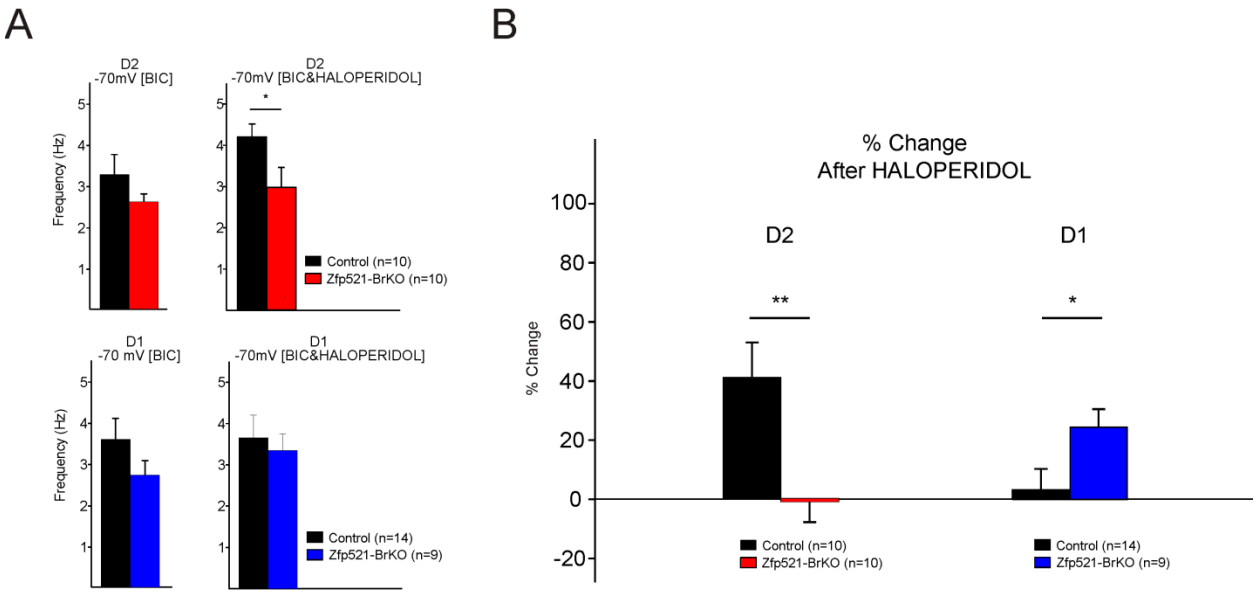

Figure 4.4 Differential effects of haloperidol on spontaneous excitatory postsynaptic currents (sEPSCs) in D1- and D2-EGFP expressing MSNs suggests impairment of striatal dopaminergic modulation of glutamatergic synaptic transmission in Zfp521-BrKO mice. (A) Average sEPSC frequencies in D1- and D2-EGFP expressing MSNs before and after acute application of haloperidol (10μM) and in the presence of the $GABA_A$ receptor antagonist, bicuculline (10μM). The increase in average sEPSC frequencies in control D2-MSNs after the application of haloperidol created a significant difference in the sEPSC frequencies between control and Zfp521-BrKO D2-MSNs (Student's t-test; $p < 0.05$). (B) Percent change in sEPSC activity in D1- and D2-EGFP expressing MSNs after haloperidol application. The expected increase in sEPSC frequency with the mixed D2-receptor antagonist haloperidol was seen in D2-MSNs from control but not Zfp521-BrKO mice (Student's t-test; $p < 0.01$). In contrast, haloperidol produced an unexpected increase in sEPSC frequency in D1-MSNs from Zfp521-BrKO mice that was significant compared to controls (Student's t-test; $p < 0.05$). Values are mean± SEM (* $p \leq 0.05$; ** $p \leq 0.01$; *** $p \leq 0.001$).

4.4 Optogenetic Evidence of Hypofunctional Striatopallidal D2-MSNs and Indirect Pathway Dysfunction in Zfp521-BrKO Mice

The pharmacological manipulation of D2-receptors by haloperidol in our behavioral and electrophysiological studies strongly implicated hypofunctional striatopallidal MSNs and suggested that deficient indirect pathway signaling may contribute to the generation of tic-like behaviors in Zfp521-BrKO mice. To dissociate D2-MSN activity from D2-receptor function and

directly address the question of deficient indirect pathway signaling mediated by hypofunctional D2-MSNs in Zfp521-BrKO mice, we employed Cre-dependent viral expression of a light-activated cation channel, channelrhodopsin-2 (ChR2), to optogenetically activate D2-MSNs and the corresponding indirect pathway and examine the effects on locomotor and tic-like behaviors in mutant and control mice (Boyden et al., 2005; Luo et al., 2008; Yizhar et al., 2011; Zhang et al., 2010).

Following the same breeding strategy used to generate Zfp521-BrKO and control mice expressing D1- or D2-EGFP, Zfp521-Hets were crossed with a BAC-Drd2-Cre mouse line from GENSAT (Gene Expression Nervous System Atlas project; www.gensat.org; Gong et al., 2003) to eventually generate Zfp521-BrKO and control mice expressing BAC-Drd2-Cre (Zfp521-BrKO; D2-Cre and control; D2-Cre). To generate a CNS-conditional knockout of Zfp521 and have D2-Cre, Zfp521-BrKO; D2-Cre mice have both Nestin-Cre and BAC-Drd2-Cre alleles. However, expression of Nestin-Cre occurs primarily during early embryonic stages (neural progenitors at around neural tube development) and in postnatal and adult stages, its expression is sparse throughout the brain and restricted to small clusters of adult neural stem cells in limited proliferative regions such as the hippocampal dentate gyrus (Dahlstrand et al., 1995; Tronche et al., 1999; Wei et al., 2002). Thus, in the mice that have both the Nestin-Cre and BAC-Drd2-Cre alleles, expression of Cre in the postnatal brain was predominately driven by the Drd2 promoter. It should also be noted that the control; D2-Cre mice used for these optogenetic experiments were either Zfp521$^{+/+}$; Nestin-Cre; BAC-Drd2-Cre or Zfp521$^{+/+}$; BAC-Drd2-Cre mice and both the expression of Cre and the behavioral response to optogenetic activation of D2-MSNs was comparable between these two control genotypes (data not shown).

To selectively express ChR2 in dorsal striatal D2-MSNs, Zfp521-BrKO and control mice expressing D2-Cre were injected with rAAV2/1-CAGGS-FLEX-ChR2-tdTomato, a recombinant adeno-associated virus (rAAV) containing a floxed inverted open reading frame (for Cre-

mediated flip-excision or FLEX) encoding ChrR2 fused with tdTomato (red fluorescent protein), driven by the ubiquitously expressed CAG promoter. In D2-MSNs, Cre-mediated recombination at the loxP sites “flips” the inverted open reading frame into the correct orientation that allows expression of ChR2-tdTomato. The rAAV2/1 pseudotype efficiently delivers its viral vector to most neuronal cell types and extensive anterograde transport of the transgenic protein allows for clear anterograde tracing of axonal projections of the infected cells with fluorescent proteins (Burger et al., 2004; McFarland et al., 2009; Taymans et al., 2007).

Following targeted stereotaxic injection of the rAAV2/1-CAGGS-FLEX-ChR2-tdTomato into the dorsal striata of Zfp521-BrKO and control mice expressing D2-Cre, we could visually verify the expression of ChR2-tdTomato primarily within the D2-MSNs by observing the labeling of tdTomato restricted to the striatum and the axonal projections to the GPe, which forms the circuit of the D2-MSN-mediated indirect pathway (Figure 4.5A). Furthermore, in mice that only express Nestin-Cre, ChR2-tdTomato expression is found only in a small number of scattered cells and did not show the same pattern or high level of expression seen in mice that also express D2-Cre (Figure 4.5A). In the same surgical procedure to stereotaxically inject the viral vector, we also implanted the optical fibers which would later be used to deliver the stimulating light into the same dorsal striatal areas that received the viral injections.

After 3 to 4 weeks following viral injection to allow for sufficient expression of ChR2 (Zhang et al., 2010), Zfp521-BrKO; D2-Cre and control; D2-Cre mice expressing ChR2 (Zfp521-BrKO; D2-ChR2 and control; D2-ChR2, respectively) were video recorded in the behavioral chamber. Optical fibers delivering blue light from a 473nm laser source were connected to the fiber optic implants and Zfp521-BrKO and control mice expressing D2-ChR2 were analyzed for locomotor activity and tic-like behaviors with and without light stimulation of D2-MSNs through ChR2. Each 3-minute testing session consisted 6 repeated cycles of a 10-second pre-laser

period followed by 10-seconds of laser activation of ChR2 and then a 10-second post-laser period.

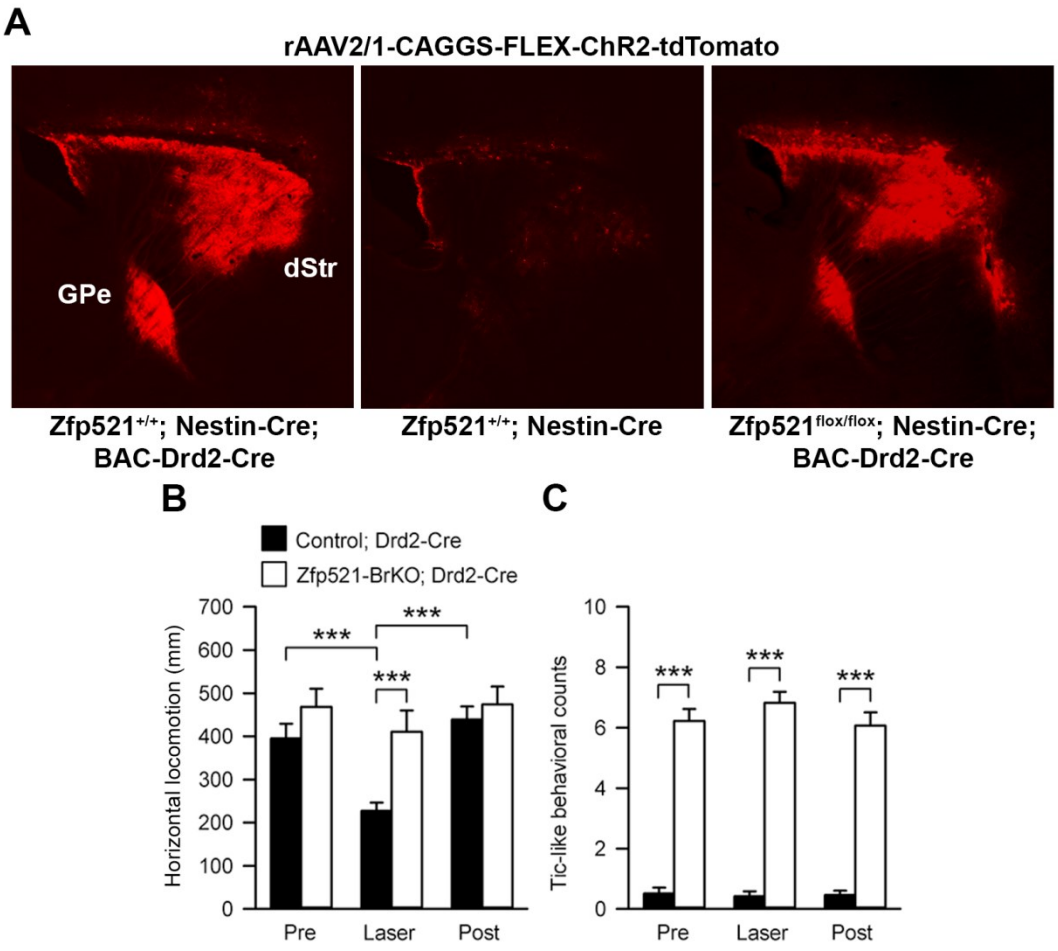

Figure 4.5 Optogenetic activation of D2-MSNs expressing channelrhodopsin-2 (ChR2) does not suppress locomotion or tic-like behaviors in Zfp521-BrKO mice. (A) Control and Zfp521-BrKO mice expressing BAC-Drd2-Cre and Nestin-Cre were stereotaxically injected with the viral vector, rAAV2/1-CAGGS-FLEX-ChR2-tdTomato, in the dorsal striatum (dStr) to selectively express the light-activated cation channel, ChR2, in striatopallidal D2-MSNs. Three to four weeks post-injection, fluorescent labeling by tdTomato (red fluorescent protein) revealed expression of the viral vector is restricted to the D2-MSNs in striatum and their axonal projections to the external segment of the globus pallidus (GPe) which forms the circuit of the indirect pathway. As a control to show that Nestin-Cre expression occurs primarily in early embryonic stages and will not the overlap with the D2-Cre-mediated viral expression of ChR2 in 2 month-old mice, control mice expressing only Nestin-Cre were also stereotaxically injected with rAAV2/1-CAGGS-FLEX-ChR2-tdTomato into the dorsal striatum. In the mice only expressing Nestin-Cre, tdTomato expression was limited to scattered cells and did not show the same expression levels or patterns as D2-Cre expressing control and Zfp521-BrKO mice. (B) Optical fibers connected to a 473nm laser source were attached to the fiber optic implants surgically placed in the same coordinates as the viral injections in control (n = 3) and Zfp521-BrKO (n = 3) mice expressing D2-ChR2. Mice were placed in the behavioral chamber, video-recorded, and analyzed for locomotor activity and tic-like behaviors in 3-minute testing sessions consisting of repeated cycles of a 10-second pre-laser period followed by a 10-second period of laser activation of ChR2 and then a 10-second post-laser period. Quantification of locomotor activity showed laser activation of ChR2 in D2-MSNs significantly reduced locomotion in control mice compared to locomotor activity during the pre- and post-laser periods (Student's t-test; $p < 0.001$ for pre- and $p < 0.001$ for post-laser comparisons) but not in Zfp521-BrKO mice. Laser activation of D2-ChR2 also significantly reduced locomotion in controls compared to Zfp521-BrKO mice (Student's t-test; $p < 0.001$). (C) Hand-scored quantification of total tic-like behaviors revealed no significant changes in Zfp521-BrKO during periods of laser-activation of D2-ChR2 compared to pre- and post-laser periods (Mann-Whitney U-test; $p = 0.272$ for pre- and $p = 0.115$ for post-laser comparisons). The absence of locomotor- and tic-suppression in Zfp521-BrKO mice by optogenetic activation of D2-MSNs expressing ChR2 provided evidence of hypofunctional striatopallidal MSNs and the indirect-pathway in mutant mice. Values are mean± SEM (* $p \leq 0.05$; ** $p \leq 0.01$; *** $p \leq 0.001$).

Automated analysis of the locomotor activity of each of three 10-second periods (pre-, laser, and post-) showed that stimulation of D2-MSNs and the indirect pathways by light activation of D2-ChR2 significantly reduced locomotion (horizontal distance traveled) in control (n = 3) but not Zfp521-BrKO mice (n = 3, Figure 4.5B). Compared to the pre- and post-laser periods, laser activation significantly reduced locomotion in control mice (Student's t-test; $p < 0.001$ for both comparisons) but reductions in locomotion were not observed in Zfp521-BrKO mice. During the 10-second periods of D2-ChR2 laser activation, control mice engaged in exploratory locomotion would freeze and then resume moving once the laser was turned off.

Hand-scoring of the tic-like behavioral counts during each of the three 10-second periods revealed that light activation of D2-MSNs and the indirect pathway through ChR2 did not suppress the tic-like behaviors in Zfp521-BrKO mice (Figure 4.5C). Mann-Whitney U-test analysis of the tic-like behavioral counts in Zfp521-BrKO mice during the pre- and post-laser periods compared to the period of laser stimulation showed no significant changes in tic-like behavioral counts ($p = 0.272$ and $p = 0.115$, respectively). In each period, the tic-like behaviors counts were significantly greater Zfp521-BrKO than control mice (Student's t-test; $p < 0.001$ for all three periods). We observed Zfp521-BrKO continued the bouts of tic-like behavior that began prior to laser activation as well as began new bouts of different tic-like behaviors during the 10-secod periods of D2-ChR2 stimulation by light. Through optogenetic activation of D2-ChR2, we directly showed the striatopallidal MSNs and the indirect pathway, which is considered to generate inhibitory output from the BG circuit to suppress cortically-driven motor behaviors, were hypofunctional in Zfp521-BrKO mice and indicated a possible deficit in the tonic inhibition of unwanted motor signals which may underlie the tic-like behaviors.

4.5 Discussion

In this chapter, we provided multiple lines of evidence from behavioral, immunohistochemical, and optogenetic experiments to support the hypothesis that a deficient

indirect pathway, mediated by hypofunctional striatopallidal D2-MSNs, is the BG circuitry dysfunction that contributes to the tic-like behaviors in Zfp521-BrKO mice. How the developmental role of Zfp521 (discussed in Chapter 3) is involved in this BG signaling deficit is currently unclear and remains an important focus of the ongoing study of Zfp521-BrKO mice. However, demonstrating hypofunctional D2-MSNs and indirect pathways in Zfp521-BrKO mice is a critical step in establishing the construct validity of this model of TS; particularly in the context of the imbalance between the striatonigral direct and the striatopallidal indirect pathways in modulating BG output as the primary functional deficit in TS.

As with TS patients, we showed in Chapter 2 that the tic-like behaviors in Zfp521-BrKO mice can be pharmacologically suppressed by the classic neuroleptic, haloperidol. One of the difficulties in treating motor tics with haloperidol, or any antagonist that targets D2-receptors, is maintaining doses that are low enough to minimize lesser side-effects such as sedation and avoid serious adverse effects such as tardive dyskinesia and catalepsy while effectively suppressing motor tics. In this chapter, we showed that although the tic-like behaviors of Zfp521-BrKO mice can be suppressed by haloperidol, at the same time, the mutant mice are highly resistant to the cataleptic effects of this mixed D2-antagonist.

As measured by the grid and bar tests, moderate doses of haloperidol induced catalepsy in control mice but Zfp521-BrKO mice remained mobile and active even when treated with high doses of haloperidol. Previous studies have reported that haloperidol-induced catalepsy is dependent on the D2-MSNs in the DMS. By quantifying cells immunohistochemically labeled for phosphorylated-H3 (a D2-MSN signaling protein selectively activated by haloperidol) in the DMS and DLS of mice treated with haloperidol, we demonstrated decreased p-H3 immunostaining throughout the dorsal striata of Zfp521-BrKO mice compared to controls. To further verify this reduced response of D2-MSNs to haloperidol in Zfp521-BrKO mice, the Levine laboratory performed patch-clamp recordings of haloperidol-treated D1- and D2-MSNs from mutant and

control mice. Electrophysiological analysis of the D1- and D2-EGFP labeled MSNs revealed haloperidol produced an increase in sEPSC frequency in control D2-MSNs but no significant response in Zfp521-BrKO D2-MSNs. Interestingly, analysis of the D1-MSNs showed that control D1-MSNs exhibited very little response to haloperidol, but Zfp521-BrKO D1-MSNs showed an unexpected increase in sEPSC frequency in response to haloperidol; this surprising finding may be critical in understanding the functional circuitry of tic-suppression and will be discussed in greater detail in Chapter 5 . Together, these studies demonstrating catalepsy-resistance and reduced signaling in response to haloperidol led us to hypothesize that the D2-MSN and the corresponding indirect pathway are hypofunctional in Zfp521-BrKO mice.

To bypass the role of D2-receptor activity, which can confound interpretation of the pharmacological studies, and directly examine the striatopallidal D2-MSNs and the indirect pathway our mouse model of TS, we optogenetically stimulated D2-MSNs expressing ChR2 in Zfp521-BrKO and control mice and analyzed the effect of indirect pathway activation on locomotion and tic-like behaviors. It has previously been shown that genetically regulated optogenetic activation (through ChR2) of D2-MSNs causes a significant reduction in ambulation in mice (Kravitz et al., 2010). Using the same genetic and optogenetic strategy, we also demonstrated that light-stimulation of D2-MSNs through ChR2 induces freezing behavior in control mice, presumably through indirect pathway-mediated inhibition of the BG motor output to the cortex. However, in Zfp521-BrKO mice, light-activation of D2-ChR2 failed to significantly reduce locomotion or suppress tic-like behaviors, providing our most compelling and direct evidence that the D2-MSNs and the corresponding indirect pathway are hypofunctional in Zfp521-BrKO mice.

If there is a common, unifying theme in TS research, it is that the neurobiology of the pathological behaviors lies in the imbalance of the tonically (and phasically) active indirect pathway that inhibits the motor cortex and puts the “brake” on unwanted behaviors and the

phasically active direct pathway that mediates the execution of volitional behaviors by focal disinhibition of select motor circuits of the cortex. There is considerable support from neuroimaging, pharmacological, and postmortem studies that show DA is one of the critical factors that mediates this functional imbalance. However, there is a clear bias towards a mechanism of a hyper-responsive direct pathway, whether it is mediated by increased innervation by dopaminergic nigrostriatal or glutamatergic corticostriatal terminals, supersensitive postsynaptic DA receptors, or overactive phasic release of too much DA (Buse et al., 2013; Singer and Minzer, 2003; Singer and Szymanski, 2002; Steeves et al., 2010; Wong et al., 2008).

In contrast, the results discussed in this chapter presents a less considered perspective of the DA hypothesis of TS: a deficient indirect pathway mediated by hypofunctional D2-MSNs may contribute to the circuitry dysfunction underlying the pathological motor behaviors in Zfp521-BrKO mice and TS patients. Although less extensive, emerging evidence from imaging and postmortem studies suggest that in a subset of TS patients, there is distinct striatal and cortical disinhibition that may result in the unregulated increase in the excitability of the motor cortex and subsequent pathological behavioral outputs (Heise et al., 2010; Lerner et al., 2012). While this disinhibition of the striatum and cortex may be correlated to decreased GABAergic interneurons or a more generalized dysfunction in GABAergic signaling (Kalanithi et al., 2005; Kataoka et al., 2010; Lerner et al., 2007), there is also evidence from a D2-receptor imaging study to suggest to that striatal disinhibition may be due to deficits in D2-receptor function (Müller-Vahl et al., 2000). Furthermore, just as we have shown that Zfp521-BrKO mice were highly resistant to the cataleptic effects of haloperidol, a retrospective study of 512 TS patients treated with neuroleptics (including haloperidol) revealed there were no reported instances of serious adverse effects from neuroleptics (even in cases with elevated doses) and the authors proceed to speculate that TS may even prevent the occurrence of such adverse effects (Müller-

Vahl and Krueger, 2011). Finally, although there was no determination of actual D2-receptor dysfunction, genotyping of the Drd2 gene in 151 children with TS and 183 normal controls revealed two polymorphisms that was significantly associated with the incidence of TS (Lee et al., 2005).

Evidence of motor tic-like behaviors resulting from striatal disinhibition was demonstrated pharmacologically in animal models by striatal microinjections of the $GABA_A$ antagonist, bicuculline, to focally disrupt the inhibitory BG motor signal to the cortex (Bronfeld et al., 2011, 2013; Worbe et al., 2009). The BG has been shown to maintain a well-preserved somatotopic organization from the cortical input to the striatum, up through to the thalamic output back to the motor cortex. In both monkeys and rats, focal disinhibition of select striatal regions were shown to induce restricted tic-like motor behaviors in the body areas corresponding to the topographic arrangement (Bronfeld et al., 2011, 2013; Worbe et al., 2009). Whether it is through pharmacological disinhibition of the striatum or a result of hypofunctional D2-MSNs and indirect pathways, as was the case in Zfp521-BrKO mice, there is now compelling evidence that disruption of striatal inhibition is critical in the pathophysiology of motor tics in both Zfp521-BrKO mice and TS patients. Past studies have generally been predicated on the view of TS as a pathological hyperactivity of the striatonigral direct pathway and the generation of too many competing and persistent aberrant motor signals to the cortex. Our study of the circuitry dysfunction of Zfp521-BrKO mice revealed it is equally important to consider TS as a deficit in the tonic and active inhibition of all the unwanted motor signals generated by the cortex that are normally filtered through the indirect pathway of the BG.

Chapter 5

Suppression of Tic-Like Behaviors in Zfp521-BrKO Mice Through D1-Receptor Agonism: Implications for D1-MSNs and the Direct Pathway

5.1 Introduction

Although we may know the biological targets of therapeutic compounds, there is still a large disconnect in our understanding of and ability to predict how a drug truly functions within the intricate environment of the brain in order modulate complex behaviors. In Chapter 2, we demonstrated that the classic neuroleptic, haloperidol, can effectively suppress tic-like behaviors in Zfp521-BrKO mice. As a mixed D2-antagonist, it is generally assumed that haloperidol blocks the signaling of the inhibitory $G_{\alpha i/o}$-coupled D2-receptors which in turn, activates the downstream indirect pathway to inhibit thalamic motor output from the BG to the cortex. The end result is the suppression of tic-like behaviors in Zfp521-BrKO mice and at higher doses, the inhibition of movement, in the form of catalepsy. However, in Chapter 3, we demonstrated that Zfp521-BrKO mice are highly resistant to haloperidol-induced catalepsy and this was likely due to the hypofunction of D2-MSNs and the indirect pathway in the mutant mice. A possible explanation to the seemingly incongruent behavioral responses to haloperidol in Zfp521-BrKO mice came from electrophysiological analysis of haloperidol-treated D1- and D2-MSN activity in the mutant and control mice. Unlike control D1-MSNs, which showed very little response to haloperidol, Zfp521-BrKO D1-MSNs showed an unexpected increase in sEPSC frequency when treated with haloperidol, suggesting that tic-suppression by haloperidol may function through a D1-MSN-mediated signaling in the mutant mice.

From a developmental viewpoint, these results suggest the intriguing hypothesis that deletion of Zfp521 causes a cell-autonomous disruption to the selection of either a D1- or D2-MSN fate in the developing MSNs. The D1-MSN response to haloperidol in Zfp521-BrKO may

be indicative of D1-MSNs aberrantly co-expressing D2-receptors and exhibiting D2-like signaling characteristics. However, without the evidence to support or refute this speculation, at present, it is more reasonable to interpret the haloperidol data from Zfp521-BrKO mice in the context of presynaptic D2-autoreceptor modulation of DA release. The role of presynaptic D2-autoreceptors in modulating the negative feedback of dopamine release to maintain both tonic and phasic DA levels (particularly in the striatum) has been well characterized (Benoit-Marand et al., 2001; Jackson and Westlind-Danielsson, 1994; Tang et al., 1994). Inversely, blocking presynaptic D2-autoreceptor function with D2-antagonists, such as haloperidol, results in an increase in DA release mediated locally at the presynaptic terminal and through activation of the dopaminergic cells of the SNc (Boyar and Altar, 1987; Bunney and Grace, 1978; Essig and Kilpatrick, 1991; Rouge-Pont et al., 2002). With hypofunctional D2-MSNs and a deficient indirect pathway, this haloperidol-induced increase in extracellular DA may be sufficient to activate D1-recpetors and mediate the unique physiological response (tic-suppression without catalepsy) to haloperidol observed in Zfp521-BrKO mice.

The hypothesis that activation of the striatonigral direct pathway can suppress tic-like behaviors may be counterintuitive, especially given that several other animal models highlight the possible hyperactivity of the striatonigral direct pathway as the signaling dysfunction in TS (Ahmari et al., 2013; Berridge and Aldridge, 2000; Canales and Graybiel, 2000; Graybiel et al., 2000). However, seemingly paradoxical therapeutics, while not common, have been shown to be effective in other neuropsychiatric disorders, such as the treatment of ADHD with the psychostimulant, methylphenidate (Goldman et al., 1998; Spencer et al., 1996). Not only has methylphenidate been shown to increase DA release and function through D1-receptors (Arnsten and Dudley, 2005; Berridge et al., 2006), a few case studies of ADHD patients that are comorbid with tics or TS have revealed that treatment of ADHD with methylphenidate also reduces the occurrence of tics (Gadow et al., 1992; Kurlan, 2002; Sverd et al., 1989).

Although neuroleptics, both classical and atypical, and more recently, alpha-2 adrenergic agonists (based on efficacy in ADHD) are the leading therapeutics for TS, several case studies suggest that striatal stimulation by dopaminergic agonists such as levodopa, amphetamines, apomorphine, and ropinirole can be effective in suppressing tics TS patients (Anca et al., 2004; Black and Mink, 2000; Feinberg and Carroll, 1979). More importantly, a limited number of studies have shown that pergolide, a ergot-derived mixed D1-, D2-, and D3-receptor agonist which has been successfully used to treat PD (Deleu et al., 2002; Fuller and Clemens, 1991; Goldstein et al., 1980; Oertel et al., 2006), is particularly successful in suppressing tics in a small subset of TS patients, especially those resistant to neuroleptic treatment (Cianchetti et al., 2005; Gilbert et al., 2000, 2003; Griesemer, 1997; Lipinski et al., 1997).

Despite the simplified view of the BG as a modulatory motor circuit, an extensive literature of anatomical, functional, molecular, and genetic studies show that the BG receives diverse signaling inputs from various sensorimotor, limbic, and associative regions of the cortex. These studies reveal the BG is in fact a complex and sophisticated system that mediates not only the planning and execution of motor behaviors, but aspects of emotion, habit-formation, reward-responses, goal-directed learning, and attention-processing (Graybiel, 2008; Redgrave et al., 2010; Tekin and Cummings, 2002; Voorn et al., 2004). In this context, we hypothesized that pharmacological activation of D1-receptors does more than simply stimulate general motor behavior; it enhances the attention-mediated, goal-directed behavioral output signals of the BG in order to suppress or override the pathological signal that normally drive the tics in TS patients and Zfp521-BrKO mice. Furthermore, we hypothesized that suppression of tic-like behaviors observed when Zfp521-BrKO mice are performing an attentionally-demanding task is similarly dependent on the more cognitive functions of the BG and is mediated by activation of the D1-receptors. In this chapter, we will show that D1-receptor agonism can effectively suppress the

tic-like behaviors in Zfp521-BrKO mice and that it is involved in the same critical circuit through which tic-suppression by attention is mediated.

5.2 Pharmacological Activation of D1-Receptors Suppresses Tic-Like Behaviors

In the previous chapter, electrophysiological analysis of D1- and D2-EGFP labeled MSNs revealed that while Zfp521-BrKO D2-MSNs were hypofunctional and not responsive to haloperidol, Zfp521-BrKO D1-MSNs showed an unexpected and significant increase in sEPSC frequency when treated with haloperidol. We inferred that the suppression of tic-like behaviors in haloperidol-treated Zfp521-BrKO mice was mediated by the activation of D1-receptors. We hypothesized that D1-receptor agonism can be effective in the suppression of tic-like behaviors in Zfp521-BrKO mice and provide an alternate drug-target for the development of novel TS pharmacotherapies.

Although pergolide is a mixed DA-receptor agonist and not specific to D1-receptors (also targets D2- and D3-receptors), a small number of case studies have reported it to be an unconventional, but effective drug in the suppression of tics in a subset of TS patients (Cianchetti et al., 2005; Gilbert et al., 2000, 2003; Griesemer, 1997; Lipinski et al., 1997). To test the efficacy of pergolide in our mouse model of TS, we injected 2 month-old control (n = 6) and Zfp521-BrKO (n = 7) with 5.0 mg/kg pergolide by intraperitoneal (i.p.) administration and video-recorded their behavior in the behavioral chamber at 15 and 60 minutes post-injection. Unbiased hand-scoring the tic-like behaviors showed that compared to the untreated baseline behavior, pergolide treatment produced a significant and relatively long-lasting suppression (up to 60 minutes post-injection) of tic-like behaviors in Zfp521-BrKO mice (Figure 5.1A). Repeated measures ANOVA revealed a significant effect of genotype ($F_{1,22} = 119.690$; $p < 0.001$) on the total tic-like behavioral counts in mice treated with pergolide and post-hoc analysis revealed a significant reduction of tic-like behaviors in mutant mice at both 15 and 60 minutes post-injection compared to the untreated baseline (Mann-Whitney U-test; $p < 0.001$ at both time points).

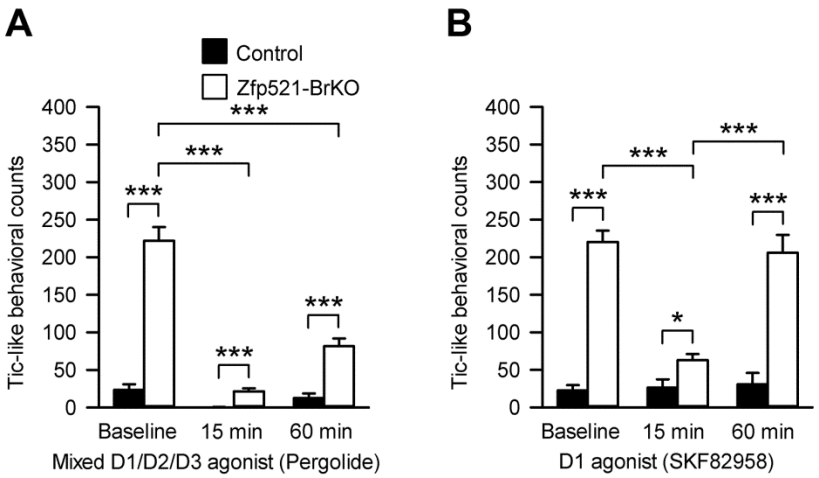

Figure 5.1 Dopaminergic agonism suppresses tic-like behaviors in Zfp521-BrKO mice. (A) Pergolide, a mixed D1-, D2-, D3-receptor agonist, significantly suppressed tic-like behaviors in 2 month-old Zfp521-BrKO mice. Control (n = 6) and Zfp521-BrKO (n = 7) were injected with 5.0 mg/kg pergolide and video-recorded in the behavioral chamber at 15 and 50 minutes post-injection. Total tic-like behaviors were quantified by unbiased hand-scoring. Repeated measures ANOVA revealed a significant effect of genotype ($F_{1,22}$ = 119.690; $p < 0.001$) on the total tic-like behavioral counts in mice treated with pergolide. Post-hoc analysis revealed a significant reduction of tic-like behaviors in mutant mice at both 15 and 60 minutes post-injection compared to the untreated baseline (Mann-Whitney U-test; $p < 0.001$ at both time points). (B) Selective activation of D1-receptors with the full D1-receptor agonist, SKF82958, also significantly suppressed the tic-like behaviors in Zfp521-BrKO mice. 2 month-old control (n = 5) and Zfp521-BrKO (n = 7) were injected with 2.0 mg/kg SKF82958 and video-recorded in the behavioral chamber at 15 and 60 minutes post-injection. Repeated measures ANOVA revealed a significant effect of genotype ($F_{1,19}$ = 66.127; $p < 0.001$) on the total tic-like behavioral counts in mice treated with SKF82958. Unlike pergolide, the tic-suppressive effect of SKF82958 was short-lasting, as post-hoc analysis revealed the significant reduction in total tic-like behavioral counts at 15 minutes (Mann-Whitney U-test; $p < 0.001$) is no longer observed at 60 minutes (Mann-Whitney U-test; $p = 0.603$). Both compounds demonstrated the efficacy of DA agonism in suppressing tic-like behaviors Zfp521-BrKO mice. Values are mean± SEM (* $p \leq 0.05$; ** $p \leq 0.01$; *** $p \leq 0.001$).

To address the behavioral effects of selectively activating D1-receptors, we next injected control (n = 5) and Zfp521-BrKO mice (n = 7) with a full D1-receptor agonist, SKF82958 (Andersen and Jansen, 1990). As with pergolide, 2 month-old mice were injected with 2.0 mg/kg SKF82958 and video-recorded in the behavioral chamber at 15 and 60 minutes post-injection for subsequent hand-scored analysis of tic-like behaviors. As shown in Figure 5.1B, treatment with a full D1-receptor agonist significantly suppressed tic-like behaviors in Zfp521-BrKO mice. Repeated measures ANOVA revealed a significant effect of genotype ($F_{1,19}$ = 66.127; $p < 0.001$) on the total tic-like behavioral counts in mice injected with SKF82958. Unlike the relatively longer-lasting pergolide, the tic-suppressive effect of SKF82958 was short-lived; post-hoc analysis revealed the reduction in tic-like behaviors in Zfp521-BrKO mice was only significant at 15 minutes post injection but not at 60 minutes post-injection compared to the untreated baseline (Mann-Whitney U-test; $p < 0.001$ at 15 minutes; $p = 0.603$ at 60 minutes). The results

from the pergolide and SKF82958 behavioral studies clearly indicated that DA-agonism, and specifically D1-receptor agonism, were effective in the suppression of tic-like behaviors in Zfp521-BrKO mice and demonstrated a novel predicative validity not reported in other mouse models of TS or OCD.

5.3 Attentional-Suppression of Tic-Like Behaviors in Zfp521-BrKO Mice is Partially Mediated by D1-Receptor Activation

We further speculated that tic-suppression by D1-receptor activation may coincide with the same signaling pathway involved in the attention-meditated or goal-driven behavioral signals from the BG. We hypothesized that antagonism of D1-receptor signaling will block the suppression of tic-like behaviors that normally occurs when Zfp521-BrKO mice are engaged in an attentionally-demanding task. To first examine the behavioral effects of the selective D1-receptor antagonist, SCH23390 (Billard et al., 1984), on unsuppressed tic-like behaviors, 2 month-old control (n = 6) and Zfp521-BrKO mice (n = 7) were injected with 0.1 mg/kg SCH23390 and tic-like behaviors were analyzed in the behavioral chamber at 90 minutes post-injection (Figure 5.2A). Analysis of the hand-scored tic-like behavioral counts showed that treatment with SCH23390 did not significantly change the occurrence of tic-like behaviors in Zfp521-BrKO mice compared to the untreated baseline measures (Mann-Whitney U-test; $p = 0.981$).

As previously discussed in Chapter 2, when Zfp521-BrKO mice are made to perform an attentionally-demanding task (balancing on a narrow, elevated beam), tic-like behaviors are significantly reduced compared to the frequency of tic-like behaviors at rest (non-attentionally engaged conditions). While placed on a narrow, elevated beam, the distraction of the novel environment and attention required to remain on the beam significantly suppressed the tic-like behaviors of Zfp521-BrKO mice to approximately 7% of the normal, baseline tic-like behavioral counts (Figure 5.2B). However, when injected with 0.1 mg/kg SCH2330 and placed on the

elevated beam after 90 minutes post-injection, we observed a significant reduction in the tic-suppression (tic-like behaviors increased to 22% of baseline) compared to when the mutant mice performed this attentionally-demanding task untreated or treated with only saline (Zfp521-BrKO, n = 6; Student's t-test; p = 0.00862 for untreated versus SCH23390-treated; p = 0.0345 for saline-treated versus SCH23390-treated). Taken together, this partial, but significant, blockade of attentional tic-suppression by D1-receptor antagonism, along with the evidence of pharmacological tic-suppression by D1-agonism, suggested that D1-receptor activation contributes to the BG circuitry mediating tic-suppression in Zfp521-BrKO and subsets of TS patients.

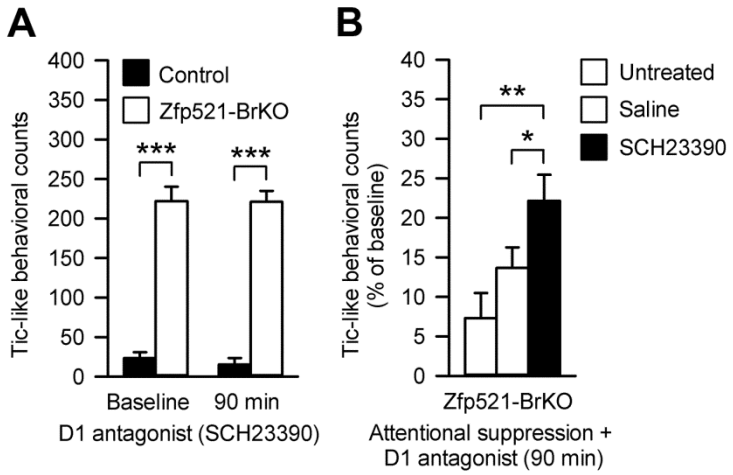

Figure 5.2 Antagonism of D1-receptors partially blocks attentional-suppression of tic-like behaviors in Zfp521-BrKO mice. (A) The selective D1-receptor antagonist, SCH23390, did not significantly alter total tic-like behaviors in Zfp521-BrKO mice. 2 month-old control (n = 6) and Zfp521-BrKO mice (n = 7) mice were injected with 0.1 mg/kg SCH23390 and total tic-like behaviors in the behavioral chamber was assessed at 90 minutes post-injection. Repeated measures ANOVA did not reveal a significant difference in total tic-like behaviors with SCH23390 treatment and additional post-hoc analysis comparing the total tic-like behaviors in Zfp521-BrKO mice at baseline and 90 minutes post-injection also did not show a significant difference (Mann-Whitney U-test; 0.981). (B) Injection of 0.1 mg/kg SCH23390 partially blocked the suppression of tic-like behaviors in 2 month-old Zfp521-BrKO mice engaged in an attentionally-demanding task. When untreated Zfp521-BrKO mice (n = 6) were placed on a narrow (3 cm which is approximately body-width), elevated bar, attentional-suppression reduced the total tic-like behaviors to 7% of the normal, baseline tic-like behavioral counts. 90 minutes post-injection of SCH23390, there was a significant block of tic-suppression and the total tics increased to 22% of baseline (Student's t-test; p = 0.00862). Saline injection did not significantly block tic-suppression compared to baseline and was significantly lower compared to SCH23390 treatment (Student's t-test; p = 0.0345). Mice were properly counter-balanced across the 3 treatment conditions to avoid exposure and practice effects on the attentionally-demanding task. Values are mean± SEM (* $p \leq 0.05$; ** $p \leq 0.01$; *** $p \leq 0.001$).

5.4 Discussion

Converging evidence from previous chapters revealed that despite a hypofunctional D2-MSN-mediated indirect pathway, the mixed D2-antagonist, haloperidol, effectively suppressed

tic-like behaviors in Zfp521-BrKO mice; most likely through the observed activation of D1-MSNs. Although we are exploring the possibility that this D1-MSN-mediated tic-suppression in Zfp521-BrKO mice may be due to an aberrant expression of D2-receptors on D1-MSNs or D1-MSNs having D2-like signaling, at present, the simplest and more likely explanation is that the haloperidol-induced activity of D1-MSNs was a result of increased DA release through presynaptic D2-autoreceptor antagonism (Boyar and Altar, 1987; Bunney and Grace, 1978; Essig and Kilpatrick, 1991; Rouge-Pont et al., 2002).

In this chapter, we demonstrated that dopaminergic agonism with the mixed D1-, D2-, and D3-receptor agonist, pergolide, effectively suppressed the tic-like behaviors in Zfp521-BrKO mice. More importantly, we also showed that specific activation of D1-receptors with a potent and selective D1-agonist, SKF82958, similarly suppressed the tic-like behaviors of Zfp521-BrKO mice. Although this suppression of tics by DA-agonism seems counterintuitive, such paradoxical treatments are not unprecedented, as in the treatment of ADHD by a psychostimulant, methylphenidate. Similarly, in the decades of TS pharmacological research, there have been several case studies that report the successful treatment of tics in TS patients with various DA agonists (Anca et al., 2004; Black and Mink, 2000; Feinberg and Carroll, 1979), including pergolide (Cianchetti et al., 2005; Gilbert et al., 2000, 2003; Griesemer, 1997; Lipinski et al., 1997).

On the surface, the suppression of motor tics by DA-agonism, specifically by D1-receptor agonism, is inconsistent with the simplified BG model which attributes activation of motor behaviors to the direct pathway and inhibition of movement to the indirect pathway. However, the extensive literature of the BG shows that it is more than a simple motor-regulatory circuit. Among the different circuits formed between the BG and various cortical regions, signaling inputs from the associative regions of the cortex, particularly the prefrontal cortex (PFC, Masterman and Cummings, 1997; Tekin and Cummings, 2002) mediates the role of the

BG in attention-processing, such as the response to novelty (Berns, 1997; Damsma et al., 1992; Kermadi and Boussaoud, 1995; Nieoullon, 2002), and goal-directed behaviors (Graybiel, 2008; Redgrave et al., 2010; Tekin and Cummings, 2002; Voorn et al., 2004). Furthermore, it has been shown that activation of D1-receptors in pyramidal neurons in the deep layer (V-VI) of the PFC (Maurice et al., 2001; Penit-Soria et al., 1987; Yang and Seamans, 1996) can regulate aspects of cognitive functions, including attention (Granon et al., 2000; Seamans and Yang, 2004; Williams and Goldman-Rakic, 1995).

Taken together, these studies suggest the likelihood of top-down processing involved in tic-suppression; this is especially evident in the suppression of tics by distraction (novelty) or concentration (engagement in a task or activity) observed in both TS patients and Zfp521-BrKO mice. We demonstrated the involvement of D1-receptor activity in the attentional-suppression of tic-like behaviors by injecting the selective D1-antagoinst, SCH23390, to partially block the tic-suppression in Zfp521-BrKO mice engaged in an attentionally-demanding task. Furthermore, contrary to what we would expect if the tic-like behaviors in Zfp521-BrKO were truly driven by hyperactive D1-MSNs (as is often theorized in other models of TS), we found that D1-antagonist treatment did not suppress the normal tic-like behaviors in Zfp521-BrKO at rest.

Throughout this dissertation, we have discussed the concept of TS as an imbalance of BG function. This aberrant signaling is thought to result from impeded selection of volitional behavioral signals by the direct pathway from among the competing pathological behavioral signals that cannot be properly inhibited by tonic and phasic activity of the indirect pathway. In TS patients and Zfp521-BrKO mice, it is possible that the volitional, direct pathway signal may be lost among or suppressed by the poorly inhibited signaling noise due to the deficient indirect pathway. With severe reduction of striatal tonic inhibition as a result of hypofunctional D2-MSNs, strengthening of the direct pathway signaling by attention or DA-agonism (especially of D1-receptors) may promote the selection of the volitional behavioral signals above the background

noise of the uninhibited pathological signals which may successfully suppress tics in both TS and Zfp521-BrKO mice.

In the chapter, we have not only gained new insights into the BG circuitry of tic-suppression by exploring D1-receptor activation, but we have further confirmed the value of this mouse as a model of TS by demonstrating predictive validity that is unique to Zfp521-BrKO mice. In addition to predictive validity for haloperidol, which is among the most common treatments prescribed for TS, Zfp521-BrKO mice demonstrated novel predictive validity for the DA-agonist, pergolide. This DA-agonist is paradoxically effective in tic suppression (without the sedative side-effect common to neuroleptics), but prescribed infrequently primarily due to the fact that its therapeutic mechanism in TS is not well understood. The broad predictive validity combined with the robust behavioral phenotype of Zfp521-BrKO mice makes it a powerful model to test novel drugs and other non-pharmacological (viral or genetic) therapeutics that can focus on unconventional targets for TS treatment, such as modulating the direct pathway to effectively promote volitional behaviors that suppress pathological tic-like behaviors.

Chapter 6

Conclusions and Future Directions

6.1 Overview

The overarching aim through all the studies presented in this dissertation was to carefully identify, characterize, and evaluate the behavioral, pathophysiological, and developmental phenotypes of a CNS-specific conditional knockout mouse model of Zfp521 that accurately recapitulates the hallmark clinical and neuropathological features of TS. Furthermore, although the striatonigral-enriched transcription factor, Zfp521(Doyle et al., 2008; Heiman et al., 2008; Lobo et al., 2006), has not previously been implicated in TS, we believe that by elucidating its molecular role in neural development, particularly in the striatum, we can gain significant insights into the BG cellular and circuitry dysfunctions underlying the pathogenesis of TS and establish the basis for new therapeutics.

Throughout this dissertation, we attempted to establish the Zfp521-BrKO mouse as an animal model of TS by demonstrating that the mutant mice fulfill the criteria for face, predictive, and construct validity. Although we demonstrated in Chapter 3 that the overall development of the striatum (including neurogenesis, differentiation, and organization of the circuitry) is largely intact despite CNS-deletion of Zfp521, we showed in Chapter 4 there is a hypofunctional striatal indirect pathway which may contribute to the tic-like behaviors in Zfp521-BrKO mice. As a potential tool for TS drug discovery, Zfp521-BrKO mice not only demonstrated predictive validity for the neuroleptic, haloperidol (one of the first-line treatments for tics in TS), but in Chapter 5, we showed that our mouse model of TS can be similarly effective in testing the tic-suppressive efficacy of DA-agonists which are generally regarded as uncommon and unconventional therapeutics for TS. In this chapter, we will discuss the significance of these studies and outline future work to further characterize the validity of Zfp521-BrKO mice as a model of TS, the BG

circuitry dysfunction that contributes to the pathological behaviors in these mice, the potential transcriptional mechanisms of Zfp521 in striatal development, and the relevance of this model in elucidating the genetic basis of TS in patients.

6.2 Validation of Zfp521-BrKO Mice as a Model of TS-Like Behaviors

Just as TS is most identified by the chronic presence of neurodevelopmental motor and vocal tics, the juvenile-onset tic-like behaviors of Zfp521-BrKO mice are this most prominent and striking features of this phenotypically robust animal model of TS. In Chapter 2, we examined the complexity of the behavioral pathology and identified the multiple components, including excessive grooming, head twitching, hind-limb flapping, and repetitive jumping, which make up the repertoire of the tic-like behaviors in Zfp521-BrKO mice. Although all Zfp521-BrKO exhibited the multiple tic-like behaviors as their dominant active behavior (up to 70% of waking activity), each mouse exhibited distinct individual variations in the frequencies of the different tic-like behaviors and the duration of the intra-tic intervals, much like the individual patterns of tics in TS patients. Furthermore, similar to how tics in TS can be influenced by external stimuli and internal processes, the tic-like behaviors in Zfp521-BrKO were also exacerbated by stress and attenuated by attention or distraction. While tics are the hallmark clinical features of TS, comorbidities including ADHD, OCD, SIBs, anxiety, as well as learning and social impairments are often just as prevalent and as disruptive to everyday life (Leckman, 2002; Robertson, 2000). Again, Zfp521-BrKO mice demonstrated exceptional face validity by exhibiting hyperactivity (analogous to ADHD), SIBs (self-inflicted lesions and hair loss from tic-like behaviors), and social impairment (in the form of deficient nest building). These comorbidities are important in that they may provide insights into the pathophysiology, particularly within the BG circuitry, that are common to these overlapping conditions that are also present other animal models of tics and stereotypies.

While the multiple tic-like behaviors and the TS-relevant comorbidities are certainly the most impressive behavioral phenotypes of the mutant mice, the strength of the face validity alone is not enough to make Zfp521-BrKO a truly comprehensive model of TS. Predictive validity is an equally important criteria that must be satisfied in order for the Zfp521-BrKO mouse to be a relevant and useful model that can advance TS research. Zfp521-BrKO mice demonstrated predictive validity for haloperidol, which continues to be one of the most commonly prescribed first-line treatments for tics in TS. Interestingly, Zfp521-BrKO also demonstrated predictive validity for pergolide, which is a DA-agonist shown to be paradoxically effective in suppressing tics in a small subset of TS patients, some who are resistant to the more conventional neuroleptic treatments of TS (Cianchetti et al., 2005; Gilbert et al., 2000, 2003; Griesemer, 1997; Lipinski et al., 1997). More importantly, while the pathological phenotypes (excessive grooming) of other genetic models of stereotypies (Sapap3 and Slitrk5 knockout mice), which are generally characterized as mouse models of OCD (Shmelkov et al., 2010; Welch et al., 2007), can be effectively treated with fluoxetine (SSRI), tic-like behaviors in Zfp521-BrKO mice were not significantly reduced with similar chronic treatment with fluoxetine. This divergence in predictive validity establishes an important distinction in the classification of Zfp521-BrKO mice as a mouse model specifically of TS rather than OCD. Overall, it is the combination of an unambiguous behavioral readout from the robust tic-like phenotypes and unique predictive validity of the Zfp521-BrKO mouse that makes it a powerful tool to study the pathophysiology of tic behaviors and drive drug discovery research for TS.

The neuropathologies observed in Zfp521-BrKO mice, specifically the selective reductions in dorsal striatal volume and PV-expression in GABAergic interneurons, recapitulated the loss of caudate volume (Hyde et al., 1995; Peterson et al., 2003) and PV-expressing interneurons (Kalanithi et al., 2005; Kataoka et al., 2010) reported from neuroimaging and postmortem studies of TS patients. These neuropathologies not only pertain to the construct

validity (the broader theme of BG deficits as pathogenic mechanisms of TS) of Zfp521-BrKO mice, but are another aspect of the face validity that speaks to the uniqueness of this mouse model of TS and the benefits of genetic manipulation to model a neurodevelopmental disorder. Pharmacological models of TS, particularly those that evoke TS-like pathological behaviors through dopaminergic-activation (psychostimulants), can satisfy some aspects of behavioral face validity and provide insights into the potential circuitry and signaling dysfunction involved in tic behaviors. However, as these models are generally pharmacological investigations of non-genetically-manipulated animals that have developed normally, they cannot fully address the developmental course of the pathogenic mechanisms of TS as it normally occurs in human patients. The critical developmental deficits (that may later manifest as neuropathologies) are best studied in a genetic model, such as Zfp521-BrKO mice, in which disruptions during early neural development may establish the pathogenic dysfunctions later in the mature animal.

Throughout this dissertation, we have focused primarily on tic-like motor behaviors of Zfp521-BrKO mice. However, any discussion of TS would be incomplete if we do not include vocal tics, which are an equally prevalent and distinctive clinical feature of TS (APA, 2013; Jankovic, 1997; Leckman, 2002). Although we did not examine dysfunctional vocalizations in our mice, previous studies have reported alterations in ultrasonic vocalizations in pups as a pathological behavioral phenotype in mouse models of autism spectrum disorders (ASDs; Peñagarikano et al., 2011; Schmeisser et al., 2012; Silverman et al., 2010; Tsai et al., 2012). In order to develop a more complete behavioral characterization of Zfp521-BrKO, studies to examine ultrasonic vocalizations in pups and sexually mature mutant mice (the two stages where vocalizations are prominent in mice) will be conducted. Although ultrasonic vocalizations in pups may be a useful behavioral phenotype to characterize at a stage (P0 to P7) where mice are extremely limited in their repertoire of motor behaviors, we must also consider that this is before the emergence of the motor tic-like behaviors at around P20 and ultrasonic vocalizations

as a behavioral phenotype may not coincide with the developmental course of the circuitry dysfunction that underlies the tic-like behaviors. Furthermore, as we strive to avoid anthropomorphizing the pathological behaviors (Crawley, 2007) of our mouse model of TS, we must keep in mind there is little evidence to equivocate ultrasonic vocalizations in mice to human language; although disruptions in vocalizations may further contribute to the face validity of Zfp521-BrKO mice, it will be difficult to interpret such tic-like vocalizations as analogous to human vocal tics in TS. With both TS and Zfp521-BrKO mice, by understanding the neurobiology of the tics outside the context of just phenomenology, we may come to show that both motor and vocal tics are both mediated by the same circuits and are simply differing examples of BG-mediated activations of different muscle groups with different behavioral consequences.

6.3 Circuitry Insights of the Zfp521-BrKO Basal Ganglia: Hypofunctional Indirect Pathway Associated with Tic-Like Behaviors and Tic-Suppression by D1-Agonsim

In the firmly-established perspective of the basal ganglia as a circuit which regulates the selection of multiple competing excitatory cortical inputs to modulate behavioral outputs, the tics associated with TS are often viewed as aberrant stimulatory outputs onto the motor cortex from the BG. This is likely a result of an imbalance of the indirect pathway which maintains the inhibitory “brake” on unwanted behaviors and the direct pathway which normally promotes behavioral output signals from the BG back to the cortex (Albin et al., 1989; DeLong, 1990; Mink, 1996, 2001). Not surprisingly, early clinical studies which reported the successful treatment of motor tics with the mixed D2-antagonist, haloperidol, formed the theoretical basis for the DA hypothesis of TS, which attributes disturbances in striatal DA levels or dysfunctions in DA-mediated signaling to the BG imbalance which underlie TS (Felling and Singer, 2011; Mink, 2001; Shapiro and Shapiro, 1968; Singer et al., 1982).

In our studies of Zfp521-BrKO mice, converging evidence, including the enrichment of Zfp521 in striatonigral MSNs (and the prominent striatal expression pattern), developmental striatal atrophy, selective reduction of PV-expression in dorsal striatal GABAergic interneurons, and pharmacological tic-suppression by haloperidol and pergolide (which both act on DA receptors), similarly implicated a striatal dysfunction and imbalanced BG circuitry in our mouse model of TS. However, diverging from the more commonly held view of a hyperactive or hyper-responsive direct pathway as the primary BG imbalance in TS, the experiments detailed in Chapter 4 support the hypothesis that a hypofunctional indirect pathway may be the prevalent BG circuitry deficit that underlies the tic-like behaviors in Zfp521-BrKO mice. Multiple lines of evidence strongly implicated hypofunctional indirect pathway D2-MSNs in Zfp521-BrKO mice: 1) resistance to haloperidol-induced catalepsy, which is mediated by D2-MSNs in the DMS (Durieux et al., 2011), 2) significant reduction of the selective expression of phosphorylated-H3 in striatal D2-MSNs by haloperidol-activated signaling, and 3) the lack of significant sEPSC frequency increases in response to bath application of haloperidol in patch-clamp recorded D2-EGFP expressing MSNs. Most importantly, we directly addressed this question of hypofunctional indirect pathway D2-MSNs (without the confounds of pharmacological manipulation of D2-receptors) in Zfp521-BrKO mice by showing that optogenetic stimulation of D2-MSNs expressing ChR2 failed to induce freezing behavior or suppress tic-like behaviors in the mutant mice.

Although the Zfp521-BrKO mouse is not the first proposed animal model of TS, conceptually, it is novel in that it is the first genetic model to show that tic-like behaviors are associated with hypofunctional indirect pathway MSNs. In other non-human primate and rodent pharmacological models of TS, the dominant view that aberrant, over-activation of the cortical-striatal-thalamo-cortical circuits prompted studies in which pathological stereotypies and tic-like behaviors were evoked by stimulation of dopaminergic signaling with amphetamines, cocaine,

L-dopa, and specific D1-receptor agonists (Berridge and Aldridge, 2000; Canales and Graybiel, 2000; Graybiel et al., 2000; Robinson and Becker, 1986; Saka et al., 2004). Even in the D1CT-7 transgenic mice, which is currently the closest genetic model to exhibit tic-like behaviors most relevant to TS, the primary signaling dysfunction that drives the pathological phenotype is the select hyperactivation of D1-receptor expressing pyramidal neurons of the somatosensory and piriform cortex which aberrantly stimulates the downstream striatal circuits (Nordstrom and Burton, 2002). However, our studies of Zfp521-BrKO mice not only revealed that the reciprocal dysfunction similarly causes tic-like behaviors, but also showed that the reduction of the inhibitory signaling from the striatal indirect pathway evokes a more complex and diverse repertoire of tic-like behaviors that is a more comprehensive and accurate representation of the clinical features in TS.

In order to further explore the indirect pathway dysfunction in Zfp521-BrKO mice, our future studies will need to focus on the molecular mechanisms underlying this disrupted BG circuit. Using the previously described Zfp521-BrKO mouse lines expressing D1- or D2-EGFP, we will separate fluorescently labeled D1- and D2-MSNs by FACS and analyze the MSN-subtype specific expression of genes by RNA-seq at different developmental stages (P0, P7, and P20). By examining and comparing the MSN-subtype-specific transcriptome of Zfp521-BrKO and control mice at important developmental ages, we will gain enormous insights into the cell-autonomous and non-cell-autonomous transcriptional activities that are significantly altered and may eventually lead to functional deficits in BG signaling when Zfp521 is deleted. Not only will this be critical in understanding the striatal pathogenesis of TS, but also in our broader understanding of the critical molecular mechanisms regulating the development, organization, and function of the direct and indirect pathways in the BG circuit.

The studies demonstrating a hypofunctional indirect pathway D2-MSNs left us with the question of how haloperidol, a mixed D2-antagonist which presumably acts, at least in part,

through the indirect pathway, can suppress tic-like behaviors in Zfp521-BrKO mice. The electrophysiological studies in Chapter 4 revealed that D1-MSNs in Zfp521-BrKO were unexpectedly activated by haloperidol and may mediate the observed tic-suppression. Although we cannot dismiss the possibility that select D1-MSNs in Zfp521-BrKO mice may aberrantly express of D2-recpectors or D1-MSNs may have D2-MSN-like signaling, the more likely explanation is that the haloperidol-induced activity of D1-MSNs is a result of increased DA release through presynaptic D2-autoreceptor antagonism (Boyar and Altar, 1987; Bunney and Grace, 1978; Essig and Kilpatrick, 1991; Rouge-Pont et al., 2002). In Chapter 5, we not only demonstrated that tic-like behaviors in Zfp521-BrKO mice can be suppressed by DA-agonism with pergolide, but we also showed that the selective D1-recptor agonist, SKF82958, was just as effective in tic-suppression. Furthermore, we demonstrated that antagonism of D1-receptors partially, but significantly, blocked attention-mediated suppression of tic-like behaviors in Zfp521-BrKO mice, indicating that the circuits mediating the two forms of tic-suppression may overlap to some degree. Given that numerous studies have shown that D1-receptor activation of pyramidal neurons in the PFC which project to the associative regions of the striatum (Masterman and Cummings, 1997; Maurice et al., 2001; Penit-Soria et al., 1987; Tekin and Cummings, 2002; Yang and Seamans, 1996) can mediate the role of the BG in attention-processing and response to novelty (Graybiel, 2008; Redgrave et al., 2010; Tekin and Cummings, 2002; Voorn et al., 2004), the important implications from our findings is that D1-receptor agonism may be involved in the top-down processing of tic-suppression and can be an effective mechanism through which we can pharmacologically suppress tics in Zfp521-BrKO mice and TS patients.

Pharmacological D1-agonism targets all the D1-receptor expressing cells and makes it difficult to interpret which signaling pathways are truly critical for both D1-agonist- and attentionally-mediated tic-suppression in Zfp521-BrKO mice. To address the question of circuit-

specific activation of tic-suppression, our continued studies will include optogenetically activating D1-ChR2 expressing cells selectively in the dorsal striatum to induce tic-suppression in Zfp521-BrKO mice. As with the optogenetic studies of viral-mediated D2-ChR2 expressing mice, we will stereotaxically injected rAAV2/1-CAGGS-FLEX-ChR2-tdTomato into the dorsal striata of Zfp521-BrKO mice expressing BAC-Drd1-Cre (Zfp521-BrKO; D1-Cre). We can then selectively laser-activate striatal D1-MSNs in order to directly examine the tic-suppressive effect of D1-MSN activation of the BG direct pathway. Furthermore, with the same mice, we can use high-frequency laser-stimulation to disrupt the dorsal D1-MSN signaling of the direct pathway to determine if it also blocks attentional-suppression of tic-like behaviors in Zfp521-BrKO mice. These future optogenetic studies will allow us to genetically dissect the critical circuits involved in tic-suppression and guide our efforts to develop novel and unconventional therapeutics for TS.

6.4 Transcriptional Mechanisms and the Developmental Role of Zfp521 in the BG and Relevance for TS

Our laboratory's initial interest in Zfp521 in BG development and function began with its identification as a striatonigral-enriched gene from our FACS-array profiling (Lobo, 2009) of striatal D1- and D2-MSNs (and later independently verified in a study using the BAC-TRAP methodology; Doyle et al., 2008; Heiman et al., 2008). Earlier studies of genes that are structurally and functionally related to Zfp521, including Zfp423 (a paralog of Zfp521) and Ebf1 (a physically interacting transcriptional partner of Zfp521), revealed that they regulate the differentiation of cerebellar, striatal, and olfactory neurons (Alcaraz et al., 2006; Cheng and Reed, 2007; Cheng et al., 2007; Lobo et al., 2008; Warming et al., 2006) as well as guide the projections of olfactory-receptor neurons (Cheng and Reed, 2007), thalamocortical projections (Garel et al., 2002), and striatonigral MSN axonal projections though the BG direct pathway (Lobo et al., 2006, 2008). These findings, along with an important study which shows Zfp521 is

critical in the early differentiation of ES cells into neuronal precursors of a neuroectodermal lineage (Kamiya et al., 2011), strongly suggest an important transcriptional role of Zfp521 throughout neural development, from differentiation during early embryonic stages to maturation in critical postnatal stages. In Chapter 3, we conducted several developmental studies to elucidate the molecular mechanisms of the striatal pathologies observed in Zfp521-BrKO mice (developmental atrophy of the dorsal striatum and reduced PV-expression in GABAergic interneurons in the dorsal striatum) in order to determine the direct role of Zfp521 in striatal development and relevance to the pathogenesis of TS.

Striatal atrophy and loss of GABAergic neurons in Dlx1/2 knockout mice were reported in a series of extensive studies by the Rubenstein laboratory. These studies revealed Dlx 1 and 2 regulate the differentiation of late-born striatal MSNs fated for the matrix, as a well as GABAergic interneurons originating from the proliferative zones of the LGE and MGE, respectively (Anderson et al., 1997; Cobos et al., 2005; Marin et al., 2000). Furthermore, these studies of the Dlx1/2 knockout mice also revealed that expression of Zfp521 in the MGE and LGE is downstream of Dlx 1 and 2 (Long et al., 2009a, 2009b). Taken together, we hypothesized that the loss of dorsal striatal volume and reduction in PV-expressing interneurons in the DMS in Zfp521-BrKO mice was in part, the result of a disruption to this Dlx1/2-medaited program of striatal MSN and interneuron differentiation and maturation due to deletion of Zfp521.

In Chapter 3, we characterized the striatal development of Zfp521-BrKO mice through immunohistochemical examination of important striatal MSN and interneuron markers. We also used BrdU birth-dating at critical developmental time points to determine if the deletion of Zfp521 disrupts the differentiation of neuronal precursors from the MGE and LGE and can account for the observed neuropathologies. Unbiased cell counting of DARPP-32 labeled MSNs, as well as D1- and D2-EGFP genetically labeled MSNs, revealed no significant changes

in the density of striatal D1- or D2-MSNs to indicate a loss of MSNs by cell death or a reduction in MSN neuropil. Developing striatal cells birth-labeled with BrdU at E11.5, E15.5, and E17.5 and examined at P0 also revealed no significant disruptions of striosome and matrix MSN development during the early and late waves of striatal neurogenesis and migration out of the VZ/SVZ, respectively. Furthermore, immunohistochemical staining of select markers to investigate the striatal organization of striosome/matrix MSNs (DARPP-32 and MuOR) and important striatal afferents (TH and VGluT1) at P0 also revealed the circuitry organization of the developing striatum is largely intact in the Zfp521-BrKO mouse. Although the largely negative results in Chapter 3 strongly suggest the neuronal composition and circuitry organization of the striatum in the Zfp521-BrKO mouse is largely intact during the course of embryonic development, it does not exclude the possibility of developmental deficits during the critical postnatal period of neural differentiation and maturation.

Although we observed a reduction of dorsal striatal PV-expression in Zfp521-BrKO that recapitulated the loss of PV-interneurons in the striata of TS patients (Kalanithi et al., 2005; Kataoka et al., 2010), later analysis of striatal interneurons with a second, activity-independent marker of interneurons originating from the MGE (which includes most cholinergic and GABAergic subtypes, including PV) did not support the findings of striatal interneuron loss (by cell death) in Zfp521-BrKO. Instead these results led us to speculate that our initial observation of striatal PV-expression deficits was due to postnatal reductions in activity-dependent PV expression in select GABAergic interneurons (Cellerino et al., 1992; Patz, 2004; Rudkin and Sadikot, 1999; Schlösser et al., 1999; Vogt Weisenhorn et al., 1998).

The collective results of our developmental studies of Zfp521-BrKO mice strongly suggest an important postnatal role of Zfp521 in striatal development that falls in line with other studies which show that activity-dependent maturation and successful establishment of axonal projections to intended targets is essential for developing striatal neurons to survive the critical

period of pruning and cell death that occurs during the first two postnatal weeks (Fentress et al., 1981; Fishell and van der Kooy, 1991; van der Kooy and Kooy, 1996). Future studies to elucidate the transcriptional role of Zfp521 in BG development and the possible pathogenesis of TS will most likely require us to carefully examine Zfp521-BrKO mice during the critical period of the first two postnatal weeks.

Furthermore, as part of the larger scope of our laboratory to elucidate the developmental and functional molecular mechanisms of the striatonigral and striatopallidal BG circuits in both normal and pathological conditions, we require new genetic tools and strategies to overcome the technical difficulties we currently face in order to further our studies of Zfp521-BrKO mice. Despite efforts to generate antibodies against Zfp521, we still lack reliable Zfp521 antibodies for molecular studies which has limited our efforts to identify the developmental lineage of cells expressing Zfp521. Although Zfp521 has been identified as a striatonigral enriched gene by FACS-array and BAC-TRAP in fully differentiated and mature MSNs (Doyle et al., 2008; Heiman et al., 2008; Lobo et al., 2006), the expression of Zfp521 in early neuronal precursors, before differentiation and maturation into their fated MSN-subtypes, remains unclear.

Without a suitable antibody, future developmental studies will require us to generate a reporter mouse expressing a Zfp521-EGFP fusion protein or a BAC-transgenic mouse expressing EGFP driven by the Zfp521 promoter (BAC-Zfp521-EGFP) in order to genetically identify the cells which express Zfp521 throughout the course of neuronal development. Determining the transcriptional lineage of Zfp521 will be critical in elucidating the cell-autonomous and non-cell autonomous molecular functions of Zfp521during striatal development and identifying the molecular deficits (and other critical circuits outside the BG) in Zfp521-BrKO mice that are relevant to the pathogenesis of TS. Alternatively, we can attempt to identify the TS-relevant cell types and circuits by crossing the conditional Zfp521 mice with other cell-type specific Cre lines or employing a genetic rescue strategy by crossing Zfp521-BrKO mice with

BAC-transgenic mice which overexpress Zfp521 driven by a promoter of interest. However, without first knowing which cells normally express Zfp521 during development, such genetic experiments can be hit-or-miss with the potential to be extremely costly, in terms of both resources and time. By using the Zfp521-EGFP reporter mice to identify the cell types which strongly express Zfp521 during neural development, we will have the critical information to more effectively and efficiently guide such future mouse genetic experiments.

Furthermore, a resource such as reporter mice expressing EGFP-tagged Zfp521will allow future studies to extensively study the transcriptional activities of Zfp521. Such studies can include, but are not limited to, co-immunoprecipitation assays to identify proteins complexed to the Zfp521-EGFP fusion protein and develop a developmental Zfp521-interactome, or chromatin immunoprecipitation (ChIP) studies to evaluate the transcriptional role of Zfp521 in chromatin remodeling through the NuRD complex (Bond et al., 2008; Matsubara et al., 2009). While the Zfp521-BrKO mouse may be invaluable as a model of TS, it is also a significant tool in our laboratory's broader efforts to understand BG development and function.

6.5 Zfp521-BrKO Mice as a Resource for Future Human Genetics Studies of TS

If there is a fundamental caveat to current animal models of TS or any other animal models of phenotypically and etiologically complex disorders, including Zfp521-BrKO mice, it is that without a clear and consistent understanding of the pathogenic mechanisms in human patients, it is difficult to gauge the construct validity of any animal model. While decades of extensive anatomical, neuroimaging, pharmacological, and postmortem studies have strongly implicated the dopamine-imbalanced BG as the primary circuit of dysfunction correlated with TS, the specific nature and details of this dysfunction remains unresolved. We can disrupt the BG circuitry and manipulate DA signaling to generate animals models of TS with convincing face and predictive validity that closely recapitulates the human condition. We can make the claim that these models satisfy the broader concept of construct validity by sharing the same

generalized BG dysfunctions as TS patients. But in the end, we are still limited in our interpretation of the construct validity of these models and lack the evidence to make the argument that the pathophysiological mechanisms which underlie the TS-like phenotypes in the animal models really represent the etiology in patients.

Despite these limitations, we believe that as a genetic model of TS that accurately recapitulates the neurodevelopmental nature of this disorder, the most significant evidence of construct validity in our mouse model will come from future human genetic studies of TS derived from sequencing and genomic analysis of Zfp521-BrKO mice. At present, genome-wide studies of TS patients (Fernandez et al., 2012; Paschou, 2013; Scharf et al., 2013; Sundaram et al., 2010) have not reported a direct association of allelic variants of Zfp521 to TS risk. However, in a recent follow-up to an Autism genome-wide association study which showed significant association of SEMA5A to autism risk, bioinformatic network-analysis (expression quantitative trait locus, or eQTL, mapping) of genes associated with SEMA5A expression levels mapped Zfp521 to a SEMA5A regulatory network, indicating potential contribution to autism risk (Cheng et al., 2013). With the suspected overlap between autism spectrum disorders and TS, particularly in BG-mediated pathological motor behaviors which are prevalent in both neurodevelopmental disorders (Baron-Cohen and Scahill, 1999; Ramocki and Zoghbi, 2008; State, 2010), this study suggests a possible relevance of Zfp521 in TS genetics.

However, even if Zfp521 itself is never confirmed as significantly with associated TS risk, our planned studies to use RNA-seq and network analysis to profile the developmental and MSN-subtype-specific gene expression in Zfp521-BrKO mice will allow us to identify networks of Zfp521-assocaited genes that may be more relevant to TS risk in future human genomic studies of TS. A recent study of APOE4 and late-onset Alzheimer's disease (LOAD) took an integrative genomic approach and applied network analysis (differential co-expression analysis, DCA) on previously published, publically available LOAD-associated transcriptome-wide gene expression

and GWAS data to identify regulatory genes and networks correlated with APOE4 expression and LOAD risk (Rhinn et al., 2013). Similarly, our planned sequencing studies of Zfp521-BrKO mice can be quickly and directly translated to human studies by taking the same integrative network approach and analyzing available data sets from TS genomic studies with the candidate genes identified from our mouse model of TS (Fernandez et al., 2012; Paschou, 2013; Scharf et al., 2013; Sundaram et al., 2010).

6.6 Concluding Remarks

The studies presented in this dissertation fulfilled our primary objective to characterize and evaluate the behavioral and pathophysiological features of a CNS-specific conditional knockout mouse model of Zfp521 that accurately recapitulates the relevant clinical and neuropathological features of TS. We established the face, predictive, and to a lesser extent, the construct validity of the Zfp521-BrKO mouse as a novel and comprehensive neurodevelopmental model of TS that will prove to be an invaluable tool for TS drug discovery. Furthermore, we are confident that genomic analysis of Zfp521-BrKO will have significant implications for future human genetic studies of TS. Continued studies of the molecular mechanisms of Zfp521 in both the normal and pathogenic context will lead to significant insights into the fundamental processes of striatal development that will be relevant to TS as well as other neurodevelopmental disorders with motor behaviors.

Materials and Methods

Animals

Zfp521 conditional allele mice ($Zfp521^{flox/flox}$) were a gift from our collaborators, Drs. Soren Warming and Neal Copeland (both at the National Cancer Institute at the time). Nestin-Cre mice were obtained from the Jackson Laboratory (JAX; www.jaxmice.jax.org). BAC transgenic Drd1a-EGFP, Drd2-EGFP, Drd1a-Cre, and Drd2-Cre mice were obtained from GENSAT (Gene Expression Nervous System Atlas project; www.gensat.org) and MMRRC (Mutant Mouse Regional Resource Centers; www.mmrrc.org). All mice were backcrossed and maintained on a C57BL/6 background (at least 6 generations). Mouse care was in accordance with *United States Public Health Service Guide for the Care and Use of Laboratory Animals* and guidelines established by the University of California, Los Angeles. Animals were group-housed in a temperature-controlled environment with 12-hour light/dark cycle and food and water available ad libitum. Veterinary care was provided by the UCLA Division of Laboratory and Animal Medicine (DLAM). Experiments and procedures were approved by the Institutional Animal Care and Use Committee at UCLA. All the genotypes, ages, and numbers of mice used for studies are given in the text.

Genotyping. All mice were genotyped by PCR analysis of DNA taken from ear biopsies at P20 using standard methods with the following sets of primers. Zfp521: 5'-Zfp521-Exon4 (5'-GCTCCTTCACATGCTCACA-3'), 3'-Zfp521-Exon4 (5'- CTGGCATGGGTAAGGCAGT-3'), and 3'-Zfp521-loxP (5'-CTCCGAGAGTTTGAGTGCAA-3'). Nestin-Cre: 5'-Nestin (5'-CCGCTTCCGCTGGGTCACTGT-3'), 3'-Nestin (5'-CTGAGCAGCTGGTTCTGCTCCT-3'), and 3'-Cre (5'-GACCGGCAAACGGACAGAAGCA-3'). BAC-D1- and BAC-D2-EGFP: 5'-D1-EGFP (5'-ACCGGAAGTGCTTTCCTTCTGGA-3'), 5'-D2-EGFP (5'-CCCTGTGCGTCAGCATTTGGAGCAAC-3'), and 3'-EGFP (5'-TAGCGGCTGAAGCACTGCA-3'). BAC-D1- and BAC-D2-Cre: 5'-D1-Cre (5'-GCTATGGAGATGCTCCTGATGGAA-3'), 5'-D2-

Cre (5'-GTGCGTCAGCATTTGGAGCAA-3'), and 3'-Cre (5'-CGGCAAACGGACAGAAGCATT-3'). The PCR cycling conditions for all primer sets were: 94°C for 5 min and then 30 cycles of 94°C for 30 sec, 56°C for 30 sec, and 72°C for 30 sec, followed by 72°C for 10 min (*Taq* DNA Polymerase; New England BioLabs).

Behavioral Tests

All behavioral tests were performed in the same room the mice were housed in, during the light cycle at approximately the same time of day for all cohorts of mice, unless noted otherwise.

Behavioral Chamber (Open Field). Unless otherwise noted, mice were individually video-recorded under normal room lighting in a clear plexiglass behavioral recording chamber (30.5 cm x 30.5 cm x 15 cm) with a transparent floor through which an angled mirror allowed video-recording of behavioral activity from below. This bottom-up view allowed for clear, unobstructed observation and analysis of even the most subtle or slightest of mouse behaviors. Mice were video-recorded for 15 minutes, with the first 12 minutes for mice to acclimate to the behavioral chamber and the last 3 minutes analyzed for behavioral quantification.

Home cage. Group-housed mice were temporarily removed from their home cages and individually returned to be video-recorded alone in their home cage for 15 minutes. Home cage behavior was recorded from a side view, along the longer side of the rectangular home cage, under normal room lighting. Mice were video-recorded for 15 minutes, with the first 12 minutes for mice to re-acclimate to their home cage after temporally being removed to allow for individual recording. The last 3 minutes were analyzed for behavioral quantification.

Elevated beam task. To engage mice in an attentionally demanding task, mice were individually placed on an elevated bar (3 cm x 30.5 cm bar; 30.5 cm above a padded surface) and video-recorded for 3 minutes. The elevated bar was approximately body-width (wide enough for mice to sit and groom) and remaining on the bar during the 3 minute video-recording was not observed to be a difficult motor task (did not require pre-training). Mice were recorded from a

top-down view to allow for unobstructed observation and analysis of all motor behaviors. Mice that fell off the bar were immediately placed back on and falls were noted in the behavioral analysis.

Quantification of tic-like and non-tic motor behaviors. Hand-scoring of all tic-like and non-tic motor behaviors was adapted from published behavioral quantification methods (Kelley, 2001). Video-recorded behavioral activity (behavioral chamber, home cage, elevated beam task, etc.) was reviewed at half-speed playback and all behaviors were quantified as "behavioral counts" by hand-scoring the prominent behaviors for each 1-second bin of a 180-second analysis period. The quantified tic-like behaviors were 1) head grooming, 2) body grooming, 3) quick head twitch, 4) rapid hind-limb flapping, and 5) jumping while the non-tic behaviors were 1) horizontal movements, 2) rearing, and 3) being stationary. Behavioral quantification was conducted by two independent scorers (could not be blind to genotype but were blind to drug treatments).

Open field analysis. In addition to analysis of tic-like and non-tic motor behaviors, the bottom-up view of the behavioral chamber also allowed for frame-by-frame automated video-analysis of spontaneous locomotor activity (entire 15 minute recording session) with customized StereoScan behavioral analysis software (CleverSys). StereoScan analysis of the open field behavior was also used to assess anxiety-like phenotypes by quantification of time spent in the perimeter and center of the behavioral chamber, as well as the number of center entries.

Light-dark box. The light-dark box chamber consisted of a covered dark area (1/3 of the box), made of black plexiglass, connected by an open doorway to an uncovered light area (2/3 of the box), made up of clear plexiglass. Mice were initially placed in the light area, adjacent to the doorway separating the two chambers and video-recorded for 10 minutes. Video-recordings were analyzed for time spent in the dark and light chambers, as well as the number of entries and head pokes from the dark chamber into the light chamber.

Nest building. Mice were temporarily single-housed for 24 hours in clean home cages, each with a new, intact nestlet (square of compressed cotton) for nest building. After being left 24 hours undisturbed, mice were carefully removed from the cages as to not disturb their nests. Nests were photographed and assessed by scorers blinded to genotype. Nest building was scored using an established 5-point rating scale: 1) Nestlet untouched, 2) Nestlet partially torn, 3) Nestlet mostly torn but no clear nest, 4) Well defined, but flat, nest, 5) Well defined nest with high walls (Deacon, 2006).

Catalepsy. Catalepsy was assessed primarily by the grid test and verified by the bar test. In the grid test, mice were placed at the top of a wire grid (15 cm x 30cm) that was inclined at 45 degrees from the surface. The time taken to move down the inclined surface to level ground was measured. Timing was stopped at 30 seconds for immobile (cataleptic) mice. In the bar test, the forepaws of the mice were placed on a bar several centimeters above the testing surface to position them into an unusual rearing-like posture. Mice were timed for how long they remained hanging upright by their forepaws on the bar, Timing was stopped at 30 seconds for cataleptic mice that remained in that unusual posture. Grid and bar tests were video-recorded for independent analysis by a second observer blinded to treatment.

Drug treatments. Unless noted otherwise, all drugs were dissolved in sterile saline solution (0.9% NaCl) and administered by i.p. injection at a volume of 0.01ml/g body weight. Drug doses (mg/kg body weight) and the time of behavioral tests or tissue collection post-injection are stated in the text. Haloperidol, fluoxetine, pergolide, SKF82958, and SCH23390 were all purchased from Sigma-Aldrich.

Quantitative RT-PCR

RNA from specified tissues (cortex, striatum, cerebellum, etc.) was extracted with the Lipid RNeasy Mini kit (Qiagen), DNAse treated (Qiagen), and quantified with a NanoDrop UV spectrophotometer (Thermo Scientific). cDNA used for qRT-PCR and generation of ISH probes

was synthesized using the QuantiTect RT kit (Qiagen) according to the manufacturer's protocols. Quantitative PCR was performed using the KAPA SYBR Fast qPCR mix with primer sets for the mRNA of specified gene targets and housekeeping genes for controls (GAPDH, β-actin, HPRT1). PCR reactions were carried out on a Roche LightCycler 480 with the following cycling conditions for all primer sets: 95°C for 3 min and then 40 cycles of 95°C for 15 sec, 56°C for 25 sec, and 72°C for 1 sec, followed by a melting curve analysis and 40°C for 10 sec. All samples were run in three replicates for each primer set. Using the $2^{-\Delta\Delta Ct}$ relative expression method (Livak and Schmittgen, 2001), the average CT values for the three replicates of each gene was normalized to the average CT values for the housekeeping gene to calculate the relative expression level.

***In situ* hybridization**

To prepare tissue for *in situ* hybridization (ISH), mice were transcardially perfused with 4% paraformaldehyde (PFA) in 0.01M phosphate buffered saline (PBS). Mouse brains were dissected, post-fixed with 4% PFA for 12 hours at 4°C, dehydrated in 30% sucrose in 0.01M PBS for 48 to 72 hours, and flash frozen in isopentane cooled with dry ice. 20 µm thick coronal sections cut on a Leica CM1850 cryostat were directly mounted onto Superfrost Plus glass slides, air-dried, and stored with desiccant at -80ºC for later ISH. Unless noted otherwise, all solutions were RNAse-free and made up in DEPC-treated water. Using primers targeting the genes of interest, probes for ISH were PCR-amplified from mouse cDNA (striatum) and subcloned into pBluescript (Stratagene). Antisense radioactive cRNA probes were generated and labeled with ^{35}S-UTP (Perkin Elmer) by in vitro transcription (IVT) using the RNAmaxx High Yield Transcription kit (Stratagene) following the manufacturer's protocols. ^{35}S-labeled cRNA probes were counted with a liquid scintillation counter and added to the hybridization solution (50% formamide, 35% Denhardt's solution, 2x SSC, 10% dextran sulfate, 0.3 mg/ml salmon sperm DNA, 0.15 mg/ml Yeast tRNA, 40 mM DTT). Slide-mounted sections were treated with

Proteinase K (1 µg/ml solution) for 15 minutes to permeabilize the tissue. Sections were hybridized in the ^{35}S-labeled hybridization solution at 60ºC (in a humidified chamber) for 48 hours. After hybridization, sections were treated with 20 µg/ml RNaseA, rinsed with a series of SSC washes (2x to 0.1x SSC), air-dried, and exposed to film for 3 to 7 days. Films were developed, scanned, and saved as images files.

Immunohistochemistry and Immunofluorescence

Mice were transcardially perfused with 4% PFA in 0.01M PBS. Mouse brains were dissected, post-fixed with 4% PFA for 12 hours at 4°C, dehydrated in 30% sucrose in 0.01M PBS for 48 to 72 hours, and flash frozen in isopentane cooled with dry ice. 40 µm thick coronal sections cut on a Leica CM1850 cryostat were cryoprotected and stored at -20ºC for later use. For immunohistochemistry, free-floating sections were washed in 0.01M PBS and treated for 30 minutes with H_2O_2 (1%) to block endogenous peroxidase activity. Sections were incubated in blocking solution (3% bovine serum albumin and 3% normal goat serum in 0.01M PBS) at room temperature for 1 hour. Sections were then incubated at 4ºC for 24 to 48 hours (specific to the individual antibody) with the primary antibody diluted to the appropriate concentration in blocking solution with 0.3% Triton X-100. After incubation in the primary antibody solution, sections were washed with 0.01M PBS and incubated for 2 hours at room temperature with the corresponding biotinylated secondary antibody (1:200; Vector) in blocking solution with 0.3% Triton X-100. Sections were then washed with 0.01M PBS and incubated for 2 hours at room temperature in an avidin-biotin complex solution (ABC R.T.U. Reagent; Vector). The immunohistochemical staining was visualized using the SG Peroxidase Substrate Kit (Vector) and then washed in 0.01M PBS. Sections were mounted onto Superfrost Plus glass slides, air-dried, dehydrated in ethanol, defatted in xylene, and coverslipped with Cytoseal XYL (Richard-Allan Scientific). Immunofluorescence staining was similar except the H_2O_2 (1%) treatment was omitted, we used a fluorescence-conjugated secondary antibody (1:200), and after incubation

with the secondary antibody and 0.01M PBS washes, sections were mounted onto slides and coverslipped with Vectashield Hard Set Mounting Medium with DAPI counterstain (Vector). Images were acquired using a Zeiss Axioskop 2 microscope and a Zeiss Laser Scanning Microscope 5 Pascal. The following primary antibodies at the given dilutions were used: DARPP-32 (1:100; Abcam), GFP (1:1000; Aves), MuOR (1:1000; Neuromics), TH (1:500; Abcam), VGluT1 (1:500; Millipore), PV (1:5000; Swant), ChAT (1:500; Millipore), Calretinin (1:200; Swant), SST (1:500; Bachem), Nkx2.1 (1:100; Epitomics), and p-H3 (1:500; Millipore).

BrdU Birth-Labeling

BrdU (5-bromo-2-deoxyuridine, a synthetic nucleoside analogue of thymidine) birth-dating was performed as previously described (Wojtowicz and Kee, 2006). Timed-pregnant dams received a single injection (i.p.) of 100 mg/kg BrdU (Sigma) dissolved in sterile saline at the time-points stated in the text. P0 pups were transcardially perfused with 4% PFA in 0.01M PBS and brains were dissected, sectioned (20 μm thick), and stored for later immunohistochemical stainings as previously described. Tail biopsies from P0 pups were collected for genotyping prior to perfusion. BrdU incorporated into cells was visualized by immunohistochemical staining with a BrdU antibody (1:200; Abcam) following the previously described procedures.

Stereological Volume Analysis and Cell Counting

To quantify the total volumes of the dorsal striatum and cortex, design-based stereological estimation (Gundersen and Jensen, 1987; West et al., 1991) of DARPP-32 immunohistochemically stained coronal sections (imaged on a Zeiss Axioskop 2 microscope) was performed using Stereo Investigator 6.0 software (MicroBrightField). The first section was randomly selected from the first ten sections that contained the dorsal striatum and every fourth section thereafter was selected for stereological analysis. DARPP-32 immunohistochemical staining was used to define the striatum from the cortex. The dorsal striatum was defined as the region of the striatum dorsal to the anterior commissure (AC). For each sequential coronal

section selected, the dorsal striatum and cortex were separately contoured (traced) and the total dorsal striatal and cortical volume was estimated using the Cavalieri Method in Stereo Investigator. For unbiased cell counting of immunohistochemically labeled cells in the dorsal striatum (DARPP-32, EGFP, PV, etc.) the dorsal striatum was first contoured under low magnification (5X). The contoured striatum was vertically divided in half at the geometric midpoint along the widest medial-lateral length of the dorsal striatum to define the dorsomedial striatum (DMS) and the dorsolateral striatum (DLS). Under higher magnification (40X or 100X), the Stereo Investigator software randomly selected three ROIs of a specified size within the contoured DMS and DLS. For each randomly selected ROI, labeled cells were counted to estimate densities of labeled cells in the DMS and DLS of matched coronal sections. In both stereological volume analysis and cell counting, investigators were blind to genotypes and treatments.

Optogenetics

Stereotaxic viral injections and implantation of optical fibers. Detailed methods for the construction of the optical fiber implants and optogenetic surgical procedures have been described previously (Yizhar et al., 2011; Zhang et al., 2010). Mice were deeply anesthetized with isofluorane (1-2%) and mounted in a stereotaxic frame with non-puncturing ear bars (Kopf Instruments). The scalp was opened and two small holes for bilateral injections were drilled with a 0.5mm burr drill bit at the site of injection above the dorsal striatum (coordinates from bregma; control: AP = +1.0 mm, ML = ±1.6 mm; Zfp521-BrKO: AP = +0.8 mm, ML = ±1.5 mm). rAAV2/1-CAGGS-FLEX-ChR2-tdTomato (University of Pennsylvania Vector Core) was bilaterally injected into the dorsal striatum (coordinates from surface of the brain; control: DV = -2.5mm; Zfp521-BrKO: DV = -2.3mm) through a 33-gauge injector cannula (PlasticsOne) using a syringe pump (KDS) at a rate of 0.2 µl/min (1.0 µl total over 5 minutes). After viral injections, the fiber optic implants (length of fiber cut so that the tip is directly above the site of injection in the dorsal

striatum) were bilaterally placed in the same dorsal striatal coordinates and secured to the skull using dental cement/epoxy. The scalp was carefully closed around the protruding fiber optic implants and sutured. Following the surgical procedure, mice were individually housed and monitored for body weight and health until recovery from the surgery (1 week). To allow sufficient time for viral expression, optogenetic behavioral tests were not conducted until 3 to 4 weeks post-surgery.

Behavioral testing with optogenetic stimulation. Behavioral testing was conducted in our standard behavioral chamber. Two fiber optic patch cables were connected to a 50/50 optical splitter which was coupled a 473nm solid-state laser (OEM Lasers). Laser output was set to deliver blue light of 1-2 mW intensity at the tip of the optical fibers implanted into the dorsal striatum. The fiber optic patch cables were suspended above the behavioral chamber and connected to the fiber optic implants of the mice with enough slack to prevent entanglement during locomotion and behavioral activities. Simulation frequency and pulse width of the laser was controlled by a 10 MHz variable pulse generator (BK Precision). The fiber optic patch cables were securely connected to the fiber optic implants and mice were placed in the behavioral chamber and video-recorded as previously described. Before the start of each testing session, mice were video-recorded but left undisturbed (no optogenetic stimulation) in the behavioral chamber for 10 minutes allow for acclimation. Each 3-minute testing session consisted of six repeated cycles of a 10-second pre-laser period (“Pre”), followed by a 10-second period of laser activation of ChR2 (“Laser”) and then a 10-second post-laser period (“Post”). For activation of D2-ChR2, we used 10-second constant-on laser stimulation (steady illumination). Mice completed 3 sessions each testing day, for a total of 18 Pre, Laser, and Post periods to be averaged for behavioral analysis (hand-scoring of video reviewed at half-speed and automated video analysis of locomotor activity with StereoScan software, same as previously described); mice were switched between each 3-minute session. Following

completion of behavioral tests, mice were perfused and histology was performed to verify injection locations and level of viral expression.

Electrophysiology

Experiments were conducted on Zfp521-BrKO; D1-EGFP, Zfp521-BrKO; D2-EGFP and their age-matched control littermates (mean age 62 days). Whole-cell patch clamp recordings in voltage-clamp mode were obtained from medium sized spiny neurons (MSNs) visualized in coronal slices (300μm thick) with the aid of infrared video. Dorsomedially located striatal MSNs were identified by somatic size and basic membrane properties (input resistance, membrane capacitance, and time constant). Series resistance was <25 MΩ and was compensated 70–80%. The patch pipette (3–5 MΩ) contained the following solutions (in mM): 125 Cs-methanesulfonate, 4 NaCl, 1 MgCl2, 5 MgATP, 9 EGTA, 8 HEPES, 1 GTP, 10 phosphocreatine, and 0.1 leupeptin, pH 7.25–7.3 using 1N CsOH (osmolality, 280–290 mOsm/l). Spontaneous excitatory postsynaptic currents (sEPSCs) were recorded in standard artificial CSF (ACSF) composed of the following (in mM): 130 NaCl, 26 NaHCO3, 3 KCl, 2 MgCl2, 1.25 NaHPO4, 2 CaCl2, and 10 glucose, pH 7.4. In specific experiments, bicuculline (BIC, 10 μM) also was added to abolish the contribution of spontaneous currents mediated by activation of $GABA_A$ receptors. In addition, cells were held at −70 mV to minimize their contribution and that of voltage-gated conductances. After characterizing the basic membrane properties of the neuron, sEPSCs were recorded for variable periods of time (usually 3–6 min). The membrane current was filtered at 1 kHz and digitized at 100 μsec using Clampex (gap-free mode). All drugs, bicuculline and haloperidol (10 μM) were bath applied for at least 5 minutes prior to recording. Spontaneous synaptic events were analyzed off-line using the Mini Analysis Program (Synaptosoft Software, Fort Lee, NJ). The threshold amplitude for the detection of an event was adjusted above root mean square noise level (generally ∼5 pA). This software was used to calculate sEPSC frequency, expressed as number of events per second (in Hertz).

REFERENCES

Abelson, J.F., Kwan, K.Y., O'Roak, B.J., Baek, D.Y., Stillman, A. a, Morgan, T.M., Mathews, C. a, Pauls, D.L., Rasin, M.-R., Gunel, M., et al. (2005). Sequence variants in SLITRK1 are associated with Tourette's syndrome. Science *310*, 317–320.

Ahmari, S.E., Spellman, T., Douglass, N.L., Kheirbek, M. a., Simpson, H.B., Deisseroth, K., Gordon, J. a., and Hen, R. (2013). Repeated Cortico-Striatal Stimulation Generates Persistent OCD-Like Behavior. Science (80-.). *340*, 1234–1239.

Albin, R.L., Young, A.B., and Penney, J.B. (1989). The functional anatomy of basal ganglia disorders. Trends Neurosci. *12*, 366–375.

Albin, R.L., Young, A.B., and Penney, J.B. (1995). The functional anatomy of disorders of the basal ganglia. Trends Neurosci. *18*, 63–64.

Albin, R.L., Koeppe, R. a, Bohnen, N.I., Nichols, T.E., Meyer, P., Wernette, K., Minoshima, S., Kilbourn, M.R., and Frey, K. a (2003). Increased ventral striatal monoaminergic innervation in Tourette syndrome. Neurology *61*, 310–315.

Alcaraz, W.A., Gold, D.A., Raponi, E., Gent, P.M., Concepcion, D., and Hamilton, B.A. (2006). Zfp423 controls proliferation and differentiation of neural precursors in cerebellar vermis formation. Proc. Natl. Acad. Sci. *103*, 19424–19429.

Alexander, G.E.E., and Crutcher, M.D.D. (1990). Functional architecture of basal ganglia circuits: neural substrates of parallel processing. Trends Neurosci. *13*, 266–271.

Alexander, G.E., DeLong, M.R., and Strick, P.L. (1986). Parallel organization of functionally segregated circuits linking basal ganglia and cortex. Annu. Rev. Neurosci. *9*, 357–381.

Allen Institute for Brain Science (2012). http://developingmouse.brain-map.org. Allen Developing Mouse Brain Atlas.

American Psychiatric Association (2013). Neurodevelopmental Disorders. In American Psychiatric Association: Diagnostic and Statistical Manual of Mental Disorders, Fifth Edition,.

Anca, M.H., Giladi, N., and Korczyn, A.D. (2004). Ropinirole in Gilles de la Tourette syndrome. Neurology *62*, 1626–1627.

Andersen, P.H., and Jansen, J. a (1990). Dopamine receptor agonists: selectivity and dopamine D1 receptor efficacy. Eur. J. Pharmacol. *188*, 335–347.

Anderson, S.A., Qiu, M., Bulfone, A., Eisenstat, D.D., Meneses, J., Pedersen, R., and Rubenstein, J.L. (1997). Mutations of the homeobox genes Dlx-1 and Dlx-2 disrupt the striatal subventricular zone and differentiation of late born striatal neurons. Neuron *19*, 27–37.

Arnsten, A.F., and Dudley, A.G. (2005). Methylphenidate improves prefrontal cortical cognitive function through alpha2 adrenoceptor and dopamine D1 receptor actions: Relevance to therapeutic effects in Attention Deficit Hyperactivity Disorder. Behav. Brain Funct. *1*, 2.

Baron-Cohen, S., and Scahill, V. (1999). The prevalence of Gilles de la Tourette syndrome in children and adolescents with autism: a large scale study. Psychol. … 1151–1159.

Benoit-Marand, M., Borrelli, E., and Gonon, F. (2001). Inhibition of dopamine release via presynaptic D2 receptors: time course and functional characteristics in vivo. J. Neurosci. *21*, 9134–9141.

Berendse, H.W., Galis-de Graaf, Y., and Groenewegen, H.J. (1992). Topographical organization and relationship with ventral striatal compartments of prefrontal corticostriatal projections in the rat. J. Comp. Neurol. *316*, 314–347.

Berns, G.S. (1997). Brain Regions Responsive to Novelty in the Absence of Awareness. Science (80-.). *276*, 1272–1275.

Berridge, K.C., and Aldridge, J.W. (2000). Super-stereotypy I: enhancement of a complex movement sequence by systemic dopamine D1 agonists. Synapse *37*, 194–204.

Berridge, C.W., Devilbiss, D.M., Andrzejewski, M.E., Arnsten, A.F.T., Kelley, A.E., Schmeichel, B., Hamilton, C., and Spencer, R.C. (2006). Methylphenidate preferentially increases catecholamine neurotransmission within the prefrontal cortex at low doses that enhance cognitive function. Biol. Psychiatry *60*, 1111–1120.

Berridge, K.C., Aldridge, J.W., Houchard, K.R., and Zhuang, X. (2005). Sequential super-stereotypy of an instinctive fixed action pattern in hyper-dopaminergic mutant mice: a model of obsessive compulsive disorder and Tourette's. BMC Biol. *3*, 4.

Bertran-Gonzalez, J., Bosch, C., Maroteaux, M., Matamales, M., Hervé, D., Valjent, E., and Girault, J.-A. (2008). Opposing patterns of signaling activation in dopamine D1 and D2 receptor-expressing striatal neurons in response to cocaine and haloperidol. J. Neurosci. *28*, 5671–5685.

Bertran-Gonzalez, J., Håkansson, K., Borgkvist, A., Irinopoulou, T., Brami-Cherrier, K., Usiello, A., Greengard, P., Hervé, D., Girault, J.-A., Valjent, E., et al. (2009). Histone H3 phosphorylation is under the opposite tonic control of dopamine D2 and adenosine A2A receptors in striatopallidal neurons. Neuropsychopharmacology *34*, 1710–1720.

Billard, W., Ruperto, V., Crosby, G., Iorio, L.C., and Barnett, A. (1984). Characterization of the binding of 3H-SCH 23390, a selective D-1 receptor antagonist ligand, in rat striatum. Life Sci. *35*, 1885–1893.

Black, K.J., and Mink, J.W. (2000). Response to levodopa challenge in Tourette syndrome. Mov. Disord. *15*, 1194–1198.

Bloch, M.H., and Leckman, J.F. (2009). Clinical course of Tourette syndrome. J. Psychosom. Res. *67*, 497–501.

Bloch, M., State, M., and Pittenger, C. (2011). Recent advances in Tourette syndrome. Curr. Opin. Neurol. *24*, 119–125.

Bloch, M.H., Leckman, J.F., Zhu, H., and Peterson, B.S. (2005). Caudate volumes in childhood predict symptom severity in adults with Tourette syndrome. Neurology *65*, 1253–1258.

Bond, H.M., Mesuraca, M., Carbone, E., Bonelli, P., Agosti, V., Amodio, N., De Rosa, G., Di Nicola, M., Gianni, A.M., Moore, M. a S., et al. (2004). Early hematopoietic zinc finger protein (EHZF), the human homolog to mouse Evi3, is highly expressed in primitive human hematopoietic cells. Blood *103*, 2062–2070.

Bond, H.M., Mesuraca, M., Amodio, N., Mega, T., Agosti, V., Fanello, D., Pelaggi, D., Bullinger, L., Grieco, M., Moore, M. a S., et al. (2008). Early hematopoietic zinc finger protein-zinc finger protein 521: a candidate regulator of diverse immature cells. Int. J. Biochem. Cell Biol. *40*, 848–854.

Boulay, D., Depoortere, R., Oblin, a, Sanger, D.J., Schoemaker, H., and Perrault, G. (2000). Haloperidol-induced catalepsy is absent in dopamine D(2), but maintained in dopamine D(3) receptor knock-out mice. Eur. J. Pharmacol. *391*, 63–73.

Bourin, M., and Hascoët, M. (2003). The mouse light/dark box test. Eur. J. Pharmacol. *463*, 55–65.

Boyar, W.C., and Altar, C. a (1987). Modulation of in vivo dopamine release by D2 but not D1 receptor agonists and antagonists. J. Neurochem. *48*, 824–831.

Boyden, E.S., Zhang, F., Bamberg, E., Nagel, G., and Deisseroth, K. (2005). Millisecond-timescale, genetically targeted optical control of neural activity. Nat. Neurosci. *8*, 1263–1268.

Braun, A.R., Stoetter, B., Randolph, C., Hsiao, J.K., Vladar, K., Gernert, J., Carson, R.E., Herscovitch, P., and Chase, T.N. (1993). The functional neuroanatomy of Tourette's syndrome: an FDG-PET study. I. Regional changes in cerebral glucose metabolism differentiating patients and controls. Neuropsychopharmacology *9*, 277–291.

Bronfeld, M., Belelovsky, K., and Bar-Gad, I. (2011). Spatial and temporal properties of tic-related neuronal activity in the cortico-Basal Ganglia loop. J. Neurosci. *31*, 8713–8721.

Bronfeld, M., Yael, D., Belelovsky, K., and Bar-Gad, I. (2013). Motor tics evoked by striatal disinhibition in the rat. Front. Syst. Neurosci. *7*, 50.

Bruun, R.D. (1984). Gilles de la Tourette's syndrome. An overview of clinical experience. J. Am. Acad. Child Psychiatry *23*, 126–133.

Bunney, B.S., and Grace, A.A. (1978). Acute and chronic haloperidol treatment: comparison of effects on nigral dopaminergic cell activity. Life Sci. *23*, 1715–1727.

Burger, C., Gorbatyuk, O.S., Velardo, M.J., Peden, C.S., Williams, P., Zolotukhin, S., Reier, P.J., Mandel, R.J., and Muzyczka, N. (2004). Recombinant AAV viral vectors pseudotyped with

viral capsids from serotypes 1, 2, and 5 display differential efficiency and cell tropism after delivery to different regions of the central nervous system. Mol. Ther. *10*, 302–317.

Buse, J., Schoenefeld, K., Münchau, A., and Roessner, V. (2013). Neuromodulation in Tourette syndrome: dopamine and beyond. Neurosci. Biobehav. Rev. *37*, 1069–1084.

Butler, A., Uryu, K., and Chesselet, M. (1998). A role for N-methyl-D-aspartate receptors in the regulation of synaptogenesis and expression of the polysialylated form of the neural cell adhesion molecule in the. Dev. Neurosci. *90095*, 253–262.

Campbell, K.M., de Lecea, L., Severynse, D.M., Caron, M.G., McGrath, M.J., Sparber, S.B., Sun, L.Y., and Burton, F.H. (1999). OCD-Like behaviors caused by a neuropotentiating transgene targeted to cortical and limbic D1+ neurons. J. Neurosci. *19*, 5044–5053.

Canales, J.J., and Graybiel, a M. (2000). A measure of striatal function predicts motor stereotypy. Nat. Neurosci. *3*, 377–383.

Cardinal, R.N., Parkinson, J. a, Hall, J., and Everitt, B.J. (2002). Emotion and motivation: the role of the amygdala, ventral striatum, and prefrontal cortex. Neurosci. Biobehav. Rev. *26*, 321–352.

De Carlos, J. a, López-Mascaraque, L., and Valverde, F. (1996). Dynamics of cell migration from the lateral ganglionic eminence in the rat. J. Neurosci. *16*, 6146–6156.

Carola, V., D'Olimpio, F., Brunamonti, E., Mangia, F., and Renzi, P. (2002). Evaluation of the elevated plus-maze and open-field tests for the assessment of anxiety-related behaviour in inbred mice. Behav. Brain Res. *134*, 49–57.

Cellerino, A., Siciliano, R., Domenici, L., and Maffei, L. (1992). Parvalbumin immunoreactivity: a reliable marker for the effects of monocular deprivation in the rat visual cortex. Neuroscience *51*, 749–753.

Centers for Disease Control and Prevention (CDC (2009). Prevalence of diagnosed Tourette syndrome in persons aged 6-17 years - United States, 2007. MMWR. Morb. Mortal. Wkly. Rep. *58*, 581–585.

Chartoff, E.H., Marck, B.T., Matsumoto, a M., Dorsa, D.M., and Palmiter, R.D. (2001). Induction of stereotypy in dopamine-deficient mice requires striatal D1 receptor activation. Proc. Natl. Acad. Sci. U. S. A. *98*, 10451–10456.

Chen, S.-K., Tvrdik, P., Peden, E., Cho, S., Wu, S., Spangrude, G., and Capecchi, M.R. (2010). Hematopoietic origin of pathological grooming in Hoxb8 mutant mice. Cell *141*, 775–785.

Cheng, L.E., and Reed, R.R. (2007). Zfp423/OAZ participates in a developmental switch during olfactory neurogenesis. Neuron *54*, 547–557.

Cheng, L.E., Zhang, J., and Reed, R.R. (2007). The transcription factor Zfp423/OAZ is required for cerebellar development and CNS midline patterning. Dev. Biol. *307*, 43–52.

Cheng, Y., Quinn, J.F., and Weiss, L.A. (2013). An eQTL mapping approach reveals that rare variants in the SEMA5A regulatory network impact autism risk. Hum. Mol. Genet. *22*, 2960–2972.

Cheung, M.-Y.C., Shahed, J., and Jankovic, J. (2007). Malignant Tourette syndrome. Mov. Disord. *22*, 1743–1750.

Chou-Green, J.M., Holscher, T.D., Dallman, M.F., and Akana, S.F. (2003). Compulsive behavior in the 5-HT2C receptor knockout mouse. Physiol. Behav. *78*, 641–649.

Cianchetti, C., Fratta, a, Pisano, T., and Minafra, L. (2005). Pergolide improvement in neuroleptic-resistant Tourette cases: various mechanisms causing tics. Neurol. Sci. *26*, 137–139.

Cobos, I., Calcagnotto, M.E., Vilaythong, A.J., Thwin, M.T., Noebels, J.L., Baraban, S.C., and Rubenstein, J.L.R. (2005). Mice lacking Dlx1 show subtype-specific loss of interneurons, reduced inhibition and epilepsy. Nat. Neurosci. *8*, 1059–1068.

Cobos, I., Borello, U., and Rubenstein, J.L.R. (2007). Dlx transcription factors promote migration through repression of axon and dendrite growth. Neuron *54*, 873–888.

Conelea, C. a, and Woods, D.W. (2008). The influence of contextual factors on tic expression in Tourette's syndrome: a review. J. Psychosom. Res. *65*, 487–496.

Correa, D., Hesse, E., Seriwatanachai, D., Kiviranta, R., Saito, H., Yamana, K., Neff, L., Atfi, A., Coillard, L., Sitara, D., et al. (2010). Zfp521 is a target gene and key effector of parathyroid hormone-related peptide signaling in growth plate chondrocytes. Dev. Cell *19*, 533–546.

Crawley, J.N. (2007). What's Wrong With My Mouse? (Hoboken, NJ, USA: John Wiley & Sons, Inc.).

Creese, I., Burt, D.R., and Snyder, S.H. (1975). Dopamine receptor binding: differentiation of agonist and antagonist states with 3H-dopamine and 3H-haloperidol. Life Sci. *17*, 933–1001.

Crittenden, J.R., and Graybiel, A.M. (2011). Basal Ganglia disorders associated with imbalances in the striatal striosome and matrix compartments. Front. Neuroanat. *5*, 59.

Cromwell, H.C., Berridge, K.C., Drago, J., and Levine, M.S. (1998). Action sequencing is impaired in D1A-deficient mutant mice. Eur. J. Neurosci. *10*, 2426–2432.

Dahlstrand, J., Lardelli, M., and Lendahl, U. (1995). Nestin mRNA expression correlates with the central nervous system progenitor cell state in many, but not all, regions of developing central nervous system. Brain Res. Dev. Brain Res. *84*, 109–129.

Damsma, G., Pfaus, J.G., Wenkstern, D., Phillips, a G., and Fibiger, H.C. (1992). Sexual behavior increases dopamine transmission in the nucleus accumbens and striatum of male rats: comparison with novelty and locomotion. Behav. Neurosci. *106*, 181–191.

Deacon, R.M.J. (2006). Assessing nest building in mice. Nat. Protoc. *1*, 1117–1119.

Deacon, T.W., Pakzaban, P., and Isacson, O. (1994). The lateral ganglionic eminence is the origin of cells committed to striatal phenotypes: neural transplantation and developmental evidence. Brain Res. *668*, 211–219.

Degos, B., Deniau, J.-M., Thierry, A.-M., Glowinski, J., Pezard, L., and Maurice, N. (2005). Neuroleptic-induced catalepsy: electrophysiological mechanisms of functional recovery induced by high-frequency stimulation of the subthalamic nucleus. J. Neurosci. *25*, 7687–7696.

Deleu, D., Northway, M.G., and Hanssens, Y. (2002). Clinical pharmacokinetic and pharmacodynamic properties of drugs used in the treatment of Parkinson's disease. Clin. Pharmacokinet. *41*, 261–309.

DeLong, M.R. (1990). Primate models of movement disorders of basal ganglia origin. Trends Neurosci. *13*, 281–285.

Ding, J.B., Guzman, J.N., Peterson, J.D., Goldberg, J. a, and Surmeier, D.J. (2010). Thalamic gating of corticostriatal signaling by cholinergic interneurons. Neuron *67*, 294–307.

Doyle, J.P., Dougherty, J.D., Heiman, M., Schmidt, E.F., Stevens, T.R., Ma, G., Bupp, S., Shrestha, P., Shah, R.D., Doughty, M.L., et al. (2008). Application of a translational profiling approach for the comparative analysis of CNS cell types. Cell *135*, 749–762.

Durieux, P.F., Schiffmann, S.N., and de Kerchove d'Exaerde, A. (2011). Differential regulation of motor control and response to dopaminergic drugs by D1R and D2R neurons in distinct dorsal striatum subregions. EMBO J. *31*, 1–14.

Eidelberg, D., Moeller, J.R., Antonini, a., Kazumata, K., Dhawan, V., Budman, C., and Feigin, a. (1997). The metabolic anatomy of Tourette's syndrome. Neurology *48*, 927–933.

Ercan-Sencicek, A.G., Stillman, A.A., Ghosh, A.K., Bilguvar, K., O'Roak, B.J., Mason, C.E., Abbott, T., Gupta, A., King, R.A., Pauls, D.L., et al. (2010). L-histidine decarboxylase and Tourette's syndrome. N. Engl. J. Med. *362*, 1901–1908.

Erenberg, G., Cruse, R.P., and Rothner, a D. (1987). The natural history of Tourette syndrome: a follow-up study. Ann. Neurol. *22*, 383–385.

Essig, E.C., and Kilpatrick, I.C. (1991). Influence of acute and chronic haloperidol treatment on dopamine metabolism in the rat caudate-putamen, prefrontal cortex and amygdala. Psychopharmacology (Berl). *104*, 194–200.

Feinberg, M., and Carroll, B.J. (1979). Effects of dopamine agonists and antagonists in Tourette's disease. Arch. Gen. Psychiatry *36*, 979–985.

Felling, R.J., and Singer, H.S. (2011). Neurobiology of tourette syndrome: current status and need for further investigation. J. Neurosci. *31*, 12387–12395.

Fentress, J.C., Stanfield, B.B., and Cowan, W.M. (1981). Observation on the development of the striatum in mice and rats. Anat. Embryol. (Berl). *163*, 275–298.

Fernandez, T. V, Sanders, S.J., Yurkiewicz, I.R., Ercan-Sencicek, a G., Kim, Y.-S., Fishman, D.O., Raubeson, M.J., Song, Y., Yasuno, K., Ho, W.S.C., et al. (2012). Rare copy number variants in tourette syndrome disrupt genes in histaminergic pathways and overlap with autism. Biol. Psychiatry *71*, 392–402.

Fishell, G., and van der Kooy, D. (1987). Pattern formation in the striatum: developmental changes in the distribution of striatonigral neurons. J. Neurosci. *7*, 1969–1978.

Fishell, G., and van der Kooy, D. (1989). Pattern formation in the striatum: developmental changes in the distribution of striatonigral projections. Brain Res. Dev. Brain Res. *45*, 239–255.

Fishell, G., and van der Kooy, D. (1991). Pattern formation in the striatum: neurons with early projections to the substantia nigra survive the cell death period. J. Comp. Neurol. *312*, 33–42.

Flandin, P., Kimura, S., and Rubenstein, J.L.R. (2010). The progenitor zone of the ventral medial ganglionic eminence requires Nkx2-1 to generate most of the globus pallidus but few neocortical interneurons. J. Neurosci. *30*, 2812–2823.

Freeman, R.D., Fast, D.K., Burd, L., Kerbeshian, J., Robertson, M.M., and Sandor, P. (2000). An international perspective on Tourette syndrome: selected findings from 3,500 individuals in 22 countries. Dev. Med. Child Neurol. *42*, 436–447.

Fuller, R.W., and Clemens, J.A. (1991). Pergolide: a dopamine agonist at both D1 and D2 receptors. Life Sci. *49*, 925–930.

Gadow, K.D., Nolan, E.E., and Sverd, J. (1992). Methylphenidate in hyperactive boys with comorbid tic disorder: II. Short-term behavioral effects in school settings. J. Am. Acad. Child Adolesc. Psychiatry *31*, 462–471.

Ganos, C., Roessner, V., and Münchau, A. (2013). The functional anatomy of Gilles de la Tourette syndrome. Neurosci. Biobehav. Rev. *37*, 1050–1062.

Garel, S., Marin, F., Grosschedl, R., and Charnay, P. (1999). Ebf1 controls early cell differentiation in the embryonic striatum. Development *126*, 5285.

Garel, S., Yun, K., Grosschedl, R., and Rubenstein, J.L.R. (2002). The early topography of thalamocortical projections is shifted in Ebf1 and Dlx1/2 mutant mice. Development *129*, 5621–5634.

Gerfen, C.R. (1984). The neostriatal mosaic: compartmentalization of corticostriatal input and striatonigral output systems. Nature *311*, 461–464.

Gerfen, C.R. (1985). The neostriatal mosaic. I. Compartmental organization of projections from the striatum to the substantia nigra in the rat. J. Comp. Neurol. *236*, 454–476.

Gerfen, C.R. (1992). The neostriatal mosaic: multiple levels of compartmental organization. Trends Neurosci. *15*, 133–139.

Gerfen, C.R., and Surmeier, D.J. (2011). Modulation of striatal projection systems by dopamine. Annu. Rev. Neurosci. *34*, 441–466.

Gerfen, C.R., Engber, T.M., Mahan, L.C., Susel, Z., Chase, T.N., Monsma, F.J., and Sibley, D.R. (1990). D1 and D2 dopamine receptor-regulated gene expression of striatonigral and striatopallidal neurons. Science *250*, 1429–1432.

Gilbert, D.L., Sethuraman, G., Sine, L., Peters, S., and Sallee, F.R. (2000). Tourette's syndrome improvement with pergolide in a randomized, double-blind, crossover trial. Neurology *54*, 1310–1315.

Gilbert, D.L., Dure, L., Sethuraman, G., Raab, D., Lane, J., and Sallee, F.R. (2003). Tic reduction with pergolide in a randomized controlled trial in children. Neurology *60*, 606–611.

Glickstein, S.B., and Schmauss, C. (2004). Focused motor stereotypies do not require enhanced activation of neurons in striosomes. J. Comp. Neurol. *469*, 227–238.

Goldman, L.S., Genel, M., Bezman, R.J., and Slanetz, P.J. (1998). Diagnosis and treatment of attention-deficit/hyperactivity disorder in children and adolescents. Council on Scientific Affairs, American Medical Association. JAMA *279*, 1100–1107.

Goldstein, M., Lieberman, a, Lew, J.Y., Asano, T., Rosenfeld, M.R., and Makman, M.H. (1980). Interaction of pergolide with central dopaminergic receptors. Proc. Natl. Acad. Sci. U. S. A. *77*, 3725–3728.

Gong, S., Zheng, C., Doughty, M.L., Losos, K., Didkovsky, N., Schambra, U.B., Nowak, N.J., Joyner, A., Leblanc, G., Hatten, M.E., et al. (2003). A gene expression atlas of the central nervous system based on bacterial artificial chromosomes. Nature *425*, 917–925.

Granon, S., Passetti, F., Thomas, K.L., Dalley, J.W., Everitt, B.J., and Robbins, T.W. (2000). Enhanced and impaired attentional performance after infusion of D1 dopaminergic receptor agents into rat prefrontal cortex. J. Neurosci. *20*, 1208–1215.

Graybiel, a M. (1984). Correspondence between the dopamine islands and striosomes of the mammalian striatum. Neuroscience *13*, 1157–1187.

Graybiel, a M. (1990). Neurotransmitters and neuromodulators in the basal ganglia. Trends Neurosci. *13*, 244–254.

Graybiel, A.M. (2008). Habits, rituals, and the evaluative brain. Annu. Rev. Neurosci. *31*, 359–387.

Graybiel, A.M., Canales, J.J., and Capper-Loup, C. (2000). Levodopa-induced dyskinesias and dopamine-dependent stereotypies: a new hypothesis. Trends Neurosci. *23*, S71–7.

Greer, J.M., and Capecchi, M.R. (2002). Hoxb8 is required for normal grooming behavior in mice. Neuron *33*, 23–34.

Griesemer, D.A. (1997). Pergolide in the management of Tourette syndrome. J. Child Neurol. *12*, 402–403.

Gundersen, H.J., and Jensen, E.B. (1987). The efficiency of systematic sampling in stereology and its prediction. J. Microsc. *147*, 229–263.

Gupta, R.K., Arany, Z., Seale, P., Mepani, R.J., Ye, L., Conroe, H.M., Roby, Y. a, Kulaga, H., Reed, R.R., and Spiegelman, B.M. (2010). Transcriptional control of preadipocyte determination by Zfp423. Nature *464*, 619–623.

Halliday, A.L., and Cepko, C.L. (1992). Generation and migration of cells in the developing striatum. Neuron *9*, 15–26.

Hata, a, Seoane, J., Lagna, G., Montalvo, E., Hemmati-Brivanlou, a, and Massagué, J. (2000). OAZ uses distinct DNA- and protein-binding zinc fingers in separate BMP-Smad and Olf signaling pathways. Cell *100*, 229–240.

Heiman, M., Schaefer, A., Gong, S., Peterson, J.D., Day, M., Ramsey, K.E., Suárez-Fariñas, M., Schwarz, C., Stephan, D. a, Surmeier, D.J., et al. (2008). A translational profiling approach for the molecular characterization of CNS cell types. Cell *135*, 738–748.

Heise, K.-F., Steven, B., Liuzzi, G., Thomalla, G., Jonas, M., Müller-Vahl, K., Sauseng, P., Münchau, a, Gerloff, C., and Hummel, F.C. (2010). Altered modulation of intracortical excitability during movement preparation in Gilles de la Tourette syndrome. Brain *133*, 580–590.

Hentges, K.E., Weiser, K.C., Schountz, T., Woodward, L.S., Morse, H.C., and Justice, M.J. (2005). Evi3, a zinc-finger protein related to EBFAZ, regulates EBF activity in B-cell leukemia. Oncogene *24*, 1220–1230.

Hesse, E., Saito, H., Kiviranta, R., Correa, D., Yamana, K., Neff, L., Toben, D., Duda, G., Atfi, A., Geoffroy, V., et al. (2010). Zfp521 controls bone mass by HDAC3-dependent attenuation of Runx2 activity. J. Cell Biol. *191*, 1271–1283.

Hoffman, D.C., and Donovan, H. (1995). Catalepsy as a rodent model for detecting antipsychotic drugs with extrapyramidal side effect liability. Psychopharmacology (Berl). *120*, 128–133.

Hornsey, H., Banerjee, S., Zeitlin, H., and Robertson, M. (2001). The prevalence of Tourette syndrome in 13-14-year-olds in mainstream schools. J. Child Psychol. Psychiatry. *42*, 1035–1039.

Huang, S., Laoukili, J., Epping, M.T., Koster, J., Hölzel, M., Westerman, B. a, Nijkamp, W., Hata, A., Asgharzadeh, S., Seeger, R.C., et al. (2009). ZNF423 is critically required for retinoic acid-induced differentiation and is a marker of neuroblastoma outcome. Cancer Cell *15*, 328–340.

Hyde, T.M., Stacey, M.E., Coppola, R., Handel, S.F., Rickler, K.C., and Weinberger, D.R. (1995). Cerebral morphometric abnormalities in Tourette's syndrome: A quantitative MRI study of monozygotic twins. Neurology *45*, 1176–1182.

Jackson, D.M., and Westlind-Danielsson, a (1994). Dopamine receptors: molecular biology, biochemistry and behavioural aspects. Pharmacol. Ther. *64*, 291–370.

Jankovic, J. (1997). Phenomenology and Classification of Tics. Neurol. Clin. *15*, 267–275.

Jankovic, J., Gelineau-Kattner, R., and Davidson, A. (2010). Tourette's syndrome in adults. Mov. Disord. *25*, 2171–2175.

Kadesjö, B., and Gillberg, C. (2000). Tourette's disorder: epidemiology and comorbidity in primary school children. J. Am. Acad. Child Adolesc. Psychiatry *39*, 548–555.

Kalanithi, P.S. a, Zheng, W., Kataoka, Y., DiFiglia, M., Grantz, H., Saper, C.B., Schwartz, M.L., Leckman, J.F., and Vaccarino, F.M. (2005). Altered parvalbumin-positive neuron distribution in basal ganglia of individuals with Tourette syndrome. Proc. Natl. Acad. Sci. U. S. A. *102*, 13307–13312.

Kamiya, D., Banno, S., Sasai, N., Ohgushi, M., Inomata, H., Watanabe, K., Kawada, M., Yakura, R., Kiyonari, H., Nakao, K., et al. (2011). Intrinsic transition of embryonic stem-cell differentiation into neural progenitors. Nature *470*, 503–509.

Kang, S., Akerblad, P., Kiviranta, R., Gupta, R.K., Kajimura, S., Griffin, M.J., Min, J., Baron, R., and Rosen, E.D. (2012). Regulation of early adipose commitment by Zfp521. PLoS Biol. *10*, e1001433.

Kapur, S., and Mamo, D. (2003). Half a century of antipsychotics and still a central role for dopamine D2 receptors. Prog. Neuropsychopharmacol. Biol. Psychiatry *27*, 1081–1090.

Kataoka, Y., Kalanithi, P.S. a, Grantz, H., Schwartz, M.L., Saper, C., Leckman, J.F., and Vaccarino, F.M. (2010). Decreased number of parvalbumin and cholinergic interneurons in the striatum of individuals with Tourette syndrome. J. Comp. Neurol. *518*, 277–291.

Kelley, A.E. (2001). Measurement of rodent stereotyped behavior. Curr. Protoc. Neurosci. *Chapter 8*, Unit 8.8.

Kelly, M. a, Rubinstein, M., Phillips, T.J., Lessov, C.N., Burkhart-Kasch, S., Zhang, G., Bunzow, J.R., Fang, Y., Gerhardt, G. a, Grandy, D.K., et al. (1998). Locomotor activity in D2 dopamine receptor-deficient mice is determined by gene dosage, genetic background, and developmental adaptations. J. Neurosci. *18*, 3470–3479.

Kermadi, I., and Boussaoud, D. (1995). Role of the primate striatum in attention and sensorimotor processes: comparison with premotor cortex. Neuroreport *6*, 1177–1181.

Khalifa, N., and von Knorring, A.-L. (2005). Tourette syndrome and other tic disorders in a total population of children: clinical assessment and background. Acta Paediatr. *94*, 1608–1614.

Kiviranta, R., Yamana, K., Saito, H., Ho, D.K., Laine, J., Tarkkonen, K., Nieminen-Pihala, V., Hesse, E., Correa, D., Määttä, J., et al. (2013). Coordinated transcriptional regulation of bone homeostasis by Ebf1 and Zfp521 in both mesenchymal and hematopoietic lineages. J. Exp. Med. *210*, 969–985.

Koós, T., and Tepper, J.M. (1999). Inhibitory control of neostriatal projection neurons by GABAergic interneurons. Nat. Neurosci. *2*, 467–472.

Van der Kooy, D., and Fishell, G. (1987). Neuronal birthdate underlies the development of striatal compartments. Brain Res. *401*, 155–161.

Van der Kooy, D., and Kooy, D. Van Der (1996). Early postnatal lesions of the substantia nigra produce massive shrinkage of the rat striatum, disruption of patch neuron distribution, but no loss of patch neurons. Brain Res. Dev. Brain Res. *94*, 242–245.

Kravitz, A. V, Freeze, B.S., Parker, P.R.L., Kay, K., Thwin, M.T., Deisseroth, K., and Kreitzer, A.C. (2010). Regulation of parkinsonian motor behaviours by optogenetic control of basal ganglia circuitry. Nature *466*, 622–626.

Krushel, L. a, Fishell, G., and van der Kooy, D. (1995). Pattern formation in the mammalian forebrain: striatal patch and matrix neurons intermix prior to compartment formation. Eur. J. Neurosci. *7*, 1210–1219.

Kurlan, R. (2002). Treatment of ADHD in children with tics: a randomized controlled trial. Neurology *58*, 527–536.

Kushner, H.I. (2009). A Cursing Brain? The Histories of Tourette Syndrome: the histories of Tourette syndrome (Harvard University Press).

Kwak, C., Dat Vuong, K., and Jankovic, J. (2003). Premonitory sensory phenomenon in Tourette's syndrome. Mov. Disord. *18*, 1530–1533.

Lajonchere, C., Nortz, M., and Finger, S. (1996). Gilles de la Tourette and the discovery of Tourette syndrome. Includes a translation of his 1884 article. Arch. Neurol. *53*, 567–574.

Lawson-Yuen, A., Saldivar, J.-S., Sommer, S., and Picker, J. (2008). Familial deletion within NLGN4 associated with autism and Tourette syndrome. Eur. J. Hum. Genet. *16*, 614–618.

Leckman, J. (2002). Tourette's syndrome. Lancet *360*, 1577–1586.

Leckman, J.F., Walker, D.E., and Cohen, D.J. (1993). Premonitory urges in Tourette's syndrome. Am. J. Psychiatry *150*, 98–102.

Leckman, J.F., Zhang, H., Vitale, A., Lahnin, F., Lynch, K., Bondi, C., Kim, Y.S., and Peterson, B.S. (1998). Course of tic severity in Tourette syndrome: the first two decades. Pediatrics *102*, 14–19.

Lee, C.-C., Chou, I.-C., Tsai, C.-H., Wang, T.-R., Li, T.-C., and Tsai, F.-J. (2005). Dopamine receptor D2 gene polymorphisms are associated in Taiwanese children with Tourette syndrome. Pediatr. Neurol. *33*, 272–276.

Lerner, a, Bagic, a, Boudreau, E. a, Hanakawa, T., Pagan, F., Mari, Z., Bara-Jimenez, W., Aksu, M., Garraux, G., Simmons, J.M., et al. (2007). Neuroimaging of neuronal circuits involved in tic generation in patients with Tourette syndrome. Neurology *68*, 1979–1987.

Lerner, A., Bagic, A., Simmons, J.M., Mari, Z., Bonne, O., Xu, B., Kazuba, D., Herscovitch, P., Carson, R.E., Murphy, D.L., et al. (2012). Widespread abnormality of the γ-aminobutyric acid-ergic system in Tourette syndrome. Brain *135*, 1926–1936.

Lipinski, J.F., Sallee, F.R., Jackson, C., and Sethuraman, G. (1997). Dopamine agonist treatment of Tourette disorder in children: results of an open-label trial of pergolide. Mov. Disord. *12*, 402–407.

Liu, F.C., and Graybiel, a M. (1992). Heterogeneous development of calbindin-D28K expression in the striatal matrix. J. Comp. Neurol. *320*, 304–322.

Liu, H., Dong, F., Meng, Z., Zhang, B., Tan, J., and Wang, Y. (2010). Evaluation of Tourette's syndrome by (99m)Tc-TRODAT-1 SPECT/CT imaging. Ann. Nucl. Med. *24*, 515–521.

Livak, K.J., and Schmittgen, T.D. (2001). Analysis of relative gene expression data using real-time quantitative PCR and the 2(-Delta Delta C(T)) Method. Methods *25*, 402–408.

Lobo, M.K. (2009). Molecular profiling of striatonigral and striatopallidal medium spiny neurons past, present, and future. Int. Rev. Neurobiol. *89*, 1–35.

Lobo, M.K., Karsten, S.L., Gray, M., Geschwind, D.H., and Yang, X.W. (2006). FACS-array profiling of striatal projection neuron subtypes in juvenile and adult mouse brains. Nat. Neurosci. *9*, 443–452.

Lobo, M.K., Yeh, C., and Yang, X.W. (2008). Pivotal role of early B-cell factor 1 in development of striatonigral medium spiny neurons in the matrix compartment. J. Neurosci. Res. *86*, 2134–2146.

Long, J.E., Cobos, I., Potter, G.B., and Rubenstein, J.L.R. (2009a). Dlx1&2 and Mash1 transcription factors control MGE and CGE patterning and differentiation through parallel and overlapping pathways. Cereb. Cortex *19 Suppl 1*, i96–106.

Long, J.E., Swan, C., Liang, W.S., Cobos, I., Potter, G.B., and Rubenstein, J.L.R. (2009b). Dlx1&2 and Mash1 transcription factors control striatal patterning and differentiation through parallel and overlapping pathways. J. Comp. Neurol. *512*, 556–572.

Luo, L., Callaway, E.M., and Svoboda, K. (2008). Genetic dissection of neural circuits. Neuron *57*, 634–660.

Macrì, S., Proietti Onori, M., and Laviola, G. (2013). Theoretical and practical considerations behind the use of laboratory animals for the study of Tourette syndrome. Neurosci. Biobehav. Rev. *37*, 1085–1100.

Maira, M., Long, J.E., Lee, A.Y., Rubenstein, J.L.R., and Stifani, S. (2010). Role for TGF-beta superfamily signaling in telencephalic GABAergic neuron development. J. Neurodev. Disord. *2*, 48–60.

Marin, O., Anderson, S.A., and Rubenstein, J.L. (2000). Origin and molecular specification of striatal interneurons. J. Neurosci. *20*, 6063–6076.

Marín, O., and Rubenstein, J. (2001). A long, remarkable journey: tangential migration in the telencephalon. Nat. Rev. Neurosci. *2*, 780–790.

Masterman, D.L., and Cummings, J.L. (1997). Frontal-subcortical circuits: the anatomic basis of executive, social and motivated behaviors. J. Psychopharmacol. *11*, 107–114.

Matsubara, E., Sakai, I., Yamanouchi, J., Fujiwara, H., Yakushijin, Y., Hato, T., Shigemoto, K., and Yasukawa, M. (2009). The role of zinc finger protein 521/early hematopoietic zinc finger protein in erythroid cell differentiation. J. Biol. Chem. *284*, 3480–3487.

Maurice, N., Tkatch, T., Meisler, M., Sprunger, L.K., and Surmeier, D.J. (2001). D1/D5 dopamine receptor activation differentially modulates rapidly inactivating and persistent sodium currents in prefrontal cortex pyramidal neurons. J. Neurosci. *21*, 2268–2277.

McCairn, K.W., Bronfeld, M., Belelovsky, K., and Bar-Gad, I. (2009). The neurophysiological correlates of motor tics following focal striatal disinhibition. Brain *132*, 2125–2138.

McFarland, N.R., Lee, J.-S., Hyman, B.T., and McLean, P.J. (2009). Comparison of transduction efficiency of recombinant AAV serotypes 1, 2, 5, and 8 in the rat nigrostriatal system. J. Neurochem. *109*, 838–845.

Mink, J.W. (1996). The basal ganglia: focused selection and inhibition of competing motor programs. Prog. Neurobiol. *50*, 381–425.

Mink, J.W. (2001). Basal ganglia dysfunction in Tourette's syndrome: a new hypothesis. Pediatr. Neurol. *25*, 190–198.

Moon Edley, S., and Herkenham, M. (1984). Comparative development of striatal opiate receptors and dopamine revealed by autoradiography and histofluorescence. Brain Res. *305*, 27–42.

Moretti, P., Bouwknecht, J.A., Teague, R., Paylor, R., and Zoghbi, H.Y. (2005). Abnormalities of social interactions and home-cage behavior in a mouse model of Rett syndrome. Hum. Mol. Genet. *14*, 205–220.

Müller-Vahl, K.R., and Krueger, D. (2011). Does Tourette syndrome prevent tardive dyskinesia? Mov. Disord. *26*, 2442–2443.

Müller-Vahl, K.R., Berding, G., Kolbe, H., Meyer, G.J., Hundeshagen, H., Dengler, R., Knapp, W.H., and Emrich, H.M. (2000). Dopamine D2 receptor imaging in Gilles de la Tourette syndrome. Acta Neurol. Scand. *101*, 165–171.

Natesan, S., Reckless, G.E., Nobrega, J.N., Fletcher, P.J., and Kapur, S. (2006). Dissociation between in vivo occupancy and functional antagonism of dopamine D2 receptors: comparing aripiprazole to other antipsychotics in animal models. Neuropsychopharmacology *31*, 1854–1863.

Nechanitzky, R., Akbas, D., Scherer, S., György, I., Hoyler, T., Ramamoorthy, S., Diefenbach, A., and Grosschedl, R. (2013). Transcription factor EBF1 is essential for the maintenance of B cell identity and prevention of alternative fates in committed cells. Nat. Immunol. *14*, 867–875.

Nieoullon, A. (2002). Dopamine and the regulation of cognition and attention. Prog. Neurobiol. *67*, 53–83.

Nordstrom, E.J., and Burton, F.H. (2002). A transgenic model of comorbid Tourette's syndrome and obsessive-compulsive disorder circuitry. Mol. Psychiatry *7*, 617–625, 524.

Oertel, W.H., Wolters, E., Sampaio, C., Gimenez-Roldan, S., Bergamasco, B., Dujardin, M., Grosset, D.G., Arnold, G., Leenders, K.L., Hundemer, H.-P., et al. (2006). Pergolide versus levodopa monotherapy in early Parkinson's disease patients: The PELMOPET study. Mov. Disord. *21*, 343–353.

Olsson, M., Björklund, a, and Campbell, K. (1998). Early specification of striatal projection neurons and interneuronal subtypes in the lateral and medial ganglionic eminence. Neuroscience *84*, 867–876.

Partridge, J.G., Tang, K.C., and Lovinger, D.M. (2000). Regional and postnatal heterogeneity of activity-dependent long-term changes in synaptic efficacy in the dorsal striatum. J. Neurophysiol. *84*, 1422–1429.

Paschou, P. (2013). The genetic basis of Gilles de la Tourette Syndrome. Neurosci. Biobehav. Rev. *37*, 1026–1039.

Patz, S. (2004). Parvalbumin Expression in Visual Cortical Interneurons Depends on Neuronal Activity and TrkB Ligands during an Early Period of Postnatal Development. Cereb. Cortex *14*, 342–351.

Pauls, D.L. (2003). An update on the genetics of Gilles de la Tourette syndrome. J. Psychosom. Res. *55*, 7–12.

Pauls, D.L., and Leckman, J.F. (1986). The inheritance of Gilles de la Tourette's syndrome and associated behaviors. Evidence for autosomal dominant transmission. N. Engl. J. Med. *315*, 993–997.

Peñagarikano, O., Abrahams, B.S., Herman, E.I., Winden, K.D., Gdalyahu, A., Dong, H., Sonnenblick, L.I., Gruver, R., Almajano, J., Bragin, A., et al. (2011). Absence of CNTNAP2 Leads to Epilepsy, Neuronal Migration Abnormalities, and Core Autism-Related Deficits. Cell *147*, 235–246.

Penit-Soria, J., Audinat, E., and Crepel, F. (1987). Excitation of rat prefrontal cortical neurons by dopamine: an in vitro electrophysiological study. Brain Res. *425*, 263–274.

Peterson, B.S., and Leckman, J.F. (1998). The temporal dynamics of tics in Gilles de la Tourette syndrome. Biol. Psychiatry *44*, 1337–1348.

Peterson, B.S., Skudlarski, P., Anderson, A.W., Zhang, H., Gatenby, J.C., Lacadie, C.M., Leckman, J.F., and Gore, J.C. (1998). A functional magnetic resonance imaging study of tic suppression in Tourette syndrome. Arch. Gen. Psychiatry *55*, 326–333.

Peterson, B.S., Thomas, P., Kane, M.J., Scahill, L., Zhang, H., Bronen, R., King, R.A., Leckman, J.F., and Staib, L. (2003). Basal Ganglia volumes in patients with Gilles de la Tourette syndrome. Arch. Gen. Psychiatry *60*, 415–424.

Phelps, P.E., Brady, D.R., and Vaughn, J.E. (1989). The generation and differentiation of cholinergic neurons in rat caudate-putamen. Brain Res. Dev. Brain Res. *46*, 47–60.

Porter, L.L., Rizzo, E., and Hornung, J.P. (1999). Dopamine affects parvalbumin expression during cortical development in vitro. J. Neurosci. *19*, 8990–9003.

Portfors, C. V (2007). Types and functions of ultrasonic vocalizations in laboratory rats and mice. J. Am. Assoc. Lab. Anim. Sci. *46*, 28–34.

Pourfar, M., Feigin, a, Tang, C.C., Carbon-Correll, M., Bussa, M., Budman, C., Dhawan, V., and Eidelberg, D. (2011). Abnormal metabolic brain networks in Tourette syndrome. Neurology *76*, 944–952.

Price, R.A., Kidd, K.K., Cohen, D.J., Pauls, D.L., and Leckman, J.F. (1985). A twin study of Tourette syndrome. Arch. Gen. Psychiatry *42*, 815–820.

Prut, L., and Belzung, C. (2003). The open field as a paradigm to measure the effects of drugs on anxiety-like behaviors: a review. Eur. J. Pharmacol. *463*, 3–33.

Ramocki, M.B., and Zoghbi, H.Y. (2008). Failure of neuronal homeostasis results in common neuropsychiatric phenotypes. Nature *455*, 912–918.

Redgrave, P., Rodriguez, M., Smith, Y., Rodriguez-Oroz, M.C., Lehericy, S., Bergman, H., Agid, Y., Delong, M.R., and Obeso, J. a (2010). Goal-directed and habitual control in the basal ganglia: implications for Parkinson's disease. Nat. Rev. Neurosci. *11*, 760–772.

Rhinn, H., Fujita, R., Qiang, L., Cheng, R., Lee, J.H., and Abeliovich, A. (2013). Integrative genomics identifies APOE ε4 effectors in Alzheimer's disease. Nature *500*, 45–50.

Robertson, M.M. (2000). Tourette syndrome, associated conditions and the complexities of treatment. Brain *123 Pt 3*, 425–462.

Robertson, M.M. (2008a). The prevalence and epidemiology of Gilles de la Tourette syndrome. Part 1: the epidemiological and prevalence studies. J. Psychosom. Res. *65*, 461–472.

Robertson, M.M. (2008b). The prevalence and epidemiology of Gilles de la Tourette syndrome. Part 2: tentative explanations for differing prevalence figures in GTS, including the possible effects of psychopathology, aetiology, cultural differences, and differing phenotypes. J. Psychosom. Res. *65*, 473–486.

Robertson, M.M., Eapen, V., and Cavanna, A.E. (2009). The international prevalence, epidemiology, and clinical phenomenology of Tourette syndrome: a cross-cultural perspective. J. Psychosom. Res. *67*, 475–483.

Robinson, T.E., and Becker, J.B. (1986). Enduring changes in brain and behavior produced by chronic amphetamine administration: a review and evaluation of animal models of amphetamine psychosis. Brain Res. *396*, 157–198.

Ross, N.R., and Porter, L.L. (2002). Effects of dopamine and estrogen upon cortical neurons that express parvalbumin in vitro. Brain Res. Dev. Brain Res. *137*, 23–34.

Rouge-Pont, F., Usiello, A., Benoit-Marand, M., Gonon, F., Piazza, P.V., and Borrelli, E. (2002). Changes in extracellular dopamine induced by morphine and cocaine: crucial control by D2 receptors. J. Neurosci. *22*, 3293–3301.

Rudkin, T.M., and Sadikot, a F. (1999). Thalamic input to parvalbumin-immunoreactive GABAergic interneurons: organization in normal striatum and effect of neonatal decortication. Neuroscience *88*, 1165–1175.

De Ryck, M., Schallert, T., and Teitelbaum, P. (1980). Morphine versus haloperidol catalepsy in the rat: a behavioral analysis of postural support mechanisms. Brain Res. *201*, 143–172.

Rymar, V. V, Sasseville, R., Luk, K.C., and Sadikot, A.F. (2004). Neurogenesis and stereological morphometry of calretinin-immunoreactive GABAergic interneurons of the neostriatum. J. Comp. Neurol. *469*, 325–339.

Sadikot, A.F., and Sasseville, R. (1997). Neurogenesis in the mammalian neostriatum and nucleus accumbens: parvalbumin-immunoreactive GABAergic interneurons. J. Comp. Neurol. *389*, 193–211.

Saka, E., Goodrich, C., Harlan, P., Madras, B.K., and Graybiel, A.M. (2004). Repetitive behaviors in monkeys are linked to specific striatal activation patterns. J. Neurosci. *24*, 7557–7565.

Sallee, F.R., Nesbitt, L., Jackson, C., Sine, L., and Sethuraman, G. (1997). Relative efficacy of haloperidol and pimozide in children and adolescents with Tourette's disorder. Am. J. Psychiatry *154*, 1057–1062.

Sanberg, P.R. (1980). Haloperidol-induced catalepsy is mediated by postsynaptic dopamine receptors. Nature *284*, 472–473.

Sanberg, P.R., Bunsey, M.D., Giordano, M., and Norman, a B. (1988). The catalepsy test: its ups and downs. Behav. Neurosci. *102*, 748–759.

Sandor, P. (2003). Pharmacological management of tics in patients with TS. J. Psychosom. Res. *55*, 41–48.

Scahill, L., Riddle, M.A., King, R.A., Hardin, M.T., Rasmusson, A., Makuch, R.W., and Leckman, J.F. (1997). Fluoxetine has no marked effect on tic symptoms in patients with Tourette's

syndrome: a double-blind placebo-controlled study. J. Child Adolesc. Psychopharmacol. *7*, 75–85.

Scharf, J.M., Yu, D., Mathews, C. a, Neale, B.M., Stewart, S.E., Fagerness, J. a, Evans, P., Gamazon, E., Edlund, C.K., Service, S.K., et al. (2013). Genome-wide association study of Tourette's syndrome. Mol. Psychiatry *18*, 721–728.

Schlösser, B., Klausa, G., Prime, G., and Ten Bruggencate, G. (1999). Postnatal development of calretinin- and parvalbumin-positive interneurons in the rat neostriatum: an immunohistochemical study. J. Comp. Neurol. *405*, 185–198.

Schmeisser, M.J., Ey, E., Wegener, S., Bockmann, J., Stempel, a V., Kuebler, A., Janssen, A.-L., Udvardi, P.T., Shiban, E., Spilker, C., et al. (2012). Autistic-like behaviours and hyperactivity in mice lacking ProSAP1/Shank2. Nature *486*, 256–260.

Seamans, J.K., and Yang, C.R. (2004). The principal features and mechanisms of dopamine modulation in the prefrontal cortex. Prog. Neurobiol. *74*, 1–58.

Selemon, L.D., and Goldman-Rakic, P.S. (1985). Longitudinal topography and interdigitation of corticostriatal projections in the rhesus monkey. J. Neurosci. *5*, 776–794.

Seuchter, S. a, Hebebrand, J., Klug, B., Knapp, M., Lehmkuhl, G., Poustka, F., Schmidt, M., Remschmidt, H., and Baur, M.P. (2000). Complex segregation analysis of families ascertained through Gilles de la Tourette syndrome. Genet. Epidemiol. *18*, 33–47.

Shapiro, A.K., and Shapiro, E. (1968). Treatment of Gilles de la Tourette's Syndrome with haloperidol. Br. J. Psychiatry *114*, 345–350.

Shapiro, E., Shapiro, A.K., Fulop, G., Hubbard, M., Mandeli, J., Nordlie, J., and Phillips, R.A. (1989). Controlled study of haloperidol, pimozide and placebo for the treatment of Gilles de la Tourette's syndrome. Arch. Gen. Psychiatry *46*, 722–730.

Shmelkov, S. V, Hormigo, A., Jing, D., Proenca, C.C., Bath, K.G., Milde, T., Shmelkov, E., Kushner, J.S., Baljevic, M., Dincheva, I., et al. (2010). Slitrk5 deficiency impairs corticostriatal circuitry and leads to obsessive-compulsive-like behaviors in mice. Nat. Med.

Silverman, J.L., Yang, M., Lord, C., and Crawley, J.N. (2010). Behavioural phenotyping assays for mouse models of autism. Nat. Rev. Neurosci. *11*, 490–502.

Singer, H., and Szymanski, S. (2002). Elevated intrasynaptic dopamine release in Tourette's syndrome measured by PET. Am. J. … 1329–1336.

Singer, H.S., and Minzer, K. (2003). Neurobiology of Tourette's syndrome: concepts of neuroanatomic localization and neurochemical abnormalities. Brain Dev. *25*, S70–S84.

Singer, H.S., Butler, I.J., Tune, L.E., Seifert, W.E., and Coyle, J.T. (1982). Dopaminergic dsyfunction in Tourette syndrome. Ann. Neurol. *12*, 361–366.

Spencer, T., Biederman, J., Wilens, T., Harding, M., O'Donnell, D., and Griffin, S. (1996). Pharmacotherapy of attention-deficit hyperactivity disorder across the life cycle. J. Am. Acad. Child Adolesc. Psychiatry *35*, 409–432.

Spina, R., Filocamo, G., Iaccino, E., Scicchitano, S., Lupia, M., Chiarella, E., Mega, T., Bernaudo, F., Pelaggi, D., Mesuraca, M., et al. (2013). Critical role of zinc finger protein 521 in the control of growth, clonogenicity and tumorigenic potential of medulloblastoma cells. Oncotarget *4*, 1280–1292.

Staley, D., Wand, R., and Shady, G. (1997). Tourette disorder: a cross-cultural review. Compr. Psychiatry *38*, 6–16.

State, M.W. (2010). The genetics of child psychiatric disorders: focus on autism and tourette syndrome. Neuron *68*, 254–269.

Steeves, T.D.L., Ko, J.H., Kideckel, D.M., Rusjan, P., Houle, S., Sandor, P., Lang, A.E., and Strafella, A.P. (2010). Extrastriatal dopaminergic dysfunction in tourette syndrome. Ann. Neurol. *67*, 170–181.

Stern, E., Silbersweig, D. a, Chee, K.Y., Holmes, a, Robertson, M.M., Trimble, M., Frith, C.D., Frackowiak, R.S., and Dolan, R.J. (2000). A functional neuroanatomy of tics in Tourette syndrome. Arch. Gen. Psychiatry *57*, 741–748.

Sundaram, S.K., Huq, A.M., Wilson, B.J., and Chugani, H.T. (2010). Tourette syndrome is associated with recurrent exonic copy number variants. Neurology *74*, 1583–1590.

Sussel, L., Marin, O., Kimura, S., and Rubenstein, J.L. (1999). Loss of Nkx2.1 homeobox gene function results in a ventral to dorsal molecular respecification within the basal telencephalon: evidence for a transformation of the pallidum into the striatum. Development *126*, 3359–3370.

Sverd, J., Gadow, K.D., and Paolicelli, L.M. (1989). Methylphenidate treatment of attention-deficit hyperactivity disorder in boys with Tourette's syndrome. J. Am. Acad. Child Adolesc. Psychiatry *28*, 574–9; discussion 580–2.

Tang, L., Todd, R.D., and O'Malley, K.L. (1994). Dopamine D2 and D3 receptors inhibit dopamine release. J. Pharmacol. Exp. Ther. *270*, 475–479.

Taymans, J.-M., Vandenberghe, L.H., Haute, C. Van Den, Thiry, I., Deroose, C.M., Mortelmans, L., Wilson, J.M., Debyser, Z., and Baekelandt, V. (2007). Comparative analysis of adeno-associated viral vector serotypes 1, 2, 5, 7, and 8 in mouse brain. Hum. Gene Ther. *18*, 195–206.

Tekin, S., and Cummings, J.L. (2002). Frontal-subcortical neuronal circuits and clinical neuropsychiatry: an update. J. Psychosom. Res. *53*, 647–654.

Tepper, J.M., and Bolam, J.P. (2004). Functional diversity and specificity of neostriatal interneurons. Curr. Opin. Neurobiol. *14*, 685–692.

Thibault, D., Loustalot, F., Fortin, G.M., Bourque, M.-J., and Trudeau, L.-É. (2013). Evaluation of D1 and D2 dopamine receptor segregation in the developing striatum using BAC transgenic mice. PLoS One *8*, e67219.

Tronche, F., Kellendonk, C., Kretz, O., Gass, P., Anlag, K., Orban, P.C., Bock, R., Klein, R., and Schütz, G. (1999). Disruption of the glucocorticoid receptor gene in the nervous system results in reduced anxiety. Nat. Genet. *23*, 99–103.

Tsai, P.T., Hull, C., Chu, Y., Greene-Colozzi, E., Sadowski, A.R., Leech, J.M., Steinberg, J., Crawley, J.N., Regehr, W.G., and Sahin, M. (2012). Autistic-like behaviour and cerebellar dysfunction in Purkinje cell Tsc1 mutant mice. Nature 1–6.

Verkerk, A.J.M.H., Mathews, C. a., Joosse, M., Eussen, B.H.J., Heutink, P., and Oostra, B. a. (2003). Cntnap2 is disrupted in a family with gilles de la tourette syndrome and obsessive compulsive disorder. Genomics *82*, 1–9.

Vogt Weisenhorn, D.M., Celio, M.R., and Rickmann, M. (1998). The onset of parvalbumin-expression in interneurons of the rat parietal cortex depends upon extrinsic factor(s). Eur. J. Neurosci. *10*, 1027–1036.

Voorn, P., Vanderschuren, L.J.M.J., Groenewegen, H.J., Robbins, T.W., and Pennartz, C.M. a (2004). Putting a spin on the dorsal-ventral divide of the striatum. Trends Neurosci. *27*, 468–474.

Wadenberg, M.L., Soliman, a, VanderSpek, S.C., and Kapur, S. (2001). Dopamine D(2) receptor occupancy is a common mechanism underlying animal models of antipsychotics and their clinical effects. Neuropsychopharmacology *25*, 633–641.

Walkup, J.T., LaBuda, M.C., Singer, H.S., Brown, J., Riddle, M. a, and Hurko, O. (1996). Family study and segregation analysis of Tourette syndrome: evidence for a mixed model of inheritance. Am. J. Hum. Genet. *59*, 684–693.

Warming, S., Liu, P., Suzuki, T., Akagi, K., Lindtner, S., Pavlakis, G.N., Jenkins, N.A., and Copeland, N.G. (2003). Evi3, a common retroviral integration site in murine B-cell lymphoma, encodes an EBFAZ-related Kruppel-like zinc finger protein. Blood *101*, 1934.

Warming, S., Rachel, R.A., Jenkins, N.A., and Copeland, N.G. (2006). Zfp423 is required for normal cerebellar development. Mol. Cell. Biol. *26*, 6913–6922.

Wei, L.-C., Shi, M., Chen, L.-W., Cao, R., Zhang, P., and Chan, Y.S. (2002). Nestin-containing cells express glial fibrillary acidic protein in the proliferative regions of central nervous system of postnatal developing and adult mice. Brain Res. Dev. Brain Res. *139*, 9–17.

Welch, J.M., Lu, J., Rodriguiz, R.M., Trotta, N.C., Peca, J., Ding, J.-D., Feliciano, C., Chen, M., Adams, J.P., Luo, J., et al. (2007). Cortico-striatal synaptic defects and OCD-like behaviours in Sapap3-mutant mice. Nature *448*, 894–900.

West, M.J., Slomianka, L., and Gundersen, H.J. (1991). Unbiased stereological estimation of the total number of neurons in thesubdivisions of the rat hippocampus using the optical fractionator. Anat. Rec. *231*, 482–497.

Williams, G. V, and Goldman-Rakic, P.S. (1995). Modulation of memory fields by dopamine D1 receptors in prefrontal cortex. Nature *376*, 572–575.

Willner, P. (1984). The validity of animal models of depression. Psychopharmacology (Berl). *83*, 1–16.

Willner, P. (1986). Validation criteria for animal models of human mental disorders: learned helplessness as a paradigm case. Prog. Neuropsychopharmacol. Biol. Psychiatry *10*, 677–690.

Wojtowicz, J.M., and Kee, N. (2006). BrdU assay for neurogenesis in rodents. Nat. Protoc. *1*, 1399–1405.

Wong, D.F., Brasić, J.R., Singer, H.S., Schretlen, D.J., Kuwabara, H., Zhou, Y., Nandi, A., Maris, M. a, Alexander, M., Ye, W., et al. (2008). Mechanisms of dopaminergic and serotonergic neurotransmission in Tourette syndrome: clues from an in vivo neurochemistry study with PET. Neuropsychopharmacology *33*, 1239–1251.

Worbe, Y., Baup, N., Grabli, D., Chaigneau, M., Mounayar, S., McCairn, K., Féger, J., and Tremblay, L. (2009). Behavioral and movement disorders induced by local inhibitory dysfunction in primate striatum. Cereb. Cortex *19*, 1844–1856.

Wu, M., Hesse, E., Morvan, F., Zhang, J.-P., Correa, D., Rowe, G.C., Kiviranta, R., Neff, L., Philbrick, W.M., Horne, W.C., et al. (2009). Zfp521 antagonizes Runx2, delays osteoblast differentiation in vitro, and promotes bone formation in vivo. Bone *44*, 528–536.

Xu, Q., Tam, M., and Anderson, S.A. (2008). Fate mapping Nkx2.1-lineage cells in the mouse telencephalon. J. Comp. Neurol. *506*, 16–29.

Yadin, E., Friedman, E., and Bridger, W.H. (1991). Spontaneous alternation behavior: an animal model for obsessive-compulsive disorder? Pharmacol. Biochem. Behav. *40*, 311–315.

Yang, C.R., and Seamans, J.K. (1996). Dopamine D1 receptor actions in layers V-VI rat prefrontal cortex neurons in vitro: modulation of dendritic-somatic signal integration. J. Neurosci. *16*, 1922–1935.

Yang, X.W., and Lu, X.-H. (2011). Molecular and cellular basis of obsessive-compulsive disorder-like behaviors: emerging view from mouse models. Curr. Opin. Neurol. *24*, 114–118.

Yizhar, O., Fenno, L.E., Davidson, T.J., Mogri, M., and Deisseroth, K. (2011). Optogenetics in neural systems. Neuron *71*, 9–34.

Zhang, F., Gradinaru, V., Adamantidis, A.R., Durand, R., Airan, R.D., de Lecea, L., and Deisseroth, K. (2010). Optogenetic interrogation of neural circuits: technology for probing mammalian brain structures. Nat. Protoc. *5*, 439–456.

Zhou, Q.-Y., and Palmiter, R.D. (1995). Dopamine-deficient mice are severely hypoactive, adipsic, and aphagic. Cell *83*, 1197–1209.

Zhuang, X., Oosting, R.S., Jones, S.R., Gainetdinov, R.R., Miller, G.W., Caron, M.G., and Hen, R. (2001). Hyperactivity and impaired response habituation in hyperdopaminergic mice. Proc. Natl. Acad. Sci. U. S. A. *98*, 1982–1987.